Influence of Pathogen Strain, Barley Cultivar, and HYD5 Protein on Fusarium Head Blight Progression and *Fusarium*-Barley Interactions During Malting

by

Adimali Kamkanamge Anuradha Ushani Jayathissa

A Thesis submitted to the Faculty of Graduate Studies of The University of Manitoba in partial fulfilment of the requirements of the degree of

DOCTOR OF PHILOSOPHY

Department of Microbiology

University of Manitoba

Winnipeg, Manitoba, Canada

ACKNOWLEDGEMENTS

I would like to express my heartfelt gratitude to my supervisor, Dr. Matthew Bakker, and my co-supervisor, Dr. Dilantha Fernando, for the incredible opportunity to be your graduate student over the past five years. Your constant support, guidance, and encouragement have been crucial for my growth, both professionally and personally. Your motivation and feedback have helped me improve my research, writing, and presentation skills. I've learned a lot from you, and I'm truly grateful for everything you've done and for your exceptional mentorship. I also want to thank my committee members, Dr. Ana Badea and Dr. Xiang Yin, for their helpful guidance and support during these years. Your input has been very valuable to me. I would like to express my sincere gratitude to Dr. James Tucker for his invaluable assistance with my barley fieldwork and for all the help in making my Brandon project a success. Thank you all so much.

Thank you to everyone in the Bakker and Fernando labs for all your support. I'm especially grateful to past Bakker lab members including Janice Fajardo, Arshani Alukumbura, Tarin Farhana, and Mehrdad Mohammadiani, as well as the current team, for all your help and the fun times we shared. Your support made everything easier, and I truly appreciate it.

I'm also thankful for the technical support provided by Patti Green, Kevin Moore, and Athena Monayao. My thanks to Dr. Maria Antonia Henriquez from Agriculture & Agri-Food Canada for sharing *Fusarium graminearum* strains HSW-15-19, HSW-15-40, HSW-15-63, HSW-15-73, and HSW-15-95. I also acknowledge Dr. Abbot Oghenekaro for supplying genomic DNA extracts of diverse *Fusarium graminearum* strains used in the high resolution melting analysis. Special thanks to Dr. Michele C. Loewen and Dr. Tanya Sharma for their assistance in developing the Δ*Hyd5* knock out strain, and to Dr. David N. Langelaan and Raymond He for collaborating to produce pure HYD5 protein. I am also grateful to the Western Grains Research Foundation, Canadian Agricultural Partnership, EvoFunPath training program, and the American Society of Brewing Chemists Research Council for their financial support.

To the entire Microbiology Department, thank you for making these past few years memorable. Your friendliness, kindness, and warm smiles have truly brightened my time here.

I also want to thank my parents, Padma and Siril Jayathissa, my brothers Rakitha, Pramod, and Ishara Jayathissa, and my husband Manoj Kohombange. Your love, care, and support have meant everything to me and have kept me going. I couldn't have done this without my family. Thank you so much.

DEDICATION

To my beloved family

CONTENTS

LIST OF TABLES

LIST OF FIGURES

ABSTRACT

Fusarium head blight (FHB) is a devastating disease in barley, primarily caused by *Fusarium graminearum*, leading to significant yield loss and mycotoxin contamination, with major economic impacts on the malting and brewing industries. This study hypothesized that variation in *Fusarium*-related issues during malting may be partially due to differences among *F. graminearum* strains. Field trials conducted from 2019–2021 used barley cultivars with varying levels of FHB resistance (Newdale and AAC Goldman) inoculated with seven *F. graminearum* isolates. Disease severity, pathogen density, and deoxynivalenol (DON) content were assessed across years, cultivars, and pathogen strains. Results showed that pathogen strain identity significantly influenced *F. graminearum* density and DON levels in barley and malt, with Newdale showing higher susceptibility than AAC Goldman.

The study also focused on the role of the hydrophobin protein HYD5 from *F. graminearum*, a surface-active protein associated with fungal pathogenesis and beer gushing. Using a CRISPR-Cas9 system, a Δ*Hyd5* knockout strain of *F. graminearum* was generated. The knockout strain showed no significant effect on visual disease severity but resulted in reduced gushing in *F. graminearum* infected malt. *Hyd5* gene expression was elevated during steeping and germination stages of malting, suggesting production of the protein during these phases. Purified HYD5 protein from *F. graminearum* was sufficient to induce beer gushing, highlighting its potential role in this malting defect. Sequence analysis of HYD5 across *Fusarium* species revealed interspecies variability, although no intraspecies variation was observed. The findings suggest that managing *Fusarium*-related malting issues, including beer gushing, requires a deeper understanding of the role of hydrophobins like HYD5 across *F. graminearum* strains and other *Fusarium* species that are active in malting environments.

1. GENERAL INTRODUCTION

Fusarium head blight (FHB) is a devastating disease affecting cereals such as wheat and barley, primarily caused by the fungus *Fusarium graminearum*. This pathogen not only reduces grain yield and quality but also contaminates the grain with mycotoxins, notably deoxynivalenol (DON), which pose serious risks to human and animal health (Bakker et al., 2018; Fernando et al., 2021). FHB development is favored by warm, humid weather following spike emergence, with optimal air temperatures between 16-30 °C promoting spore germination (McMullen et al., 2012; Schöneberg et al., 2018). Symptoms of FHB include premature bleaching of one or more spikelets in the barley head/spike, and affected seeds may appear shriveled and discolored (Siou et al., 2014).

In barley, especially malting barley, the effects of *F. graminearum* are not confined to the field. The malting process, which converts barley into malt for brewing, creates conditions that encourage fungal growth and mycotoxin production. The malting provides an ideal environment for fungal activity due to moderate temperatures, high humidity, and readily available nutrients (Mastanjević et al., 2018, 2019). As a result, *F. graminearum* can negatively affect malt quality by accumulating DON and potentially causing beer gushing, a phenomenon where beer foams excessively upon opening (Janssen et al., 2018). Beer gushing is linked to hydrophobins, small proteins produced by filamentous fungi including *Fusarium* species. These proteins form hydrophobic layers on fungal surfaces and have been implicated in gushing due to their role in carbon dioxide (CO_2) micelle formation, which leads to excessive foaming (Sarlin et al., 2005). While all strains of *F. graminearum* can produce hydrophobins, variability among strains in hydrophobin production and other virulence factors, like the rate and timing of DON production, can lead to inconsistent effects on malt quality and beer production (Linder et al., 2005; Sarlin et al., 2005).

Hydrophobins are characterized by their conserved eight-cysteine residues that form disulfide bridges, stabilizing their structure (Bayry et al., 2012). These proteins play crucial roles in fungal development, including sporulation, aerial hyphae formation, and surface adhesion, particularly in interactions with plant and animal hosts (Valsecchi et al., 2018; Wessels, 2000).

The *F. graminearum* genome encodes multiple hydrophobin genes, with *Hyd5* being particularly significant in the context of barley-malting interactions. While HYD5 does not appear to affect fungal morphology or water-air interface penetration, it plays a role in the

hydrophobicity of fungal mycelia and is associated with beer gushing (Minenko et al., 2014). During malting, *Fusarium* strains can produce hydrophobins in greater quantities, potentially leading to beer gushing even in malt derived from visually healthy barley (Sarlin et al., 2007). Thus, understanding the diversity of *F. graminearum* strains and their differential production of hydrophobins is critical to managing both FHB in barley and its downstream impacts in the malting and brewing industries.

Fusarium affects not only DON contamination in barley and malt and beer gushing but also yeast behavior during the fermentation process. This issue is known as premature yeast flocculation (PYF). PYF occurs when flocculation-competent yeast settles out of the fermentation medium too early or heavily, leading to poorly attenuated wort and a final product with undesirable flavors. This phenomenon is triggered by non-starch polysaccharides released during the breakdown of malted barley husks due to *F. graminearum* contamination (Xie et al., 2022).

This thesis investigates the roles of *F. graminearum* strains, their hydrophobin production, and their impacts on FHB disease progression and barley malt quality. By focusing on the variability among strains in virulence factors such as DON and hydrophobins, this study aims to provide insights into the broader implications of fungal diversity for agriculture and brewing.

CHAPTER 1: LITERATURE REVIEW

1. Cultivated barley: *Hordeum vulgare*

Barley (*Hordeum vulgare* L.) is a cereal grain with a long history, having been among the first crops domesticated around 10,000 years ago in the Middle East (Zohary et al., 2013). Initially, barley was mainly consumed as food by humans, but over time its primary uses have shifted towards animal feed, malting, and brewing. In recent years, approximately two-thirds of the global barley production has been allocated for feed, one-third for malting, and only about 2 % is directly consumed as food (Baik and Ullrich, 2008). Despite these trends, barley remains an essential dietary staple in some cultures, particularly in regions of Asia and northern Africa (Newman & Newman, 2006). Historically, barley has been valued for its hearty flavor and high nutritional content, boasting more fiber, beta-glucan, and starch granules than wheat and other cereal grains. Additionally, barley is rich in starch, minerals, vitamins, and protein, making it an excellent food supplement (Huang, 2020; Sullivan et al., 2013). The health benefits associated with barley consumption are one of its primary advantages in various food products.

In addition to its use as food, barley plays a crucial role in brewing, serving as the main raw material after water (Gupta et al., 2010). Its unique chemical composition and brewing properties make it the preferred grain for malt production worldwide, significantly influencing beer quality and the cost-effectiveness of the brewing process (Zhou, 2010). While other grains like wheat, rye, oats, rice, and corn can also be used to produce malt, barley remains the most favored due to its high content of carbohydrates, proteins, enzymes, and flavor compounds, which contribute to the desired characteristics of beer (Gupta et al., 2010). The protein content of barley affects the chemical makeup and enzyme activity of the resulting malt. Because of its extensive use in the beer industry, barley has gained prominence as an industrial crop, attracting interest from entrepreneurs, farmers, and researchers alike (Narwal et al., 2017).

2. Fusarium head blight (FHB)

FHB is a destructive fungal disease in cereal crops and corn caused primarily by *F. graminearum*. In 1884, the disease was first described in England, where it was considered a major threat to wheat and barley crops during the early years of the twentieth century (Smith, 1885). The pathogen can overwinter as spores or mycelium on infected plant residues, and within infected seeds (Hofgaard et al., 2016). Pathogen need warm, humid weather at the flowering time of the crop combined with air temperatures between 16-30 °C to promote

spore germination (Czembor et al., 2015). Spores can also overwinter in infected seeds, potentially impacting seedling vigor and survival (Okungbowa & Shittu, 2014).

The fungus produces asexual spores (macroconidia) on infected residues, which can be dispersed to plants and other plant debris by rain-splash, irrigation or wind (Leplat et al., 2016). When conditions are warm, humid, and wet, bluish-black perithecia develop on the surface of these residues and forcibly discharge sexual spores (ascospores) into the air (Manstretta & Rossi, 2015). These ascospores are picked up by the wind and may travel great distances in the air and have the potential to infect fields in the neighboring regions (Maldonado-Ramirez et al., 2005; Schmale et al., 2006). Infection occurs when the ascospores and/or macroconidia land on the susceptible parts of the host plant (Alisaac & Mahlein, 2023). Extruded anthers during barley flowering are the site of primary infection (Alukumbura et al., 2022; Schroeder & Christensen, 1963). If the *Fusarium* infect the flowers just after their extrusion, the fungus will colonize and kill the florets, with no kernel development. Florets that are infected later with *F. graminearum* will produce diseased kernels that are shrivelled and wilted in appearance (Ilgen et al., 2009).

FHB symptoms in barley begin with the premature bleaching of spikelets within the head of the barley plant. During favourable weather, the fungus produces salmon-orange to pink colored spores near the base of the spikelets or just beneath the glumes. The seeds in blighted heads do not fill properly and appear shrivelled and bleached.

F. graminearum and other members of the *F. graminearum* species complex are the major pathogens causing FHB in cereal crops, which can lead to yield losses and trichothecene mycotoxins contaminations deoxynivalenol (DON), nivalenol (NIV), and several acetylated derivatives (Nicolli et al., 2018).

3. The malting process

Malting is the process of converting or modifying barley into the main ingredient used in brewing. Malting is a 5–7 day process that includes three main steps and begins with cleaning the grains followed by steeping, germination, and kilning (Krstanović et al., 2021). During the malting process, large and structurally complex compounds (starch, proteins, and nucleic acids) in the barley are partially or fully degraded into simpler components (sugars, amino acids, and nucleotides) by hydrolytic enzymes (Rani & Bhardwaj, 2021).
Adequate precleaning of barley is essential before they can enter the steep vessel, so that the finished product contains the minimum amount of contaminants that may affect the beer

qualities and flavour. The barley that has been precleaned and is ready for malting is moved into circular steel bins with a large capacity. The recommended warm storage of barley is 12-15 °C at 12 % seed moisture content (Izydorczyk, 2004). The malting companies sometimes deliberately store the barley for a few months because *Fusarium* will slowly decline in vigour.

Malting starts with the steeping stage, in which the dried grains are imbibed in the necessary amount of water to elevate the moisture level to around 42-47 % (P. Schwarz & Li, 2010). Steeping consists of a series of immersions in water which takes up to 48 hours. Each wet period is followed by a dry period during which the water is drained, and CO_2 is removed using fans. These conditions help the barley to develop normally and stimulate germination. Once the steeping is complete, the grain should have reached sufficient moisture levels with a high percentage of chitted kernels, i.e., showing a white-colored protrusion of the growing cotyledon/rootlet emerging from the embryo of the grain (Rani & Bhardwaj, 2021).

Germination accelerates embryo development, manifested by the growth of the rootlets and shoot length increments, which coincides with endosperm modifications. During germination, the germinating grain bed is turned regularly to prevent rootlets from matting, allowing adequate airflow and maintaining a loosely packed grain bed. Gemination is controlled by aerobic and humid conditions at 16-20 °C for 3-6 days, depending on the process conditions and starting materials (Kranz et al., 2015).

In kilning, the green malt (moist malted barley) is transferred to the kilning chamber, where it develops the final desired character and flavor. Heated air is passed through the grain bed to arrest germination. The kilning process dries the grain down to 3-5 % moisture, and this ensures the product's stability for storage, transportation, and maintaining the enzymatic potential of the grain. Kilning is conducted in a stepwise manner with a gradual increase of the temperature from 50 to 85 °C over a 21-hour period. Finally, the malt is cooled, and the dried rootlets are removed before storage since the rootlets pick up moisture quickly (Neylon et al., 2020).

4. *Fusarium* activity as a quality factor in malt production

In barley, *Fusarium* directly integrates into the grain in the barley head and extensively degrades endosperm by penetrating and feeding on the available nutrients (Lewandowski et al., 2006). After harvest, barley is stored for some time before malting, but *Fusarium* may still develop further during this storage time. Although the conditions in grain storage

facilities are not conducive to the development of fungi, the fungi primarily associated with the grains harvested from the field may continue growing during storage. Such growth during storage would only occur under improper storage conditions, such as if the moisture content is too high (Bokulich & Bamforth, 2013). For most end uses of cereal grains, impacts of *Fusarium* or other pathogens are primarily associated with fungal activity in the field, as drying and proper storage largely halt fungal activity in the harvested grain. However, the malting industry faces unique challenges with *Fusarium* that are not experienced in other industries because the malting process itself creates conditions that favour new fungal growth. Thus, *Fusarium* infections in barley are the most important pathogens in the malting and brewing industries because they can proliferate during the malting process (Mastanjević et al., 2018).

Fungi exposed to favourable process conditions (readily available nutrients, exposure to lower temperatures, good aeration, high air humidity, emergence in water and overall high grain moisture during germination) will enhance their growth and the synthesis of secondary metabolites. High moisture content in steeped grain combined with lower temperatures enables fungal spores to germinate and start mycelial growth. The low moisture level in kilning, together with high temperatures for the fungi, appears to have a profound effect on reducing mycelial growth. *Fusarium* proliferation during malting is mainly caused by the grain's initial infection and the grain's nutritive characteristics (Bakker et al., 2024; Sarlin et al., 2005). The infection in malts can also be spread through transportation. Schwarz et al., (2001) described that visual evidence of *Fusarium* spp. infection can be observed during the malting process, particularly through the steeping and germination phases. White, aerial fungal mycelium develops during severe infections, giving the grain a fluffy, hairy look. The most intense mycelium growth can be seen in the germ itself and can result in its death. Because of that, heavily infected grains lose their ability to germinate. In general, pronounced effects on a reduction of thousand kernel weight, a reduction in test weight, increased grain moisture content, and an increase in soluble protein content and soluble nitrogen content were reported in *Fusarium* infected kernels (Schwarz et al., 2002). *Fusarium* infection can also change the color, viscosity, soluble nitrogen, free amino nitrogen, beta-glucan level and pH value in malt and wort. Further, the infected malt can affect other quality parameters as well such as germinative capacity (the percentage of seeds that would normally germinate under optimal conditions), endosperm protein and starch degradation (Mastanjević et al., 2018).

4.1 *Fusarium* traits related to malt quality parameters: Aggressiveness

Spreading of the mycelium within the barley head is likely to be a major component of *F. graminearum* aggressiveness (Miedaner et al., 2001). The aggressiveness of a pathogen is a quantitative measurement of a disease induced by the pathogenic isolate on the susceptible host. It is the most important fungal trait affecting FHB disease invasion and stability of barley resistance. Aggressiveness can be measured through various quantitative traits, also called aggressive components expressed during the host-pathogen interaction. These traits are infection efficiency, lesion size, lesion cover, necrosis, spore production rate and percent disease index (Sultana et al., 2018). However, the pathogen aggressiveness is usually evaluated by measuring the disease severity, a combined variable resulting from the integrated effect of infection efficiency. Infection efficiency is defined as the probability of an individual spore deposited on a receptive host surface, while disease severity is measured as a proportion of diseased spikelets per spike (Pariaud et al., 2009).

The aggressiveness of different strains may vary for a given species, with the more aggressive ones affecting barley plants faster and more intensively. Several reports have underlined the variation for aggressiveness in FHB causal agents. However, the physiological factors leading to different virulence levels among FHB isolates are still unclear, although the synthesis and secretion of cell walls degrading enzymes and mycotoxins production are assumed to play an important role (Dusabenyagasani et al., 1999).

Variations in aggressiveness have been identified among *F. graminearum* strains sampled from various parts of the world, within a country or state and even within populations from individual fields (Carter et al., 2002; Malbrán et al., 2012). However, most of the work regarding the aggressiveness of *F. graminearum* isolates was conducted under greenhouse conditions. Thus, the information about the aggressiveness of the *F. graminearum* strains under field conditions is lacking. It is found that aggressiveness is not geographically structured in a single location since fungal isolates with different levels of aggressiveness can be found within the same population of *F. graminearum* (Mesterhazy et al., 2020). Overall, the comparative aggressiveness of fungal isolates associated with FHB on barley is poorly understood. More effective and accurate disease assessment methods are required to successfully identify FHB pathogens' aggressiveness.

4.2 Deoxynivalenol and its derivatives

Severe FHB occurrence can be expected in warm and wet weather conditions during anthesis (Gilbert & Tekauz, 2000). The disease not only reduces grain yield and quality but also limits grain utilization due to contamination with mycotoxins. Mycotoxins are secondary metabolites produced by fungi under certain conditions (Bills & Gloer, 2016). The most frequently detected mycotoxin in cereal grains at very high concentrations is deoxynivalenol (DON), a low molecular-weight inhibitor of protein synthesis (Sobrova et al., 2010).

DON is detected most frequently and at the highest concentrations in association with *F. graminearum* and *F. culmorum* (Warth et al., 2012). Kernels can harbor *Fusarium* infection without showing visible symptoms, leading to a hidden risk of DON contamination (Peiris et al., 2010). Ingestion of contaminated grains or by-products is toxic to humans and animals and can have severe long-term consequences, including immunosuppression, neurotoxicity, and nutrient uptake alteration (Morooka et al., 1972). Thus, a maximum limit for DON in food and feed has been recommended in many countries. The Codex Alimentarius Commission has established maximum tolerable levels for DON. For cereal-based foods for infants and young children, the limit is set at 0.2 ppm. For flour, meal, or flakes made from wheat, maize, or barley, the maximum tolerable level is 1 ppm. For wheat, maize, and barley intended for further processing—where additional treatments can reduce DON levels before these grains are used in food products—the limit is set at 2 ppm (Chen et al., 2019).

DON can be degraded or detoxified into various derivatives by acetylation, oxidation, de-epoxidation, or glycosylation (Maul et al., 2012; Sun & Wu, 2016; H. Zhang et al., 2016). In addition to DON, derivatives like the acetylated forms 3-acetyl deoxynivalenol (3-ADON) and 15-acetyl deoxynivalenol (15-ADON) are of particular importance and contribute to the total DON-induced toxicity. Combinations of trichothecenes are often present in grain samples, and 10-20 % of DON exists as mixture of 3-ADON and/or 15-ADON (Knutsen et al., 2017; Pinton et al., 2012; Ran et al., 2013). However, to date, health authorities consider DON and its acetylated derivatives to have different toxic effects. Pinton et al., (2012), compared the intestinal toxicity of DON and its acetylated derivatives and observed the effect of DON is different from the acetylated derivatives. DON derivatives have been considered markers for detecting DON in cereal crops because DON shows a co-occurrence with its derivatives (Boevre et al., 2015). Most 3-ADON and 15-ADON is de-acetylated into DON during digestion by animals (Righetti et al., 2017). Therefore, 15-ADON and 3-ADON have at least equal toxicity to animals compared to DON. The problem of these DON derivatives

has become of increasing concern for consumers and producers since their presence could increase the total amount of toxins in food and feed (Castañares et al., 2014). Thus, the acetylated forms of DON have attracted increasing attention.

5. Diversity of *Fusarium graminearum* populations in Canada

Fusarium graminearum is a widely distributed pathogen (Zeller et al., 2003). FHB pathogen diversity studies have revealed two major genetic populations within the species *F. graminearum* in the Upper Midwest of the US and the western and Maritime Provinces of Canada. The dominant genetic population (NA1) consists largely of isolates with the 15-ADON chemotype, prevalent in the eastern Canadian provinces of Québec and Ontario (Kelly et al., 2016; Lofgren et al., 2018). In contrast, the second genetic population (NA2) consisting of 3-ADON chemotypes may have been introduced into North America in the last several decades. The frequency of NA2 was rare before 2004 and has rapidly increased in parts of the midwestern US and western and Atlantic provinces of Canada (PARRY et al., 1995).

Recently *F. graminearum* strain that produces a novel 7-hydroxy, 8-deoxy trichothecene structure has been identified. This new trichothecene has been called NX-2, and the structure of the molecule is identical to that of 3ADON except for the absence of a keto group at the 8-carbon position (Varga et al., 2015). The NX-2 producing population of *F. graminearum* is exclusively found in the northern US and southern Canada, where they are observed at low frequency (<3 %). These results indicate that *F. graminearum* population dynamics in North America have been influenced by a complex selective landscape (Zhang et al., 2007) and populations may be differentially adapted across the continental scale. Unfortunately, the literature has not yet explored the genetic variation in *F. graminearum* populations that could contribute to phenotypic divergence in FHB pathogens.

Trichothecenes are considered virulence factors in wheat (Zhang et al., 2012), and chemotype differences may contribute to the invasion of NA2/3ADON isolates in some regions. However, NA2 isolates can also deposit more toxins in grain, grow faster and spread rapidly than NA1 isolates on wheat (Lee et al., 2001), indicating that other fitness traits may be involved in pathogen adaptive shifts. Before 2000, 15-ADON producers were dominant in Canada, while they have been gradually replaced by the 3-ADON producers in some major wheat-growing regions. For example, 3-ADON genotype frequency in western Canada has been increased by more than 14-fold between 1998 and 2004 (Ward et al., 2008). An analysis

of the trichothecene genotypes of *F. graminearum* collected from winter wheat fields in the eastern US revealed an increasing prevalence of the 3-ADON genotype, with a gradient moving from the southern regions toward the northeastern US and closer to Canada (Foroud et al., 2012).

While three populations produce different trichothecene chemotypes, *in planta* the trichothecenes are predominantly found in their deacetylated form. Both 3ADON and 15ADON are converted to DON, and NX-2 is converted to 3,7,15-trihydroxy-12,13-epoxytrichothec-9-ene (NX-3) (Woelflingseder et al., 2020).

6. Techniques for detecting *Fusarium*

There is an increased incidence of FHB in barley due to climate change threatening food safety and encouraging the movement of various pathogens into new geographic regions. Thus, the risk of quality problems associated with *Fusarium* infections in the malting and brewing industry present a continual challenge. Germinative capacity of infected barley samples can be significantly lowered by *Fusarium* infection depending on the barley variety, the crop year, and the *Fusarium* species (Gilbert & Tekauz, 2000).

Effective tools for detecting Fusarium contamination in barley and malt are essential for addressing these challenges. They allow for early identification, accurate mycotoxin level assessment, and mitigation of risks affecting both the malting and brewing industries as well as consumer health. To this end, several analytical methods are available; however, the most used method is the visual assessment to screen cereal batches for fungal infection, as it assumes a direct connection between symptoms (if they can be observed) and the potential fungal contaminants. The exceedance of a defined limit of *Fusarium* infected/red kernels (usually five to seven kernels in a 200 g sub-sample) stops further processing and can lead to price reductions or the rejection of the entire batch/shipment of barley (Linkmeyer et al., 2016). Visible symptoms provide low predictability for *Fusarium* contamination, but a significant correlation has been observed between the number of red kernels and fungal deoxyribonucleic acid (DNA) contents in severe infections (Góral et al., 2019).

The occurrence of *Fusarium* can be analyzed by nucleic acid-based or immunological methods. *Fusarium* contamination has been quantified in barley using enzyme linked immuno sorbent assay (ELISA) or latex agglutination technology based on detecting extracellular polysaccharides released in the substrate. This was known to be a sensitive and selective method for determining the *Fusarium* infection on either single kernels or larger

samples of barley at harvest and during malting (Vaag, 2023). However, ELISA is much slower than the latex agglutination method. Further, immunoassays can also be used to detect mycotoxin produced on barley and occurring in malt and beer (Ramakrishna et al., 1990).

7. *Fusarium* hydrophobins as predictors of beer gushing

Beer is one of the most popular and widely consumed alcoholic drinks worldwide. It contains essential nutrients like carbohydrates, amino acids, minerals, vitamins, and polyphenols (Bamforth, 2002). The main sensory characteristics that define beer quality and acceptance are flavor, aroma and color. Among them, color plays the most significant role as it creates the first impression, attraction and perception for the consumers. Traditional beer colors range from pale straw, yellow, golden, copper, and amber to brown and black. In craft beers, various brewing processes can influence the color, resulting in a wider range of hues (Ualema et al., 2024).

One notable issue affecting beer quality is gushing. Gushing is the spontaneous overflowing of beer from the package (usually a bottle) immediately upon opening (Virkajärvi et al., 2017). There are two types of beer gushing (Haikara et al., 2001). Primary gushing is mainly induced by fungal proteins, so-called gushing factors, which are present in malt or in other cereal raw materials of beer. Secondary gushing, also called non-malt-related gushing, may occur if beer contains haze, impurities from bottles, metal ions, calcium oxalate crystals, cleaning agent residues or oversaturation with CO_2. Although primary gushing has been reported to be mainly caused by *Fusarium* fungi, some other genera such as *Aspergillus*, *Nigrosora*, *Penicillium* and *Stemphylium* are also reported to induce gushing (Kleemola et al., 2001). Beer gushing can cause significant economic losses to the brewer. Gushing affects the beer quality and consequently causes financial problems for breweries. Providing constant beer quality is one of the biggest challenges for the brewing industry. In addition to causing massive economic losses to malting and brewing industries, beer gushing also makes consumers reconsider the brand they are buying, and drives them away from the product, giving the brewery a bad reputation.

While gushing-inducing factors produced by fungi have been studied for decades, none of them have been fully characterized. Reports suggest that these factors are polypeptides or peptide-containing substances. Studies indicated that low molecular mass ($\leq$ 20 kDa) fungal proteins called hydrophobins act as the factors promoting primary beer gushing (Sarlin et al., 2005; Wösten & Wessels, 1997).

7.1 What are hydrophobins?

Hydrophobins are highly surface-active, amphiphilic molecules produced by filamentous fungi (Wessels, 1996). Hydrophobins show very little sequence conservation in general, apart from the unique pattern of eight cysteines (Cys) residues implicated in the formation of four disulfide bridges (Cys1–Cys6, Cys2–Cys5, Cys3–Cys4, Cys7–Cys8). Hydrophobins are unique to the fungal kingdom. Fungal genome analyses have indicated that hydrophobins generally exist as small gene families with two to ten members, although certain species contain more members; for example, *Coprinus cinereus* possesses 33 putative hydrophobins (Littlejohn et al., 2012; Sunde et al., 2008). Based on hydropathy plots, solubility and the type of layer they form, hydrophobins are divided into two classes: class I and II (Wessels, 1997). Class I hydrophobins assemble into highly insoluble polymeric monolayers, often forming fibrillar structures known as rodlets within fungal cell walls. The rodlets are extremely stable, can only be solubilized with harsh acid treatments, and the soluble forms can polymerize back into rodlets under appropriate conditions. The monolayers formed by class II hydrophobins lack the fibrillar rodlet morphology and can be solubilized with organic solvents and detergents (Bayry et al., 2012).

The hydrophobins can self-assemble at water-air interfaces in response to the environment and aggregate to form amphipathic membranes. By self-assembling at the water-air interfaces, hydrophobins would allow fungi to escape the aqueous environment (Wösten & De Vocht, 2000). This property enables hydrophobins to play a role in a broad range of fungal growth and development (Wessels, 1997). Indeed, hydrophobins coat the surface of the otherwise hydrophilic cell wall polysaccharides of spores, hyphae, and fruiting structures and expose their hydrophobic layer to the outside, conferring water repellent properties to these fungal surfaces (Wessels, 1997; Wösten et al., 1994, 1999).

The genome of *F. graminearum* contains five different genes encoding for hydrophobins, named *Hyd1-5*. *Hyd1-4* are predicted to belong to Class 1 hydrophobins, while *Hyd5* seems to be the only gene coding for a Class II hydrophobin (Sarlin, 2012a). *Hyd2* is involved in fungal growth, and *Hyd3* is involved in attachment to hydrophobic surfaces (Quarantin et al., 2019). Both of these hydrophobins are involved in the hyphal ability to penetrate through the water-air interface and likely in adhesion of conidia to the surface of the plant spike, thus contributing to *F. graminearum* virulence (Quarantin et al., 2019). *Hyd5* does not affect colony and hypha morphology and is not involved in the penetration of hyphae through the water-air interface, but it does affect the hydrophobicity of aerial mycelia (Minenko et al.,

2014). The Class II hydrophobin HYD5 has been suggested as the causative agent for gushing in beer (Sarlin, 2012b).

7.2 Beer gushing and *Fusarium Hyd5*

In beers and other carbonated liquids, HYD5 can aggregate around hydrophobic CO_2 molecules. This aggregation leads to the formation of nanostructures that trap CO_2 within them. Upon the release of pressure when opening a bottle of beer, these nanostructures act like "nano bombs," rapidly releasing the trapped CO_2 in a sudden burst. This explosive release of gas results in a phenomenon known as gushing, where the beer foams uncontrollably and can overflow from the bottle. The presence and behavior of hydrophobins are thus critical factors in determining a beer's susceptibility to gushing, as they can significantly influence the stability and release of CO_2 within the liquid (Khalesi et al., 2015). Fungal hydrophobins can induce the gushing of beer even at low concentrations (Sarlin et al., 2005). The ability of hydrophobins to induce gushing varies, and this is assumed to be due to differences in their structures resulting from variations in their amino acid sequences. The overall low sequence conservation indicates that the Cys-residues are important for structural reasons while the other residues can vary significantly to give specific properties for the variants (Wessels, 2000). However, detailed physicochemical study of different hydrophobins has been hindered by the difficulties of producing and purifying hydrophobins in sufficient amounts (Khalesi et al., 2015). Thus, knowledge is limited on the variation in hydrophobins among *F. graminearum* isolates.

7.3 Hydrophobins and host-pathogen interactions

Hydrophobins are recognized as pathogenicity factors, although their precise role in fungal virulence is still not fully understood. In *Magnaporthe grisea*, the rice blast fungus, the hydrophobin Mpg1 is thought to act as a developmental sensor for appressorium formation, aiding in the interaction with hydrophobic leaf surfaces required for pathogenicity. Deleting the *MPG1* gene resulted in reduced virulence, while the deletion of another hydrophobin gene, *MHP1*, led to a loss of viability and diminished capacity to infect and colonize susceptible rice cultivars (Lau & Hamer, 1996; Talbot et al., 1996). Similarly, in *Beauveria bassiana*, the non-specific hydrophobic interaction between the fungal spore coat hydrophobin and the insect epicuticle is key in establishing fungal pathogenicity (Bayry et al., 2012). Further evidence comes from *Clonostachys rosea*, where deletion mutants lacking the class II hydrophobin *Hyd3* exhibited reduced colonization of *Arabidopsis thaliana* roots. Interestingly, double mutants lacking both *Hyd1* and *Hyd3* showed enhanced root

colonization compared to the wild type (Dubey MK et al., 2014). A similar pattern was observed in *Trichoderma virens*, where the class II hydrophobin *TvHydii* influenced root colonization of *Solanum lycopersicum*. Knockout or overexpression of *TvHydii* led to decreased or increased root colonization, respectively (Guzmán-Guzmán et al., 2017). In *F. graminearum*, deletion of *Hyd2* and *Hyd3*, as well as the triple mutant *Hyd2-3-4*, resulted in reduced virulence when using spray inoculation on wheat spikelets. This impairment in virulence was attributed to the fungus reduced ability to overcome the water-air interface and attach to the hydrophobic surfaces of the spike tissues (Quarantin et al., 2019).

7.4 Beer gushing prediction

The most effective way to prevent gushing is to use raw materials with no gushing potential. Currently, it is common practice in the brewing industry to determine the gushing potential of malt prior to its actual processing (Specker, 2014). A malt lot, which has been tested to have a potential to induce gushing, will either be rejected by a brewery or is blended with gushing negative malt in order to reduce the gushing potential. By blending, the concentration of gushing inducing material, i.e. hydrophobin proteins, is thought to reach a level below a critical limit. Sarlin et al., (2005) experimentally determined a minimum level of 250 ppm hydrophobin in malt, above which malt show a positive gushing potential. However, the critical level cannot be clearly defined in commercial malting contexts because of the different gushing inducing capabilities of different hydrophobin proteins.

Counting of *Fusarium* infected kernels or determining mycotoxin levels as a marker for *Fusarium* infection have been used as an indirect measure to determine the gushing inducing potential of malt lots (Schwarz, 2017). However, estimating the gushing potential by calculating fungal contamination of barley or malt proved insufficient. Also, determining mycotoxins produced by fungi, which was linked to the fungal biomass only to a limited extent, was used as predictive test for gushing occurrence. However, different levels of mycotoxins are produced by different fungal species, and the production of the compounds varies with factors such as environmental conditions, agricultural practise or cereal cultivar. Therefore, also mycotoxin content of grain proved not to be a reliable predictor for gushing (Schwarz et al., 1996).

There are a few gushing prediction methods developed for malt, wort, beer and other beverages. The substances causing gushing are rarely identified, but the potential of raw materials for gushing can be determined. *Fusarium* fungi are able to produce hydrophobins in

the field during the growing period of barley, and during the malting process, especially during the steeping and germination steps (Kulkarni et al., 2020). Hydrophobins survive through the brewing process, ending up in the final beer, where they can induce gushing when present in sufficiently high levels. The correlation between the hydrophobin level and the gushing potential in beer suggests that a hydrophobin analysis could be used for evaluating the risk of gushing in malt (Piacentini et al., 2021). The possibility of formation of new hydrophobins during the malting process complicates using hydrophobin ELISA to measure the gushing potential directly from fungal hydrophobins in barley. Detection of hydrophobin coding genes from *Fusarium* in barley could be used as a more accurate predictor, although numerous factors may influence the extent of *Fusarium* activity during malting. Determining the presence of gushing-inducing factors (i.e., genes and or proteins) improves the accuracy of gushing prediction. Therefore, analyzing malt for hydrophobins to detect and exclude problematic batches offers a practical approach to reducing beer gushing issues (Sarlin et al., 2005).

8. Genome editing in fungi

Genome editing technology is a flexible engineering tool for gene manipulation of microorganisms, including fungi. Gene editing in fungi has evolved through several technological advancements, each offering unique advantages and limitations. Early methods, such as restriction enzymes enabled targeted DNA cleavage but lacked precision due to short recognition sequences. More advanced tools, like zinc-finger nucleases and transcription activator-like effector nucleases, improved specificity by recognizing longer DNA sequences in the genome. While zinc-finger nucleases offered better precision, transcription activator-like effector nucleases further enhanced target recognition and were easier to design (Gaj et al., 2013). Additionally, RNA interference has been widely used for gene silencing, which allows researchers to selectively silence specific genes by introducing small RNA molecules (Leung and Whittaker, 2005). Despite these advancements, earlier methods often faced challenges such as off-target effects, design complexity, and limited efficiency, paving the way for more robust genome-editing technologies like CRISPR-Cas9.

8.1 CRISPR-Cas9 gene editing in *Fusarium graminearum*

CRISPR (clustered regularly interspaced short palindromic repeats)-Cas9 is an advanced tool for targeted genome editing, originally discovered in bacteria as a defence mechanism against viral infections (Ishino et al., 2018). This technology has become invaluable for studying *F.*

graminearum. By using CRISPR-Cas9, researchers can precisely target and modify specific genes within the *F. graminearum* genome, allowing for detailed investigation into the biological functions and mechanisms of pathogenicity. This approach is particularly effective for exploring genes involved in virulence, such as those responsible for the biosynthesis of DON. The ability to induce targeted mutations, deletions, or insertions through CRISPR-Cas9 not only deepens our understanding of fungal biology and host-pathogen interactions but also aids in developing new strategies for disease control and crop protection (Gosavi et al., 2020).

CRISPR-Cas9 is a flexible genome editing tool applicable to a broad range of organisms, including both prokaryotes and eukaryotes. It utilizes RNA (ribonucleic acid)-guided nucleases to make precise changes to the genome, allowing for systematic exploration of genetic elements and variations in various species. The Cas9 nuclease, key to this system, is directed by small RNAs that pair with target DNA, enabling accurate and efficient edits. This approach is ideal for high-throughput and multiplexed gene editing across diverse cell types and organisms (Khanzadi & Khan, 2020).

8.2 Precise genome editing using Cas9 nuclease

Cas9 enables genome editing by introducing double-strand breaks (DSBs) at specific locations in the genome (Rodgers & Mcvey, 2016). These breaks are repaired through one of two main pathways: non-homologous end joining (NHEJ) or homology-directed repair (HDR). NHEJ is an error-prone process that often results in insertions or deletions (indels), making it useful for gene knockouts. Indels in coding regions can lead to frameshift mutations and early stop codons, ultimately causing gene inactivation. Additionally, multiple DSBs can be used to remove larger sections of the genome (Rodgers & Mcvey, 2016).

In contrast, HDR is a more accurate but less common repair pathway that relies on an external repair template. This template can be double-stranded DNA with homology arms or single-stranded DNA oligonucleotides, allowing for precise edits like single-nucleotide changes. HDR, unlike NHEJ, typically occurs only in dividing cells, and its success depends on various factors such as the cell type, genomic location, and the type of repair template used (Yang et al., 2020).

8.3 Cas9 – an RNA-guided nuclease for genome editing

The CRISPR-Cas9 system, which originates from the microbial adaptive immune defense, utilizes RNA-guided nucleases to cleave foreign genetic material. There are three primary

types of CRISPR systems (I-III) found among different bacterial and archaeal species. Each system is defined by a unique set of CRISPR-associated (Cas) genes, noncoding RNAs, and a distinctive pattern of repeating sequences. These repeats are interspersed with short segments of external DNA, known as protospacers, which together form the CRISPR RNA (crRNA) array (Koonin & Makarova, 2019).

The type II CRISPR system, which is particularly well-studied, consists of the Cas9 nuclease, a crRNA array that encodes guide RNAs, and a trans-activating crRNA (tracrRNA) that helps process the crRNA into functional segments. Each crRNA segment carries a 20-nucleotide guide sequence that directs Cas9 to its DNA target through Watson-Crick base pairing. In the widely used CRISPR-Cas9 system derived from *Streptococcus pyogenes*, the target DNA must be located directly upstream of a 5'-NGG Protospacer Adjacent Motif (PAM). To simplify this system, crRNA and tracrRNA often merged into a single-guide RNA (sgRNA). By modifying the 20-nucleotide guide sequence within the sgRNA, Cas9 can be directed to nearly any target sequence adjacent to a PAM site, enabling highly accurate and versatile genome editing (Chylinski et al., 2014).

8.4 Limitations of the Cas9 system

There are some limitations to using Cas9 for gene editing. Cas9 is directed to specific regions of the genome by a 20-nucleotide sequence in the sgRNA. For effective targeting, a PAM sequence must be present right after the 20-base-pair target sequence. Different Cas9 variants have distinct PAM sequences; for example, SpCas9 requires a 5’-NGG PAM sequence. Another option is the Cas9 homolog Cpf1, which targets AT-rich PAM sites. Cpf1 recognizes a TTN PAM sequence, making it suitable for editing genomes with low GC content.

Relying on commercially sourced CRISPR components like Cas9 enzymes and synthesized guide RNAs can be costly. One way to cut these expenses is to produce purified Cas9 and gRNA components directly in the lab (Al Abdallah et al., 2017).

CHAPTER 2: Impacts of pathogen strain and barley cultivar on fusarium head blight in barley and during malting

This chapter has been published as a peer-reviewed journal article:

Jayathissa A, Tucker J, Badea A, Fernando WGD, Bakker M. 2024. Impacts of pathogen strain and barley cultivar on fusarium head blight in barley and during malting. **Plant Pathology** 73:1874-1885. DOI: 10.1111/ppa.13918.

Committee members:

Badea, Ana (Department of Plant Science, University of Manitoba)

Yin, Xiang (Department of Microbiology, University of Manitoba)

External examiner: Zhong, Shaobin (Department of Plant Pathology, North Dakota State University)

Contribution of authors:

Jayathissa, Anuradha U: Conducted the experiments, collected data, analyzed the results, and organized the manuscript's findings.

Bakker, Matthew G: Main supervisor. Provided guidance throughout the project, including project planning, experimental design, conducting experiments, data collection, analysis, and manuscript writing.

Fernando, W G Dilantha: Co-supervisor. Provided knowledge in plant research and guidance in writing the manuscript.

Badea, Ana and Tucker, J: Assisted with barley field trials and data collection at Agriculture and Agri-Food Canada, and provided guidance in manuscript preparation.

An extension of this work has also been published, as:

Bakker MG, Jayathissa AU, Fernando WGD, Badea A, Tucker JR. 2024. Microbiome dynamics during malting of barley grains infested by *Fusarium graminearum* strains. Plant Pathology. 73:1886-1900. DOI: 10.1111/ppa.13946

As I did not analyze the microbiome data reported in this second publication, it does not appear as part of this thesis. Nevertheless, the work that is described in this thesis was essential in providing the experimental samples that formed the basis of this paper.

ABSTRACT

Fusarium head blight (FHB) is a devastating disease in barley, causing significant losses for the malting and brewing industries. We hypothesized that the variation observed in *Fusarium*-related issues during malting may be partially attributable to differences among *Fusarium graminearum* strains. Field trials in 2019–2021 used barley cultivars with different FHB resistance: Newdale (intermediate) and AAC Goldman (moderately resistant). Barley plants were grown under disease-conducive conditions and plots were inoculated with conidial suspensions of each of seven different *F. graminearum* monoclonal isolates plus a non-inoculated control. Disease severity (as a percentage of symptomatic spikelets) differed significantly among years (2020 > 2019 > 2021). *Fusarium graminearum* density in barley varied significantly across years (2019 > 2021 > 2020). Pathogen strain identity and cultivar (Newdale > AAC Goldman) had significant effects on *F. graminearum* density in barley. The harvested barley was micromalted. The deoxynivalenol (DON) content in barley and malt significantly differed among years and cultivars, with the highest levels in 2019 and in Newdale. Pathogen strain identity significantly influenced DON content in barley and malt. *F. graminearum* density in malt showed significant variation among years (2021 > 2019 > 2020) and was influenced by the pathogen strain identity, while cultivar did not significantly affect *F. graminearum* density in malt. Gushing varied significantly across years but was not affected by cultivar or pathogen strain identity and was independent of *F. graminearum* density. My finding that *F. graminearum* strain identity altered impact in barley and malt may explain variability of FHB impacts.

1. INTRODUCTION

Fusarium head blight (FHB) is a significant disease in barley, primarily caused by *Fusarium graminearum*. The pathogen infects the barley heads, reducing the grain yield and quality. The FHB disease also leads to the contamination of grain with a dangerous mycotoxin, deoxynivalenol (DON), that impacts human and animal health (Bakker et al., 2018; Fernando et al., 2021). FHB development is favoured by warm humid weather following spike emergence and air temperatures of 16-30 °C, which promote spore germination (McMullen et al., 2012; Schöneberg et al., 2018). FHB symptoms include premature bleaching of one or more spikelets within the barley head. The affected seeds in blighted heads exhibit poor filling, appearing shrivelled, bleached, and brown in colour (Siou et al., 2014). It is important to note that barley may have DON contamination even in the absence of visible symptoms (Cowger et al., 2020).

For most end uses of cereal grains, the impacts of *F. graminearum* are primarily associated with fungal activity in the field. However, the malting industry faces unique challenges with FHB that are not experienced in other industries because the malting process creates conditions that favour new fungal growth (Beccari et al., 2017). Malting is the process of converting or modifying barley into malt, the main ingredient in brewing. It is a 5-7 day process that includes three main steps: steeping, germination, and kilning (Krstanović et al., 2021). The favourable conditions during malting, such as readily available nutrients, moderate temperatures, good aeration, high humidity and overall high grain moisture during germination support the growth of fungal mycelium and synthesis of secondary metabolites (Mastanjević et al., 2018, 2019).

Fusarium activity during malting has a negative impact on the quality of finished malt, including via accumulation of the mycotoxin DON and potentially contributing to beer gushing, affecting the overall quality and stability of the grain (Janssen et al., 2018). However, it remains difficult to predict when malt quality defects related to Fusarium will arise despite the knowledge of these effects. The unpredictable nature of *Fusarium*-related issues in malting may stem from various factors, including the variability among strains of *F. graminearum* and their differential impacts on malt quality (Mastanjević et al., 2018). Thus, it is crucial to understand the impact of the intraspecific diversity of *F. graminearum* strains on disease progression, including during the malting environment, to develop effective criteria for grading barley or predicting final quality from microbiological assessment at the early stages of malting (Liang et al., 2015). *Fusarium* species and strains within species possess a

range of traits related to the above-mentioned malt quality issues. Aggressiveness, DON production and hydrophobin production are some of the important fungal traits that affect grain quality. Within *F. graminearum*, we would expect all strains to be able to cause disease on barley and to be able to produce DON and hydrophobins. Still, the magnitude of these processes probably differs among strains.

Variations in aggressiveness exist among *F. graminearum* strains worldwide (Walkowiak et al., 2015), including different regions, countries, states (Xue et al., 2006) and even within individual fields (Malbrán et al., 2012). Fabre et al., (2019) found that the differences in *F. graminearum* aggressiveness were not due to the presence of unique, strain-specific molecules. Instead, they were based on the strain's ability to produce these molecules in sufficient quantities. The strain's genetic makeup largely determined variation in protein levels, with some influence from the host plant variety. *F. graminearum* and some related species can also produce DON, which makes the barley unsuitable for malting and brewing (Bertuzzi et al., 2018). DON is also identified as one of the indicators of the quality and safety of barley used for malting (Salas et al., 1999). Gilbert et al., (2002) revealed a high level of diversity in rates of DON production among *F. graminearum* isolates from Canada.

Fusarium species can also secrete hydrophobins, which are small (between 5 and 20 kDa) surface-active proteins. These proteins serve in fungal growth, acting as structural components and playing a role in how fungi interact with their environment. Hydrophobins have implications for beer quality, especially in relation to beer gushing. Beer gushing is the excessive and spontaneous over-foaming of beer when a container is first opened, where manufacturing defects, such as excessive carbonation, are not to blame (Shokribousjein et al., 2011). Hydrophobins have been identified as the main inducers of primary beer gushing (Sarlin et al., 2005). They are typically known for their role in fungal growth as structural components of the fungal cell wall, and for roles in the interaction of fungi with their environment (e.g., impacting adherence to hydrophobic surfaces or altering the surface tension of water) (Minenko et al., 2014; Quarantin et al., 2019). While all strains of *F. graminearum* produce hydrophobins, the specific characteristics (e.g., amino acid sequence), quantities, or timing of production of these hydrophobins could differ among strains, leading to variations in their impact on beer gushing (Linder et al., 2005; Sarlin et al., 2005).

We hypothesized that the variability in *Fusarium*-related issues during malting may reflect differences among *Fusarium* strains, because the identity of the *Fusarium* strains infecting

barley differs among locations and over time (Oghenekaro et al., 2021; van der Lee et al., 2015). There may be episodes of *Fusarium*-related issues during malting primarily when the most damaging strains of *F. graminearum* are present. From 2019 to 2021, we conducted an experiment where we produced barley of two different cultivars. Each cultivar was individually infected with several strains of *F. graminearum*. The harvested barley was then malted at a laboratory scale in order to study *F. graminearum* activity during malting, and how the impact of *F. graminearum* infection differs among strains of the pathogen.

2. MATERIALS AND METHODS

2.1 Inoculum preparation

The inoculum was prepared individually for each of seven different *F. graminearum* strains that had been collected from various regions of Manitoba. Five of the strains (HSW-15-73, HSW-15-19, HSW-15-95, HSW-15-40 and HSW-15-63) were obtained from the Henriquez Spring Wheat (HSW) collection of *Fusarium* isolates at Agriculture and Agri-Food Canada, Morden, Manitoba, and two of the strains (WRS1915 and WRS2065) were from Agriculture and Agri-Food Canada, Brandon, Manitoba. To ensure that this set of isolates included sufficient genetic diversity to result in measurable differences in the impact on malt quality, the strains were selected from different trichothecene chemotypes, geographic origins, and host plant species (Table 1).

Table 1 *Fusarium graminearum* strains used in this work.

Strain	Chemotype	Crop isolated from	Location of origin	Reference
HSW-15-19	3-ADON	Wheat	Notre Dame, Manitoba	Unpublished
HSW-15-40	15-ADON	Wheat	Killarney, Manitoba	Unpublished
HSW-15-63	15-ADON	Wheat	Tourond, Manitoba	Unpublished
HSW-15-73	3-ADON	Wheat	Arborg, Manitoba	Unpublished
HSW-15-95	15-ADON	Wheat	St. Joseph, Manitoba	Unpublished
WRS1915	15-ADON	Barley	Foxwarren, Manitoba	(Tucker et al., 2019)
WRS2065	3-ADON	Barley	Selkirk, Manitoba	(Tucker et al., 2019)

F. graminearum isolates were cultured on potato dextrose agar (PDA; Difco) for 3 days at 28 °C. Conidial suspensions were produced in mung bean broth, which was prepared by boiling 40 g of mung beans in distilled water for 20 min. The resulting broth was then passed through a coffee filter to remove any solid particles and made up to a final volume of 1 L. The broth was then autoclaved for 15 min at 121 °C. Each strain was inoculated to a 250 mL flask with 150 mL mung bean broth by transferring a mycelial disc from PDA. Flasks were incubated with shaking (150 rpm) at 28 °C. After 1 week, the conidial suspensions were harvested and filtered through sterile cheesecloth. The spore concentrations were determined by direct count using a haemocytometer and adjusted in sterile water to a standard concentration of 7×10^4 spores/mL.

2.2 Field experiment

Two cultivars of hulled two-row spring malting barley were selected for their differential patterns of resistance to FHB: Newdale is intermediate to FHB, while AAC Goldman is moderately resistant to FHB (Legge et al., 2008, 2018). A field experiment was conducted over three growing seasons (2019–2021) at the Agriculture and Agri-Food Canada, Brandon Research and Development Centre. Plots consisted of a 5 m double row, with rows spaced 0.3 m apart, and were assigned using a randomized split block design with three blocks. Each block contained eight plots (each of seven different *F. graminearum* strains, plus a non-inoculated control). Plots were randomized within each block, and a new randomization was performed each year. A guard row was planted around the perimeter of the experiment and between blocks. Inoculum was applied with a backpack sprayer, after 75 % of the plots had headed. Irrigation was used to promote successful pathogen establishment. Plots were sprayed again 2 days following the initial application. After plots were sprayed, irrigation using a sprinkler was supplied between 04:00-06:00 and 18:00-20:00 daily until onset of maturity.

Plots were rated for *Fusarium*-damaged kernels 24 days after inoculation. Each plot recorded the number of kernels per spike for two spikes, and the number of visually symptomatic kernels was recorded for ten randomly selected spikes. FHB severity was calculated within each plot as follows:

$$Severity = \left(\frac{Mean\ number\ of\ symptomatic\ kernels}{Mean\ number\ of\ kernels\ per\ spike}\right) X\ 100$$

To minimize cross-contamination between samples at harvest, the plot combine was blown out with compressed air prior to harvest, and the wind speed was turned up between plots. Harvested barley was dried under low heat (30 °C) for several days, passed through an SLN sample cleaner (Pfeuffer), and stored at ambient temperature in plastic tubs.

2.3 Micromalting

Barley infected with each *F. graminearum* strain was micromalted via a lab-based malting procedure. In a sterile crystallizing dish (90 × 50 mm), 40 g of barley was mixed with 80 mL of sterile Milli-Q water and incubated at room temperature for 16 h (1st steep). The first steep water was drained completely, and the grain was allowed to sit for an 8-h air rest (1st air rest) with the lid closed, and with a mixing of the grain halfway through the air rest period. The grain was submerged with 40 mL of sterile Milli-Q water for 5 min (2nd steep) and drained

completely. The dishes were left at room temperature for a 16-hour air rest (2nd air rest) with the lids closed.

The dishes were moved to a 14 °C incubator for the germination phase. After 8 h of incubation, the grain was submerged with sterile Milli-Q water for 5 min and drained completely, simulating a spray watering of the grain during germination. The germination phase continued for an additional 64 h, mixing and turning once daily. The grain was transferred to an aluminium pan for kilning and put into a drying oven (Binder BD-720) at 70 °C for 20 h. After kilning, the kernels were rubbed against a screen to break off and discard the rootlets. The cleaned kernels were collected as finished malt and were ground. The ground malt was passed through a no. 10, 2.00 mm sieve and subsampled for the measurements of DON content and *F. graminearum* density, and for testing of gushing propensity.

2.4 Measuring DON content in barley and malt

The DON content of barley and malt was determined using the Veratox for DON 5/5 kit (Neogen). This method uses a competitive direct ELISA of DON in cereal matrices. Ground barley or malt (5 g) was mixed with water (25 mL) for 3 min. The extract was centrifuged for 10 min at 4500 g, and the clear extract was filtered with a filter syringe to collect the sample filtrate and put it into a sample collection tube. The DON content in the samples were measured according to the manufacturer's guidelines.

2.5 Measuring *Fusarium graminearum* density in barley and malt

F. graminearum density was assessed by quantitative PCR (qPCR). According to the manufacturer's directions, total DNA was extracted from 0.1 g of pulverized tissue using the GeneJET Plant Genomic DNA Purification Mini Kit (Thermo Fisher Scientific). The purity and concentration of DNA samples were measured via spectrophotometry (NanoDrop One, Thermo Fisher Scientific). To avoid variable DNA extraction efficiency introducing biases into estimates of *F. graminearum* density, pathogen density was expressed as a ratio of *F. graminearum* gene copies to barley gene copies within each extract. For this purpose, the abundance of the barley actin gene was measured using primers Hv.Actin forward (5′-GTCTCCAGCTCCTGTTCATAAT-3′), Hv.Actin reverse (5′-GAGAGGTTACTCCTTCACAACC3′) and Hv.Actin.probe (5′-TCCCTTACAATTTCCCGCTCAGCT-3′; 5′ FAM, internal ZEN, 3′ IowaBlack). For the amplification of *F. graminearum* DNA, the rDNA internal transcribed spacer (ITS) region

was amplified using primers ITS2.Fusarium forward (5′ AGCGTCATTTCAACCCTCAA-3′), ITS2.Sambuc reverse (5′-TACTACGCTATGGAAGCTCGAC-3′) and ITS2.gram.probe (5′-AGCTG[+C][+A]GTCCTGCTGCACTC-3′; 5′ FAM, 3′ IowaBlack; [+N] indicates a locked nucleic acid). All the primers and probes were designed in this work.

Each 20 µL PCR reaction mixture consisted of PrimeTime Master mixture (Integrated DNA Technologies), forward and reverse primers each at 0.5 µM, 1 ng/µL template DNA, probe at 0.23 µM and molecular biology-grade water. Thermocycling consisted of polymerase activation at 95 °C for 3 min; 40 cycles of denaturation at 95 °C for 15 s and annealing/extension at 60 °C for 1 min, using a QuantStudio 7 Pro Real-Time PCR System (Thermo Fisher Scientific). The initial abundance of the template DNA is defined by the formula $N_0 = (N_T/2^{Cq})$, where N_0 is the initial abundance of the target gene in the DNA extract, N_T is the threshold amplicon abundance and C_q is the cycle number at which the fluorescence signal crosses the fluorescence intensity threshold. Thus, the ratio of interest was calculated as

$$Fusarium\ density = \left(\frac{N_{0\_Fusarium}}{N_{0\_Barley}}\right) = 2^{(C_{q\_Barley} - C_{q\_Fusarium})}$$

2.6 Beer gushing

A modified Carlsberg method (Mastanjević et al., 2017) was used to assess the gushing potential of each experimental malt sample (Figure 1). The Canadian Malting Barley Technical Centre, Winnipeg, MB, provided the beer for this assessment, which was all from a single brewing batch.

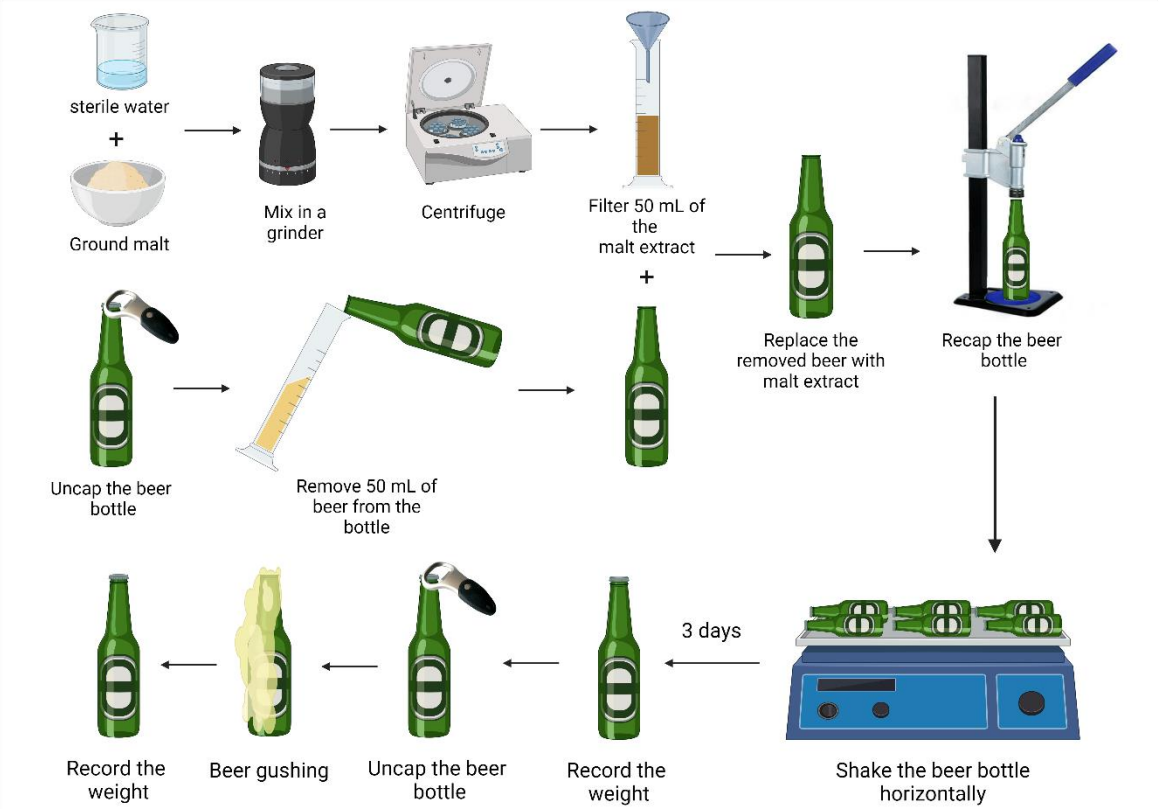

Figure 1: Modified Carlsberg method for assessment of the gushing propensity of malt.

Beer bottles were taken out of the fridge and equilibrated to room temperature. In a Waring blender (200 mL), 20 g of whole malt was mixed with 80 mL of distilled water for 30 s. The malt extract was centrifuged for 10 min at 4500 g at 25 °C and then the supernatant was filtered through a fluted filter paper (12.5 cm; VWR Grade 413). For each sample, a beer bottle was uncapped, and 50 mL of beer was removed into a 250 mL graduated cylinder containing 30 mL of water (to facilitate measurement by reducing the beer foaming). An equal volume (50 mL) of filtered malt extract was used to replace the beer that had been removed. Using a bench bottle capper, the beer bottle was recapped with a new bottle cap. The bottle was shaken horizontally with a movement parallel to the longitudinal direction of the bottle (100 oscillations per minute; E6013 shaker, Eberbach Corporation) for 3 days at room temperature, using a foam insert on the shaker table to hold the bottles in position. After shaking, the bottle was stored for 1 h standing upright at room temperature. The weight of the beer bottle was recorded. The bottle was placed in a laboratory tray, the bottle inverted three times, and the cap removed using a bottle opener. The outside of the bottle was dried off with a paper towel and the final weight of the bottle + cap was recorded. The extent of beer gushing was measured by calculating the weight loss in grams.

2.7 Statistical analysis

The statistical analyses were carried out using R v. 4.1.2 (R Core Team, 2021). We constructed multivariable linear models to explore the relationships between experimental factors and various measures of *Fusarium* damage including FHB severity in barley, *F. graminearum* density in barley and malt, DON content in barley and in malt, and beer gushing. Models are summarized in Table 2. The Tukey honestly significant difference method was used for post hoc contrasts to determine significant differences between years, barley cultivars or pathogen strains. The significance level for all statistical tests was set at $p < 0.05$. We calculated Pearson correlations between different variables related to FHB. To visualize the correlation matrix and to create graphics we used the packages 'ggcorrplot' (Kassambara & Kassambara, 2019) and 'ggplot2' (Wickham, 2011).

3. RESULTS

3.1 FHB severity

Despite the somewhat controlled conditions (i.e., provision of inoculum and irrigation), disease severity differed significantly among years (2020 > 2019 > 2021; analysis of variance (ANOVA) with Tukey contrasts, $p < 0.05$). I attribute this to prevailing weather conditions, such as 2021 being a drought year with above average temperatures and low precipitation.

In keeping with previously established ratings for the two barley cultivars, FHB severity was significantly greater in Newdale than in AAC Goldman ($p = 8.6 \times 10^{-15}$). There was a significant Year × Cultivar interaction (Table 2); specifically, in 2019, FHB severity was approximately three times greater in Newdale than in AAC Goldman (9.1 vs. 3.1), while in 2020 and 2021, severity differed less between the two cultivars (37.8 vs. 21.4 and 3.6 vs. 1.4, respectively).

Pathogen strain identity was a significant predictor of FHB severity, but in post hoc contrasts, none of the strains were found to produce significantly different FHB severities from each other. Among years, the relative impact of different pathogen strains was also variable; for example, in cultivar Newdale, the numerically highest FHB severities in 2019 and 2020 were caused by *F. graminearum* HSW-15-63; however, in 2021, HSW-15-63 produced the lowest FHB severity on Newdale among all seven *F. graminearum* strains that were tested (Figure 2).

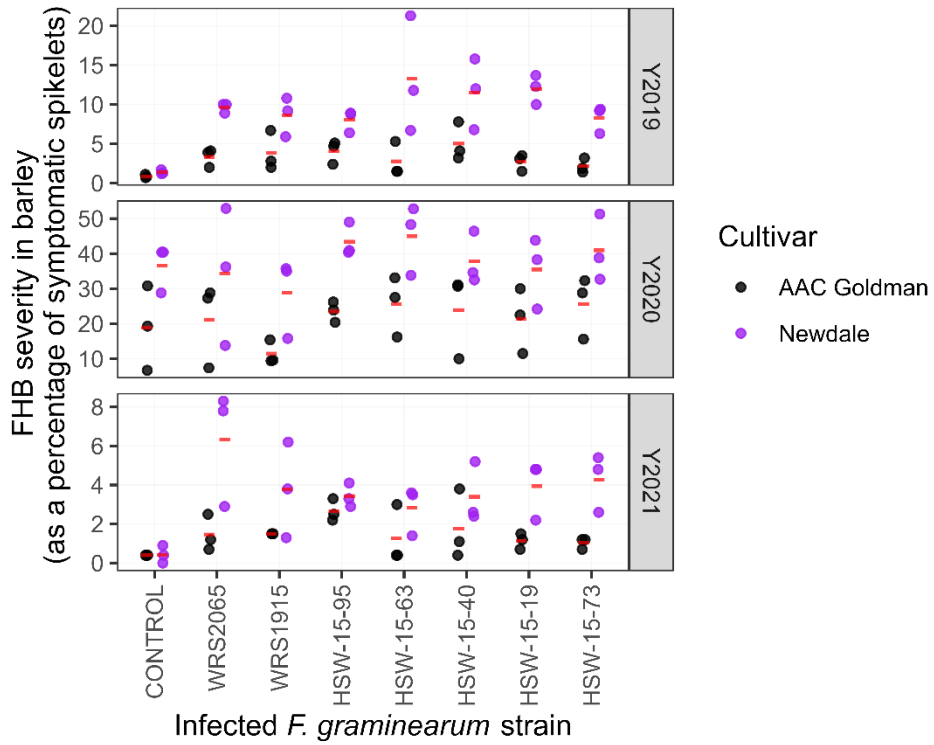

Figure 2: The severity of fusarium head blight in barley [(mean number of symptomatic kernels/mean number of kernels per spike) X 100] for plots that were inoculated individually with each of seven different *F. graminearum* strains, plus a non-inoculated control. Two barley cultivars (denoted by colour) were tested across three growing seasons. Short red horizontal lines indicate means for each barley cultivar per *F. graminearum* strain. No significant differences were found among the strains.

3.2 *Fusarium graminearum* density in barley

There were significant differences in *F. graminearum* density observed across years, with the highest density recorded in 2019, followed by 2021 and 2020 (ANOVA with Tukey contrasts; $p < 0.05$). The barley cultivar used had a significant effect on the *F. graminearum* density in barley, with Newdale supporting higher levels than AAC Goldman (T-test; $p = 3.5 \times 10^{-3}$), which is consistent with their respective FHB resistance ratings. Again, the Year × Cultivar interaction was significant (Table 2). In each of these years (2019, 2020, 2021), Newdale consistently supported approximately two times higher *Fusarium* levels compared to AAC Goldman. Specifically, in 2019, Newdale had a *F. graminearum* density (unitless ratio) of 74.3 while AAC Goldman had 36.5. In 2020, Newdale had 9.7, and AAC Goldman had 4.4. Similarly, in 2021, Newdale exhibited a *F. graminearum* density of 22.1, while AAC Goldman had 13.1.

There were significant differences among pathogen strains in the fungal density that was attained in barley. The *F. graminearum* densities in barley infected with HSW-15-19, HSW-15-40, HSW-15-63 and HSW-15-95 were significantly higher than in the non-inoculated

control. Barley infected with HSW-15-40 exhibited significantly greater density of *F. graminearum* compared to barley infected with WRS1915 (Figure 3).

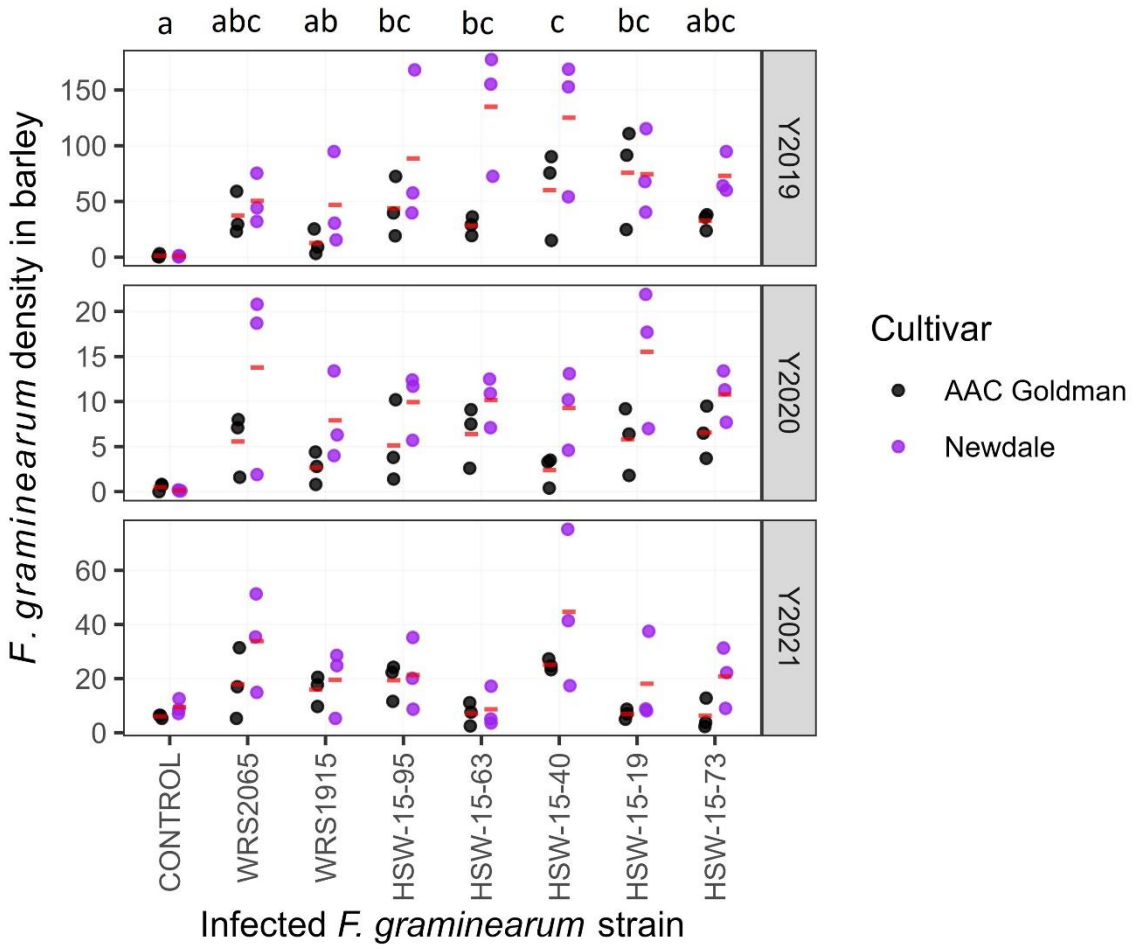

Figure 3: *Fusarium graminearum* density in barley (i.e., copies of *F. graminearum* ITS2 per copy of the barley gene for actin, in DNA extracts from pulverized whole kernels) that had been inoculated individually with each of seven different *F. graminearum* strains, plus a non-inoculated control. Two barley cultivars (denoted by colour) were tested across three growing seasons. Short red horizontal lines indicate means for each barley cultivar per *F. graminearum* strain. Above the panels, treatments that do not share a lowercase letter differ significantly from each other (see Table 2 for details of statistical testing).

There was an apparent divergence between visual assessment of FHB severity in 2020 compared to the measured *F. graminearum* density in grain harvested at the end of that growing season (Figure 4).

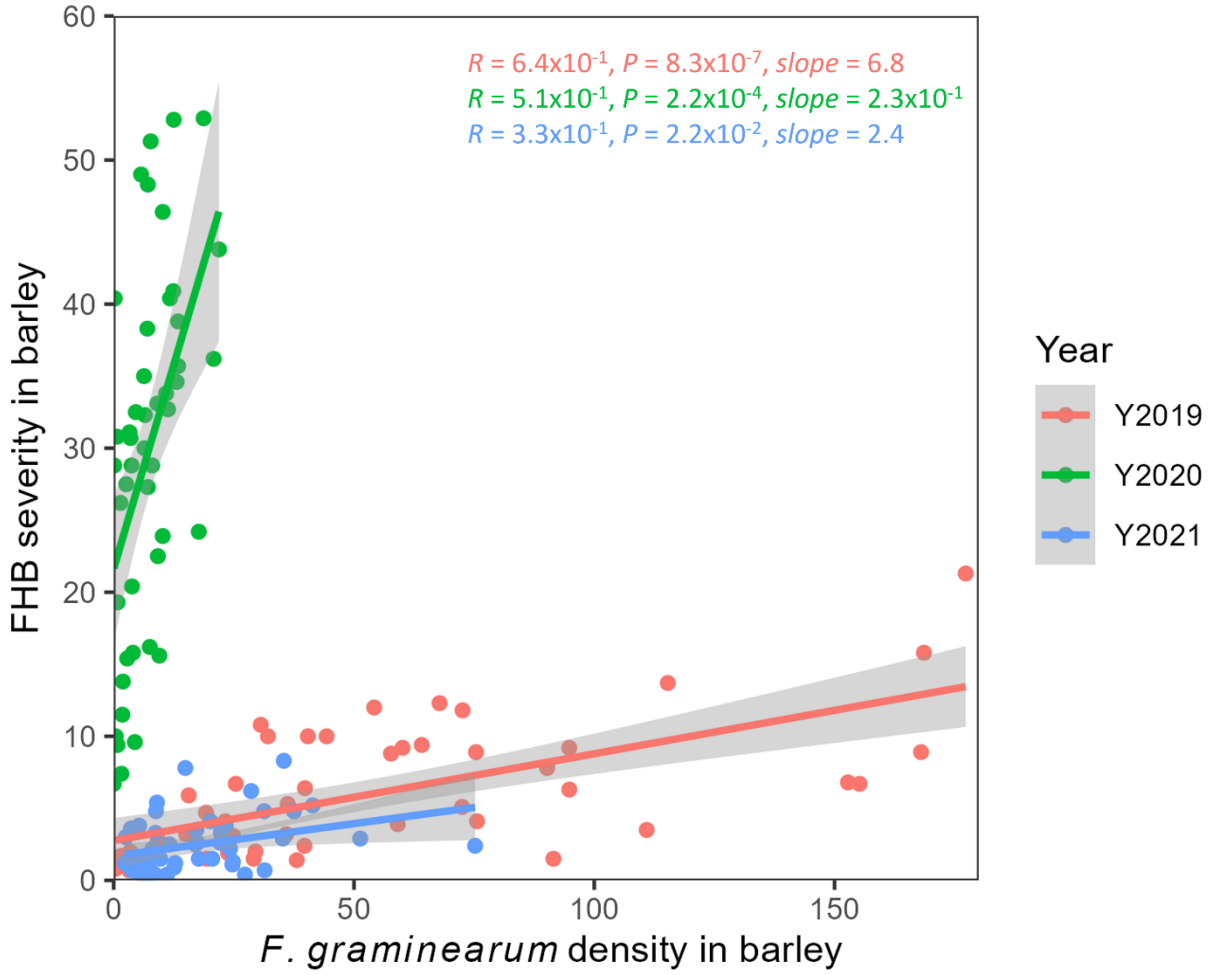

Figure 4: Relationships between *Fusarium* density (i.e., copies of *F. graminearum* ITS2 per copy of the barley gene for actin, in DNA extracts from pulverized whole kernels) in barley and fusarium head blight severity [(average number of symptomatic kernels/average number of kernels per spike) X 100] in barley that had been inoculated with each of seven different *F. graminearum* strains, plus a non-inoculated control across 2019-2021 growing seasons. Shaded areas represent 95% confidence interval for the fitted line. Different colours represent different years.

3.3 DON in barley

The mean DON content in barley was highest in 2019 (8.29 ppm), followed by 2021 (1.74 ppm), and lowest in 2020 (1.70 ppm). The differences in DON content between 2019 versus. 2020 and 2019 versus 2021 were statistically significant (ANOVA with Tukey contrasts; $p < 0.05$), but the difference in DON content between 2021 and 2020 was not statistically significant (ANOVA with Tukey contrasts; $p = 0.997$). The barley cultivars showed significant variation in DON content, with Newdale having higher levels than AAC Goldman ($p = 1.3 \times 10^{-11}$); this was again consistent with the FHB resistance ratings of these cultivars. There was a significant Year × Cultivar interaction term (Table 2); in 2019, DON content was substantially greater in Newdale than in AAC Goldman (11.6 vs. 5.0 ppm). However, in 2020

and 2021, the difference in DON content between the two cultivars was less pronounced, with values of 2.3 versus 1.1 ppm and 2.3 versus 1.2 ppm, respectively.

The DON content was found to be significantly influenced by the strain of *F. graminearum* used for inoculation. Barley infected with HSW-15-19, HSW-15-40, HSW-15-73 or HSW-15-95 showed higher DON contents compared to the non-inoculated control treatment (ANOVA with Tukey contrasts; $p \leq 0.05$). The observed order of DON content in barley from highest to lowest was as follows: HSW-15-19, HSW-15-40, HSW-15-73, HSW-15-95, HSW-15-63, WRS2065, WRS1915, non-inoculated control (Figure 5).

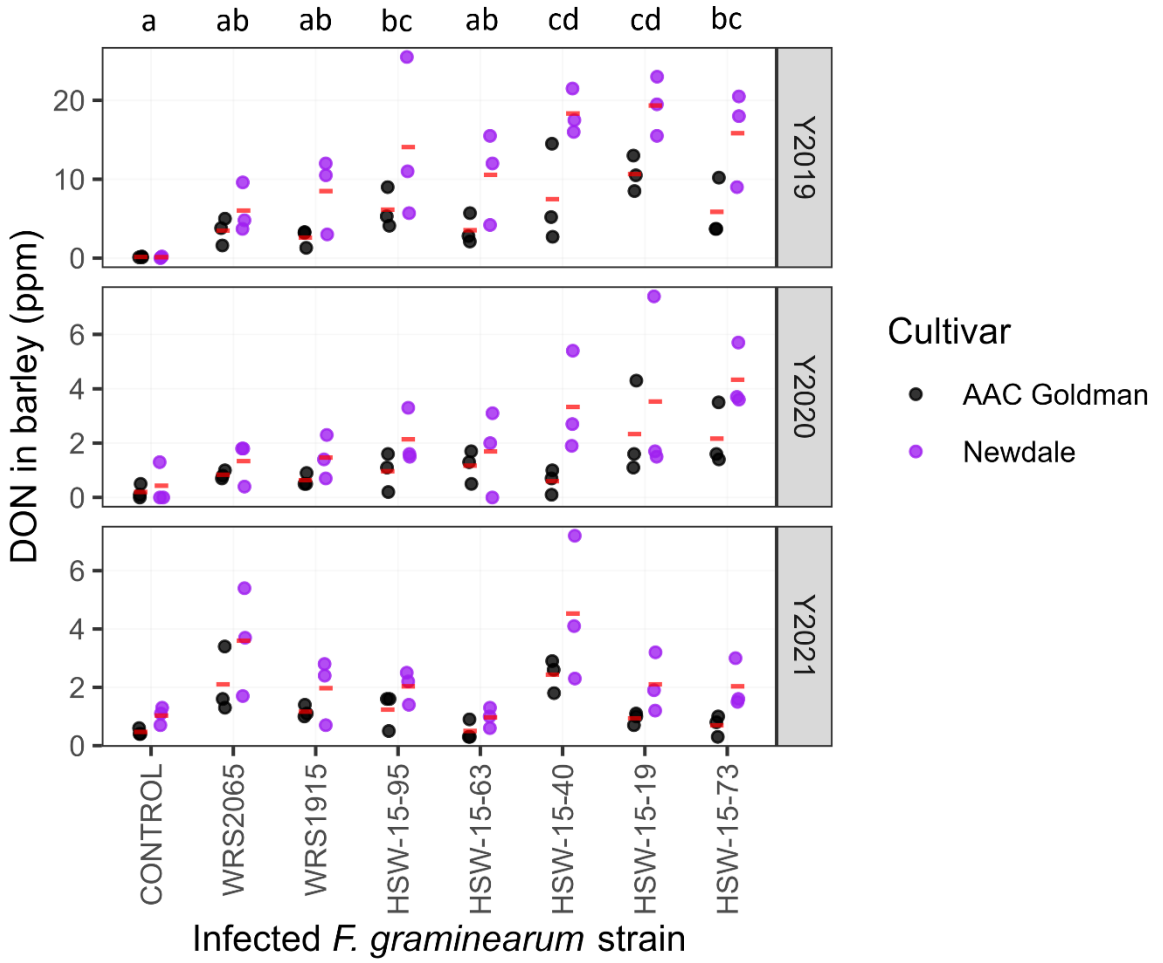

Figure 5: Deoxynivalenol (DON) content in barley (i.e., concentration in parts per million in pulverized whole grain measured by ELISA) that had been inoculated individually with each of seven different *Fusarium graminearum* strains, plus a non-inoculated control. Two barley cultivars (denoted by colour) were tested across three growing seasons. Short red horizontal lines indicate means for each barley cultivar per *F. graminearum* strain. Above the panels, treatments that do not share a lowercase letter differ significantly from each other (see Table 2 for details of statistical testing).

Even though the visual assessment of disease severity was comparatively higher in 2020, there was no corresponding increase in DON content in 2020 barley. However, there was still a significant relationship between DON content and FHB severity in 2020 (Figure 6; R = 0.41 to 0.61 among years).

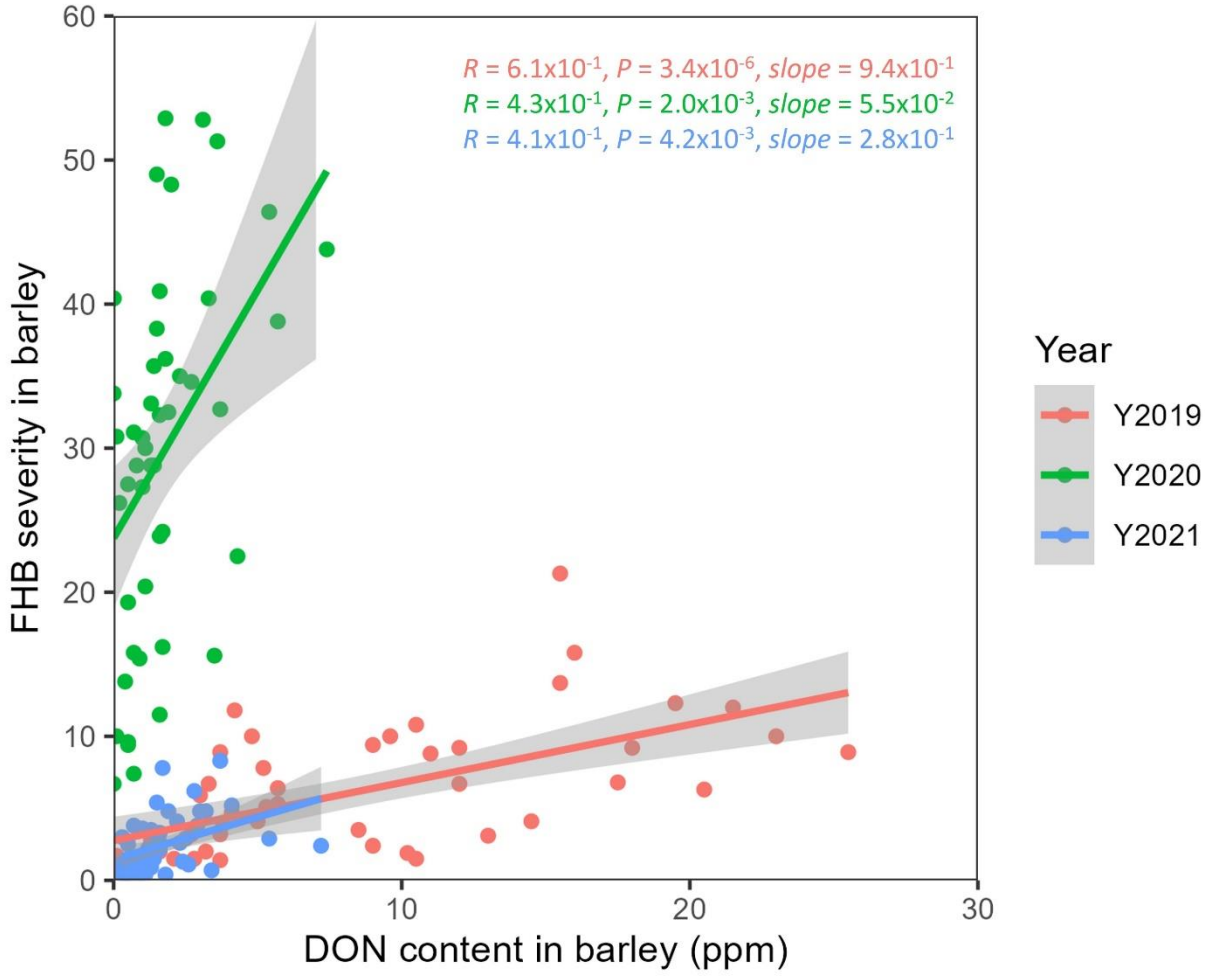

Figure 6: Relationship between DON content in barley and fusarium head blight severity in barley that had been inoculated with each of seven different *F. graminearum* strains, plus a non-inoculated control across 2019-2021 growing seasons. Shaded areas represent 95% confidence interval for the fitted line. Different colours represent different years.

In a model that included year, barley cultivar and pathogen strain identity, the *F. graminearum* density in barley was also a significant predictor of DON content in barley (Table 2). In all three years, DON content was significantly and positively correlated with *F. graminearum* density in barley (Figure 7; R = 0.66 to 0.94 among years).

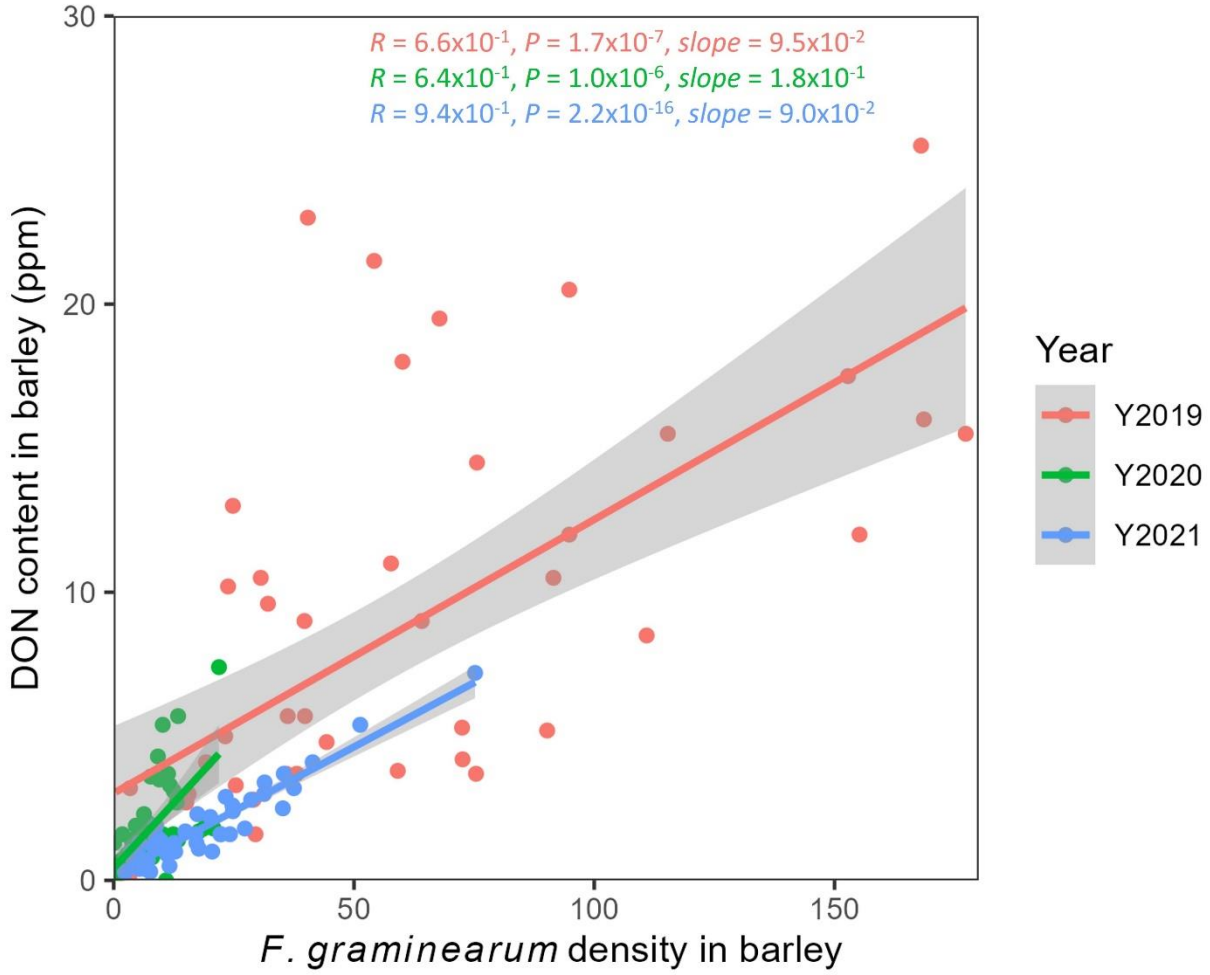

Figure 7: Relationship between *F. graminearum* density in barley and deoxynivalenol (DON) content in barley that had been inoculated with each of seven different *F. graminearum* strains, plus a non-inoculated control across 2019-2021 growing seasons. *F. graminearum* density is strongly positively correlated with DON content in barley. Shaded area represents 95% confidence interval for the fitted line. Different colours represent different years.

3.4 *Fusarium graminearum* density in malt

After additional opportunity for growth and activity during the malting process, there were significant differences in *F. graminearum* density in malt among years, with significantly lower densities in 2020 compared to 2019 and 2021 (ANOVA with Tukey contrasts; $p < 0.05$). Unlike other Fusarium-related variables, the barley cultivar did not significantly affect *F. graminearum* density in malt (Table 2).

Furthermore, the density of *F. graminearum* in malt also exhibited significant variation depending on the specific strain of *F. graminearum* that had infected the barley, although the density *of F. graminearum* in malt was significantly higher than the control for only one pathogen strain, HSW-15-40 (Figure 8).

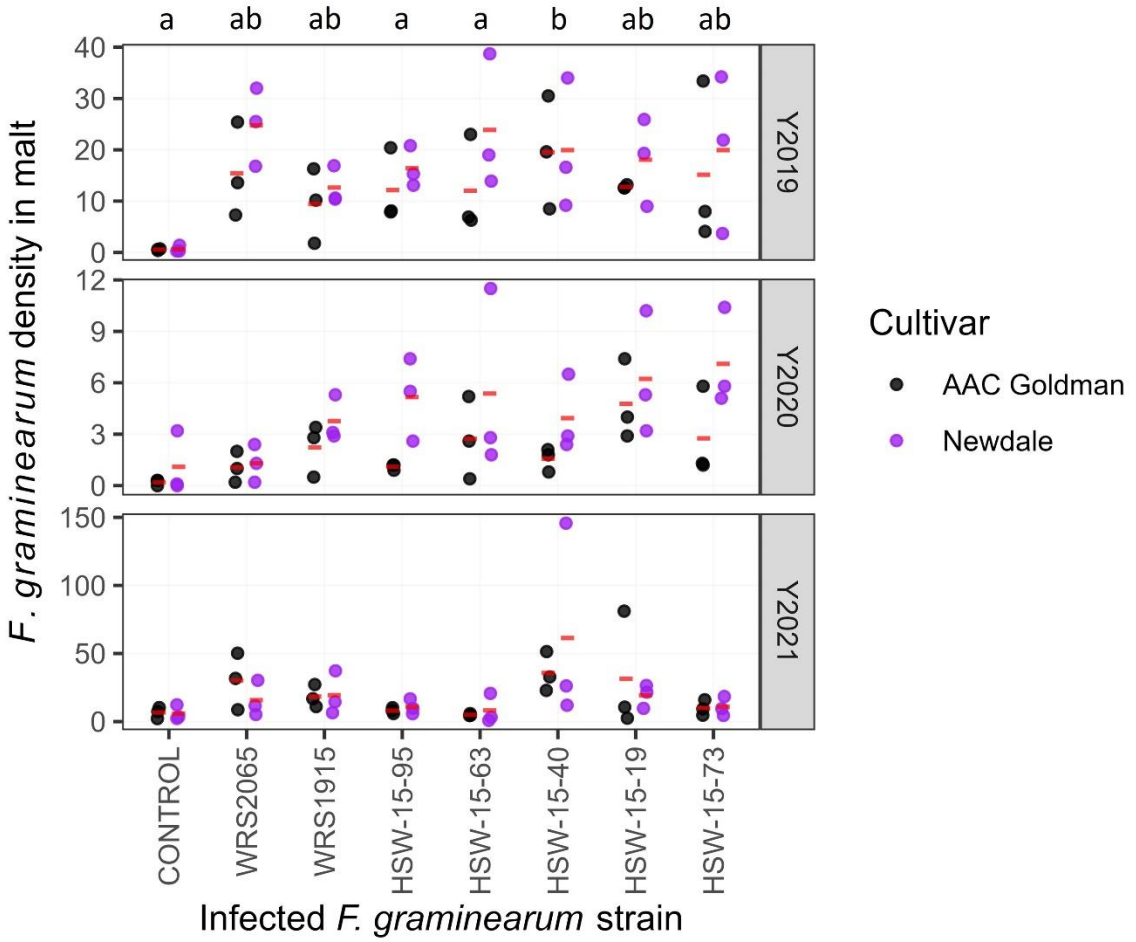

Figure 8: *Fusarium graminearum* density in malt (i.e., copies of *F. graminearum* ITS2 per copy of the barley gene for actin, in DNA extracts from pulverized whole malted kernels) produced from barley that had been inoculated individually with each of seven different *F. graminearum* strains, plus a non-inoculated control. Two barley cultivars (denoted by colour) were tested across three growing seasons. Short red horizontal lines indicate means for each barley cultivar per *F. graminearum* strain. Above the panels, treatments that do not share a lowercase letter differ significantly from each other (see Table 2 for details of statistical testing).

3.5 DON in malt

Significantly higher concentrations of DON in malt were observed in 2019 than in 2020 or 2021 (ANOVA with Tukey contrasts; $p < 0.05$), mirroring what was found for DON concentration in barley. The DON content in malt was also significantly different among barley cultivars, with malted Newdale having higher levels than malted AAC Goldman ($p = 5.1 \times 10^{-7}$). There was a significant Year × Cultivar interaction (Table 2); in 2019, DON content was approximately three times greater in Newdale than in AAC Goldman (3.8 vs. 1.4 ppm). In 2020 Newdale exhibited DON content about two times higher than in AAC Goldman (1.4 vs. 0.7 ppm). However, in 2021, the difference in DON content between the two cultivars was less pronounced, with values of 1.4 versus 0.9 ppm, respectively.

Moreover, the level of DON in malt varied significantly depending on the specific strain of *F. graminearum* that infected the barley, with several pathogen strains producing concentrations of DON in the malt that were significantly greater than in the non-inoculated control (Figure 9). The DON content in malt infected with HSW-15-19 (3-ADON), HSW-15-40 (15-ADON) or HSW-15-73 (3-ADON) was significantly higher compared to the control, with the order of DON content in malt, ranked from highest to lowest, being HSW-15-19, HSW-15-40 and HSW-15-73. In a model that included year, barley cultivar and *F. graminearum* density in barley, pathogen strain identity was also a significant predictor of DON content in malt (Table 2).

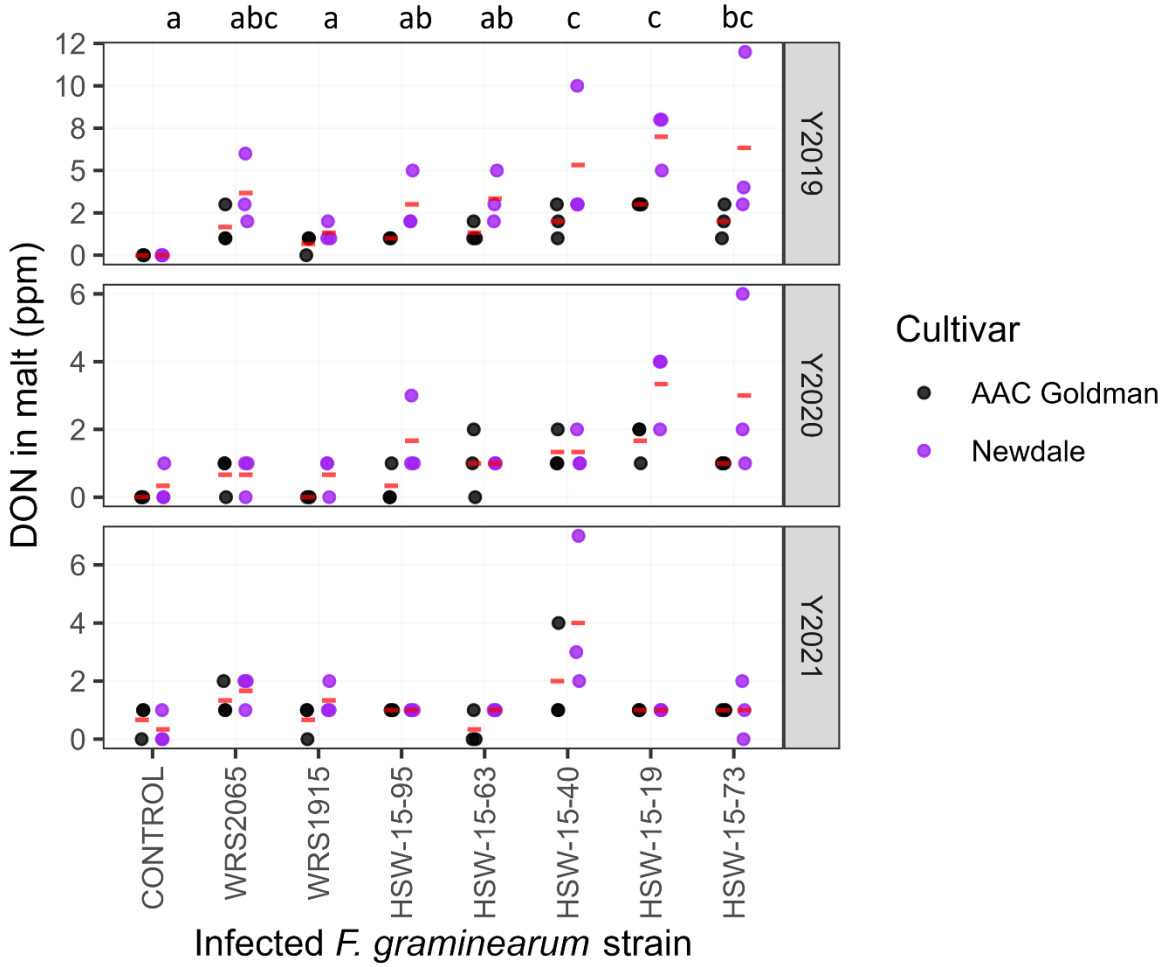

Figure 9: Deoxynivalenol (DON) content in malt (i.e., concentration in parts per million in pulverized malt, measured by ELISA) produced from barley that had been inoculated individually with each of seven different *Fusarium graminearum* strains, plus a non-inoculated control. Two barley cultivars (denoted by colour) were tested across three growing seasons. Short red horizontal lines indicate means for each barley cultivar per *F. graminearum* strain. Above the panels, treatments that do not share a lowercase letter differ significantly from each other (see Table 2 for details of statistical testing).

3.6 *Fusarium graminearum* density in malt versus DON in malt

F. graminearum density in malt was significantly correlated with the DON content in malt across all three years (Figure 10). A strong correlation was found in 2019 (R = 0.62), while the correlation was weaker in 2020 and 2021 (R = 0.45 and 0.44, respectively). This shows that there is a correlation between the levels of *Fusarium* and DON content in malt, although it may vary in strength between different years. In 2021, I observed a notably flat slope for this relationship compared to 2019 and 2020.

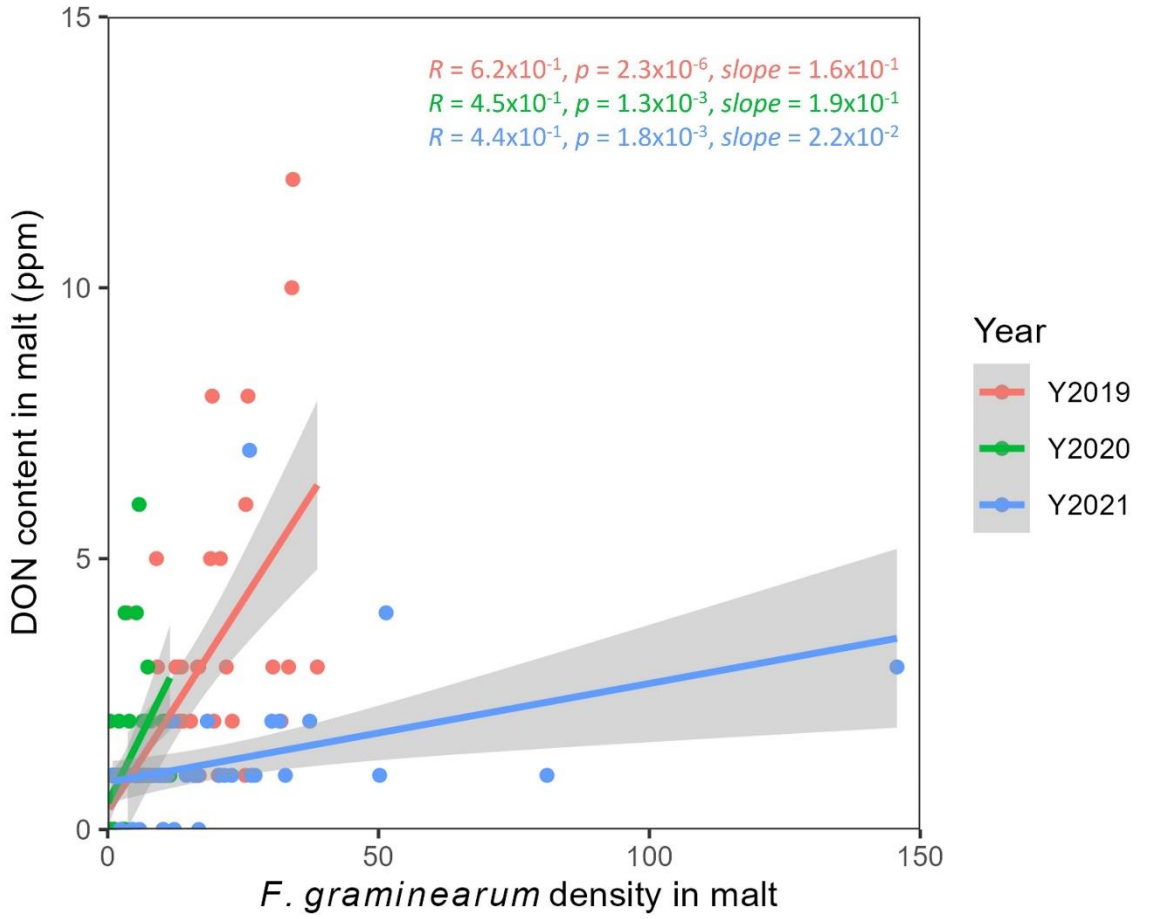

Figure 10: Relationships between *Fusarium graminearum* density and deoxynivalenol (DON) content in malt produced from barley that had been inoculated individually with each of seven different *F. graminearum* strains, plus a non-inoculated control. Shaded area represents 95% confidence interval for the fitted line. Different colours represent different years.

3.7 Beer gushing

Gushing was significantly different across years (2020 > 2019 > 2021; ANOVA with Tukey contrasts; $p < 0.05$). However, no significant differences were observed in gushing between the barley cultivars or among pathogen strains (Table 2). Inoculated barley did not produce malt with greater gushing activity than my non-inoculated barley (Figure 11).

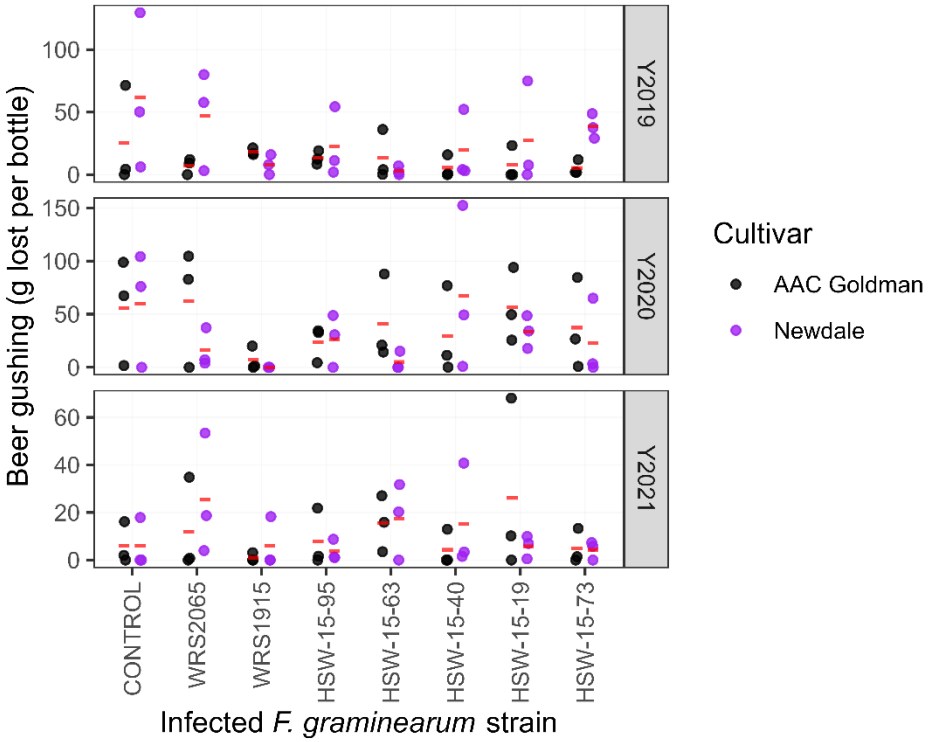

Figure 11: Beer gushing potential of malt (i.e., grams lost per bottle because of over foaming) produced from barley that had been inoculated individually with each of seven different *F. graminearum* strains, plus a non-inoculated control. Two barley cultivars (denoted by colour) were tested across three growing seasons. Short red horizontal lines indicate means for each barley cultivar per *F. graminearum* strain.

Table 2 Summary of analysis of variance results (*p* values) exploring the relationships between experimental variables (row headings) and various measures of *Fusarium* damage (column headings). Rows within each column indicate factors included within the same statistical model.

	FHB severity	***F. graminearum* density in barley**	**DON content in barley**	***F. graminearum* density in malt**	**DON content in malt**	**Gushing propensity of malt**
Year	$<2.0 \times 10^{-16}$***	$<2.0 \times 10^{-16}$***	$<2.0 \times 10^{-16}$***	3.2×10^{-7}***	1.4×10^{-8}***	2.9×10^{-4}***
Barley cultivar	8.6×10^{-15}***	3.5×10^{-3}**	1.3×10^{-11}***	2.4×10^{-1}	5.1×10^{-7}***	6.2×10^{-1}
Pathogen strain	2.4×10^{-2}*	4.5×10^{-5}***	1.8×10^{-12}***	1.1×10^{-3}**	4.1×10^{-9}***	8.8×10^{-2}
Year × Cultivar	1.2×10^{-8}***	1.2×10^{-3}**	9.2×10^{-4}***	7.5×10^{-1}	1.8×10^{-2}*	6.6×10^{-2}
Year × Strain	7.2×10^{-2}	4.0×10^{-4}***	5.3×10^{-5}***	1.2×10^{-2}*	4.1×10^{-2}*	6.7×10^{-1}
F. graminearum density in barley	5.6×10^{-2}	N/A	$<2.0 \times 10^{-16}$***	2.8×10^{-4}***	2.0×10^{-3}**	9.0×10^{-1}
F. graminearum density in malt	N/A	N/A	N/A	N/A	5.5×10^{-4}***	6.5×10^{-2}

Note. These damage measures encompass Fusarium head blight (FHB) severity (evaluated visually), *F. graminearum* density (measured via quantitative PCR), deoxynivalenol (DON) content (measured via ELISA), and gushing potential (measured via Carlsberg test). Linear models for explaining measured values of each dependent variable (i.e., each column) included all terms for which a *p* value is listed; rows with 'N/A' represent variables that were not included in the model for that dependent variable.
***$p \leq 0.001$, **$p \leq 0.01$, *$p \leq 0.05$

3.8 *Fusarium graminearum* density in malt versus gushing

The statistical relationship between the *F. graminearum* density in malt and the extent of beer gushing was negative in sign, but not statistically significant (Figure 12).

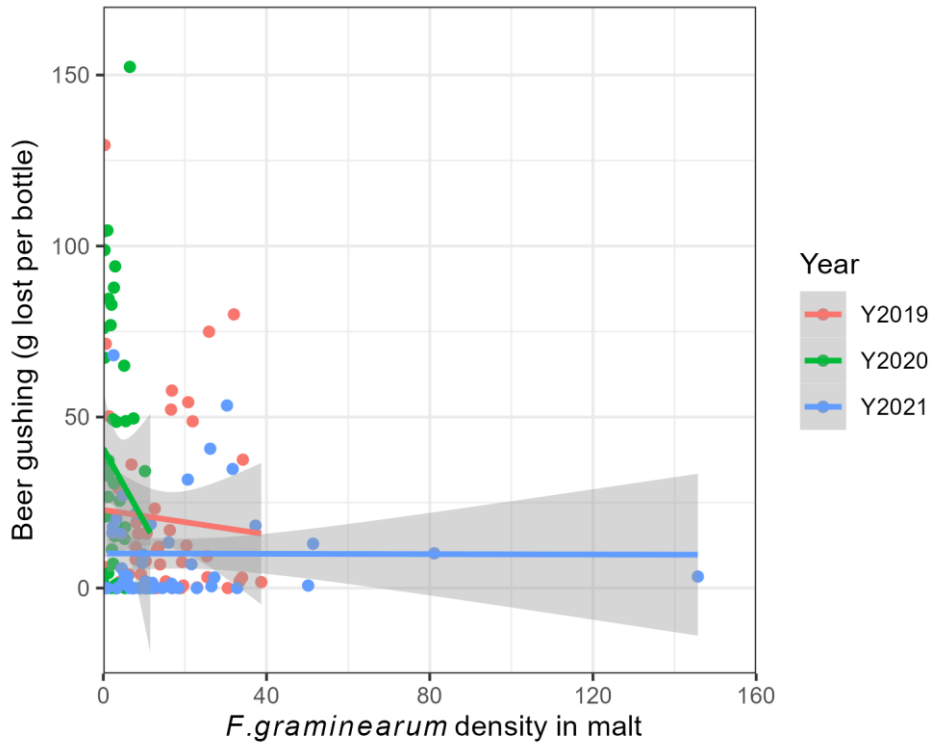

Figure 12: *F. graminearum* density in malt was not significantly correlated with gushing. Shaded areas represent 95 % confidence interval for the fitted line. Different colours represent different years.

3.9 Effect of DON chemotype on fungal traits

The set of pathogen strains that was used here included both 15-ADON and 3-ADON chemotypes. Across pathogen strains, chemotype did not play a significant role in determining the disease severity, *F. graminearum* density in barley, DON content in barley or *F. graminearum* density in malt. However, chemotype was a significant factor when analysing the DON content in malt (ANOVA with Tukey contrasts; $p = 0.0027$, with 15-ADON strains producing lower DON content in malt than 3-ADON strains; mean of 1.5 and 2.2 ppm, respectively). Malt infected with 15-ADON strains also had a lower propensity for gushing compared to malt infected with 3-ADON strains (ANOVA with Tukey contrasts; $p = 0.041$ mean gushing values of 15.6 for 15-ADON strains and 24.5 for 3-ADON strains).

Both *F. graminearum* density in barley and DON content in malt were strongly correlated with DON content in barley. A moderately high-positive correlation was found between F. graminearum density in barley and DON content in malt. Medium correlation was found in *F.*

graminearum density barley vs. *F. graminearum* density malt, *F. graminearum* density malt vs. DON content in malt, FHB severity in barley vs. beer gushing. DON content in barley demonstrated a low correlation with *F. graminearum* density in malt. There was a negative correlation between FHB severity in barley and *F. graminearum* density in malt. Beer gushing was not associated with any of the *F. graminearum* related issues except FHB severity in barley. In contrast, FHB severity was only associated with *F. graminearum* density in malt and beer gushing (Figure 13).

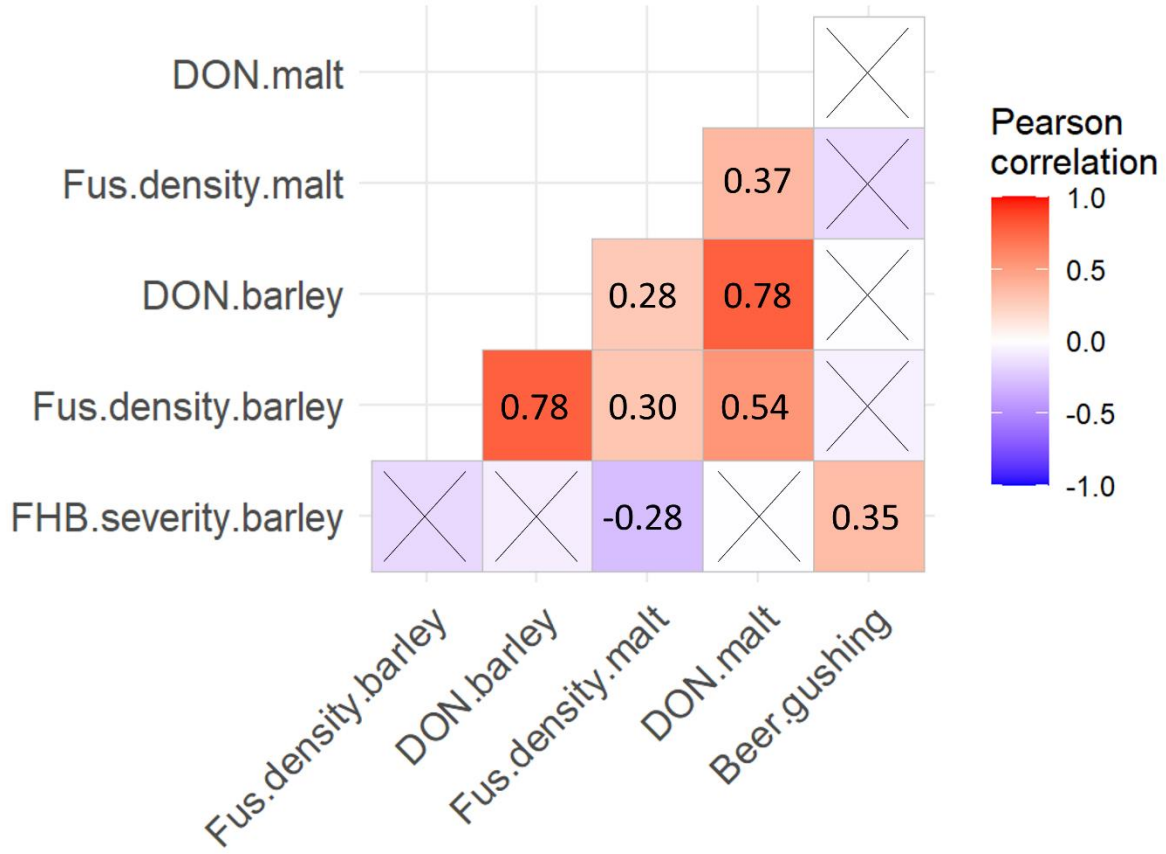

Figure 13: Heatmap indicating the range of correlations among different variables related to fusarium head blight disease, by a colour spectrum ranging from blue (negative correlation) to red (positive correlation). Numbers within the boxes represent Pearson correlation coefficients (R). Cells with 'X' show nonsignificant coefficients ($p > 0.05$).

4. DISCUSSION

This study was designed with the specific aim of investigating the activity of *F. graminearum* on barley and during malting and understand how this pathogen's impact varies among different strains. One key strength of this study was that I introduced different strains of *F. graminearum* to barley plants in the field, rather than a , more straightforward approach of

adding different pathogen strains superficially prior to the malting process; for example, my approach incorporates the pattern of natural infection occurring within and underneath the hull. Such infections will probably create a different interaction with the plant during malting compared to a case where the inoculum consisted of freely dispersed macroconidia at the malting stage. Inoculating in this way will make my results better reflect what happens in industrial malting settings (Jin et al., 2021; Roy, 2021).

Different *Fusarium* species and strains may be prevalent in different geographic regions, and their abundance can fluctuate from year to year due to various factors such as climatic conditions, agricultural practices and pathogen evolution (Laurent et al., 2017). In my study, I observed that none of the strains exhibited consistent trends in disease severity over the years. For instance, in Newdale, the highest recorded FHB severities in 2019 and 2020 were attributed to the *F. graminearum* strain HSW-15-63. However, in 2021, HSW-15-63 exhibited the lowest FHB severity on Newdale compared to the other six *F. graminearum* strains tested. Thus, while strains of *F. graminearum* do differ in their effects, these differences interact in complex ways with environmental conditions or other features of the agricultural ecosystem.

At the same time, there were some indications in this study that visible disease symptoms were influenced by more than just development of FHB due to my inoculated strains. In particular, 2020 stood out for its substantially higher visual severity scores, without corresponding increases in *F. graminearum* density. There appears to have been some amplification of disease severity symptoms in 2020, perhaps due to a concurrent infection or physiological condition. Indeed, high FHB ratings in the non-inoculated control for 2020 suggest natural infection by some other pathogen, which my qPCR assay for F. graminearum would not have picked up and that would not have produced DON (thus contributing to poor correlations between these variables and visual severity scores). Visual assessment relies on symptoms, such as discolouration, shrivelling or fungal growth on the heads of infected plants. However, as highlighted by Mesterhazy, (2020), this process can be challenging when there are other diseases or symptoms present, such as net blotch and spot blotch, that may resemble FHB symptoms. In the opposite direction, visual severity can also underestimate *Fusarium* activity; late-stage *Fusarium* infections can lead to higher DON levels despite the absence of visible kernel damage (Cowger et al., 2020).

DON is considered as a virulence factor in causing disease on wheat and barley (Zhang et al., 2012). Studies have also observed variations in DON contamination levels across different

geographic regions (Okorski et al., 2022). Additionally, some isolates may exhibit more toxin deposition in grain, grow faster and spread rapidly on plants (Foroud et al., 2012; Lee et al., 2001). My research revealed that isolates collected from barley showed lower DON production than the isolates collected from wheat, which implies a lack of host specificity (Harris et al., 2016). Isolates originating in wheat were very capable of causing disease in barley. Notably, one strain of *F. graminearum*, HSW-15-40, achieved significantly higher density and DON content in both barley and malt. However, in most cases, I did not find significant differences in the impact among *F. graminearum* strains, suggesting that the strains in my study may have similar pathogenicity and virulence capabilities under the environmental conditions that were tested here.

After factoring in the year, barley cultivar and *F. graminearum* density in barley, the significant influence of pathogen strain identity on DON content in malt indicates that variations in DON production among *F. graminearum* strains cannot be solely attributed to differences in growth extent. The comparably flat slope in 2021 when comparing *F. graminearum* density in malt to DON content suggests that more *Fusarium* biomass was required to produce the same amount of DON in 2021, while in 2019 and 2020, a given amount of DON was made with relatively less biomass. Environmental alterations could have affected the growth dynamics of the *Fusarium* fungi, influencing their ability to produce DON efficiently. (Alouane et al., 2021; Laurent et al., 2017).

The persistent resistance differences between Newdale and AAC Goldman, throughout the malting process, have significant implications for barley breeding programs and malt quality control. Based on the relative performance of these two varieties, it appears that the improvement of genetic resistance toward FHB in the field will provide continued benefits in the malting environment. Selection for improved FHB resistance in AAC Goldman took place only under field conditions, yet this study indicates that it has also lowered DON accumulation under malting conditions. However, the more resistant cultivar did not support lower *F. graminearum* density in malt than the less resistant cultivar. This may be explained by *F. graminearum* growth in this environment being primarily based on the hull tissue, which is senescent and unable to mount responsive defences (Jin et al., 2021). Another possibility is that the resistance disparity between these cultivars is relatively low and can easily be exceeded. If the growth of *F. graminearum* becomes excessively dominant in that environment, the contrast in resistance may not be evident. Even in the aspects where the cultivars do show distinctions, there might have been a more pronounced contrast between

them under milder disease pressure, such as in production conditions with lower inoculum availability and without supplemental overhead irrigation.

In my study, *F. graminearum* alone did not explain the occurrence of gushing in the malt samples. This was surprising, as *F. graminearum* has been frequently suggested to play a role in gushing. According to Virkajärvi et al., (2017), quantifying *Fusarium* sp. Given their role as major gushing inducers, DNA in barley and malt through qPCR is a promising approach for estimating the severity of Fusarium contamination. Similarly, Habschied et al., (2014) Indicated that the infection of wheat by *F. culmorum* significantly affects and increases the gushing potential in malt. However, other microbial or chemical factors may play a larger role in causing gushing than *F. graminearum* density.

Gushing is attributed to the presence of excreted hydrophobins, or other less well-characterized peptides (Sarlin, 2012b; Shokribousjein et al., 2011). Hydrophobin production is common among filamentous fungi, so other fungi in my experiment may have contributed to gushing, perhaps overwhelming or obscuring any role of *F. graminearum* in this process. For example, fungi other than *Fusarium* may have proliferated with reduced competition in my non inoculated control. If these fungi also produce hydrophobins, that might explain why my inoculated barley did not produce malt with greater gushing activity than my non inoculated barley. Previous research (Gyllang & Martinson, 1976; Kitabatake & Amaha, 1977) has suggested that gushing is probably caused by fungal growth at different stages of the beer production chain, involving various fungal species such as *Alternaria*, *Aspergillus*, *Cladosporium*, *Fusarium*, *Penicillium*, *Rhizopus* and *Stemphylium*. In my study, I examined the correlation between gushing and visual disease severity, with the severity score possibly indicating the presence of multiple fungi. The results indicated that there may be a link between gushing and total fungal load, or between gushing and some fungus other than *F. graminearum* (Yin, 2021).

A helpful frame for interpreting the observed connections between *F. graminearum* and FHB-related factors (Figure 13) is to consider which functions are solely attributable to *F. graminearum*, and which functions or traits may result from the activities of a broader range of fungi. For example, DON production in this system is very likely due entirely to the activity of *F. graminearum*; I may expect, therefore, to see a high correlation between *F. graminearum* abundance and DON concentration. In contrast, visible disease symptoms may be caused by other species of *Fusarium* (including some that do not produce DON) or other

fungal genera. Similarly, gushing may be induced by a wide range of fungi that, like *F. graminearum*, produce hydrophobin proteins. Therefore, weaker correlations may be expected between *F. graminearum* abundance, incidence or severity of disease symptoms, or the magnitude of gushing.

Notwithstanding the irrigation that was applied to promote successful infection, yearly variation in prevailing weather conditions probably impacted disease development in the field. In 2019, there was a higher disease severity, primarily due to the prevalence of wet weather at flowering, which was the primary factor driving the spread of FHB. The drier growing conditions probably had a dominant role in reducing *Fusarium* infection in 2021, which was less favourable for disease. (Environment and Climate Change Canada, 2022).

In conclusion, this study underscores the impact of FHB on barley and malt, with significant variations observed in disease severity, *F. graminearum* density and DON content across different years and barley cultivars. The infection caused by different *F. graminearum* strains also played a crucial role in influencing these factors. The micromalting process had a limited effect on DON accumulation in malt. Moreover, the variation in gushing across the years highlights the complexity of factors influencing gushing in beer, with *F. graminearum* density not being a good predictor of gushing occurrence in the malt samples tested. This study emphasizes the complexity of FHB and its impact on barley and malt, calling for continued efforts to better understand and address this economically significant disease in the malting and brewing industry.

CHAPTER 3: The role of HYD5 protein in *Fusarium*-barley interactions

This chapter has been submitted for publication to the Canadian Journal of Plant Pathology and is currently in review as:

Jayathissa, A.U., He, R., Sharma, T., Langelaan, D. N., Fernando, W.G.D., Bakker, M.G. (2024) The role of HYD5 protein in *Fusarium*-barley interactions. Submitted to Canadian Journal of Plant Pathology.

Committee members:

Badea, Ana (Department of Plant Science, University of Manitoba)

Yin, Xiang (Department of Microbiology, University of Manitoba)

External examiner: Zhong, Shaobin (Department of Plant Pathology, North Dakota State University)

Contribution of authors:

Jayathissa, Anuradha U: Conducted the experiments, analyzed the data, and wrote the manuscript. Designed the experiments to meet the research goals, collected and analyzed the data, and organized the findings in the manuscript.

Bakker, Matthew G: Main supervisor. Provided guidance throughout the project, including project planning, experimental design, conducting experiments, data collection, analysis, and manuscript writing.

Fernando, W G Dilantha: Co-supervisor. Provided knowledge in plant research and guidance in writing the manuscript.

Sharma, T: Contributed to CRISPR-Cas9 gene editing in Fusarium graminearum and supported the development of the Hyd5 gene knockout strain.

He, R and Langelaan, D. N: Performed HYD5 protein purification from Fusarium graminearum and supported related protein experiments.

ABSTRACT

Hydrophobins are specialized amphiphilic proteins in filamentous fungi, characterized by conserved cysteine residues that stabilize their structure. They play crucial roles in fungal growth, pathogenesis, and environmental interactions. This study focuses on the role of a particular hydrophobin, HYD5, in *Fusarium graminearum*, a pathogen responsible for fusarium head blight in cereals. It also examines the association of HYD5 with an applied industrial malting and brewing quality defect known as beer gushing. We utilized an in vitro CRISPR-Cas9 system to create a Δ*Hyd5* knockout strain of *F. graminearum*. Experiments with barley demonstrated that *Hyd5* is expressed *in planta* growth on barley heads. The Δ*Hyd5* knockout strain of *F. graminearum* showed no significant effect on visual disease severity on barley heads that had been inoculated through spraying. Elevated *Hyd5* gene expression during the steeping and germination stages of malting suggested that HYD5 is produced during these phases. Compared to the wildtype pathogen strain, introduction of the Δ*Hyd5* knockout strain to the malting environment resulted in reduced gushing, while purified HYD5 protein from *F. graminearum* (heterologously expressed in *E. coli*) was sufficient to induce dramatic beer gushing. High-resolution melting analysis identified genetic variants in the *Hyd5* gene among *F. graminearum* strains, though no intraspecies variation in the HYD5 protein sequence was found. Interspecies comparisons revealed significant variability in HYD5 sequences across *Fusarium* species. Testing with *F. avenaceum*, for which HYD5 shares 80 % amino acid identity with the *F. graminearum* version of the protein, demonstrated strong growth during malting and no significant difference in gushing compared to *F. graminearum* infected malt. This study underscores the role of HYD5 in fungal pathogenesis and beer quality. It suggests that managing beer gushing will require a deeper understanding of hydrophobin behavior, across *Fusarium* species and perhaps across a broader range of fungi that are active in the malting environment.

1. INTRODUCTION

Hydrophobins are small, amphiphilic proteins, found only in filamentous fungi (Wessels, 2000; Wösten, 2001). They are characterized by the presence of eight conserved cysteine residues, which can form four disulfide bridges to stabilize the protein structure (Bayry et al., 2012). Based on their solubility and sequence characteristics, hydrophobins can be classified into two major classes: Class I and Class II (Linder et al., 2005; Sarlin et al., 2005). Class I hydrophobins form amyloid-like rodlets that are integral components of cell walls. These rodlets are extremely insoluble in water, organic solvents, and detergents, and can only be solubilized using strong acids. In contrast, Class II hydrophobins form amphipathic monolayers without the fibrillar rodlets and can be dissolved in aqueous organic solvents and detergents (Wessels, 1997; Wösten, 2001). Some fungi produce only one class of hydrophobin, while others may produce both, suggesting diverse functional roles (Askolin et al., 2006; Jensen et al., 2010). Class I hydrophobins are usually associated with structural integrity, while Class II hydrophobins are more involved in dynamic processes like host-pathogen interactions or surface adhesion (Valsecchi et al., 2018).

Hydrophobins are expressed at different stages of the fungal life cycle, and appear to be important during sporulation, fruiting body formation, and growth of vegetative hyphae (Linder, 2009). Studies have shown that hydrophobins play an important role in fungal pathogenesis where they act as virulence factors in enhancing fungal infection (Dubey MK et al., 2014). Hydrophobins mediate the boundaries between hydrophilic and hydrophobic microenvironments by altering the surface properties of fungal structures. Their amphiphilic nature allows them to form hydrophobic layers on surfaces, which repel water and enable fungi to transition from submerged to aerial conditions. This ability to modify surfaces helps fungi adapt to various environments, facilitating processes such as spore dispersal, surface attachment, and the formation of protective structures (Linder et al., 2005). They have also been reported to be involved in the attachment of fungal structures and the emergence of aerial hyphae from submerged conditions (Wösten & Wessels, 1997).

In addition to having a high concentration of hydrophobic amino acids, a key common characteristic observed in hydrophobins is the presence of eight cysteine residues (Schuren & Wessels, 1990a) that play a key role in protein structure via formation of disulfide bonds. Apart from the conserved cysteines, hydrophobin amino acid sequences usually show a low structural similarity level. For example, at the nucleotide level, the sequences of hydrophobin genes are quite different; even among the three hydrophobin genes in *Schizophyllum*

commune (*Sc3, Sc4, Sc1*) there is only 45 % homology in their coding sequences. At the amino acid level, allowing for some variations still shows about 39 % similarity and 41 % identity. However, including proteins like RodA from *Aspergillus nidulans* and Eas from *Neurospora crassa* reduces the similarity further to 11 % identity and 23 % similarity (Schuren & Wessels, 1990b; Wessels, 1994).

By self-assembling at water-air interfaces, hydrophobins allow fungi to overcome the surface tension of water and escape the aqueous environment (Szilvay et al., 2007; Wessels, 1996). Hydrophobins coat the surface of the otherwise hydrophilic cell wall polysaccharides of conidia, spores, hyphae, and fruiting structures, and expose their hydrophobic layer to the outside, conferring water repellent properties. In fact, several null hydrophobin fungal mutants show an easily wettable phenotype, indicating that hydrophobins confer surface hydrophobicity to aerial hyphae and spores (Beckerman & Ebbole, 1996; Talbot et al., 1996; Wösten, 2001).

The role of hydrophobins has been studied in various fungal pathogens of plants. In the rice blast fungus, *Magnaporthe grisea*, the *mpg1* hydrophobin is crucial for efficient conidiogenesis and pathogenicity on the host plant (Talbot et al., 1993), as well as for attachment to the leaf surface (Talbot et al., 1996). The Δmpg1 mutant shows a reduced ability to form appressoria, likely because its germ tubes cannot firmly attach to the hydrophobic plant cuticle and properly sense surface features (Talbot et al., 1993). Another hydrophobin in *M. grisea*, *mhp1*, is necessary for conidial development, viability, and surface hydrophobicity. The Δmhp1 mutant demonstrates reduced appressorium formation, leading to a significant decrease in pathogenicity (Kim et al., 2005).

The genome of the plant pathogen *Fusarium graminearum*, a hemi-biotrophic fungus causing fusarium head blight (FHB) disease in cereals including barley, contains five genes encoding for hydrophobins, named *Hyd1-Hyd5* (Quarantin et al., 2019; Sarlin et al., 2012). All five hydrophobins contain a secretion signal peptide and a conserved pattern of eight cysteines. However, while *Hyd1-Hyd4* are classified as class I hydrophobins, *Hyd5* is distinct as it belongs to class II. *Hyd2* and *Hyd3* have been suggested to play roles in fungal growth and the attachment of fungal germlings to hydrophobic surfaces, respectively. Both genes are essential for the ability of hyphae to penetrate through the water–air interface and for conidia to adhere to the wheat spike surface. As a result, strains lacking these genes (Δ*Hyd2* and Δ*Hyd3*) exhibited reduced virulence toward the host plant (Quarantin et al., 2019). A previous

study that examined the role of *F. graminearum Hyd5* gene, found that the HYD5 protein did not influence colony or hyphal morphology, or the penetration of hyphae through the water-air interface, but did impact the hydrophobicity of aerial mycelia (Minenko et al., 2014). However, these findings do not fully indicate whether HYD5 is important for infection of the plant or for virulence.

When the host plant supporting fungal growth is barley, there may be unique importance for HYD5, due to activity during malting and impacts on downstream processes such as brewing. HYD5 has been identified as a possible causal factor for a quality defect known as gushing in beer (Denschlag et al., 2013; Lutterschmid et al., 2011). Hydrophobin-induced gushing is considered a beer quality problem but is largely outside of the brewer's control as further hydrophobin production is believed to take place during malting. Fungi in the genus *Fusarium* can proliferate and produce hydrophobins during the malting process. For example, one study found a higher amount of hydrophobins in malt compared to in the corresponding raw barley (Sarlin et al., 2007). These hydrophobins can survive throughout the malting and brewing processes and end up in the final beer (Laitila, 2007; Sarlin et al., 2007). The current model for understanding gushing posits that under the pressurized, high-CO_2 conditions present in bottled beer, hydrophobins aggregate around hydrophobic CO_2 micro-bubbles, forming micelles; upon release of pressure when the container is opened, these micelles break down, causing a sudden release of gaseous CO_2 that carries beer up and out of the container (Sarlin, 2012a; Shokribousjein et al., 2011). The economic impacts of beer gushing, and the difficulty that maltsters and brewers have in predicting gushing, motivate additional study about hydrophobins produced by *Fusarium*. This study investigated the role of HYD5 in *Fusarium*-barley interactions and its association with beer gushing.

2. MATERIALS AND METHODS

2.1. Testing the role of HYD5 during growth *in planta* and during malting

2.1.1 Targeted *Hyd5* gene deletion in *Fusarium graminearum* using CRISPR-Cas9

To generate a Δ*Hyd5* knockout (KO) strain, I produced macroconidia of *Fusarium graminearum* DAOMC 233423 in carboxymethyl cellulose broth (CMC, per L: 2.0 g CMC, 0.2 g K_2HPO_4, 0.2 g $MgSO_4 \cdot 7H_2O$, 0.1 g $(NH_4)_2SO_4$). Cultures were incubated at 28 °C for 3 days with shaking at 180 rpm. Macroconidia were washed and resuspended to a concentration of 1×10^8 spores/mL. For protoplasting, spores were incubated in yeast extract peptone dextrose media until germ tubes formed. The mycelium was then treated with protoplasting solution (500 mg Driselase, 200 mg of Yatalase, 200 mg Lysing enzyme L1412 from *Trichoderma harzianum* dissolved in 20 mL of 1.2 M KCl). The mixture was incubated at 28 °C with shaking at 80 rpm for 30 minutes. After this initial incubation period, protoplast formation was monitored every 10 minutes, continuing until approximately half of the mycelium was digested and a sufficient number of protoplasts had formed, which typically took around 20 additional minutes. Protoplasts were subsequently washed and resuspended in STC buffer (1.2 M sorbitol, 10 mM Tris-HCl [pH 8.0], 50 mM $CaCl_2$). I designed CRISPR RNA sequences (crRNAs; see Table 3) for both 5' and 3' ends of the *Hyd5* gene at locations near the start and stop codons, to ensure effective knockout. A homologous repair template (HRT), containing a hygromycin resistance cassette flanked by sequences matching the first 35 base pairs upstream of the 5' cut site and downstream of the 3' cut cite (referred to as 5' HRT and 3' HRT sequences in Table 3) was amplified and used for homologous recombination (Figure 14). Cas9 ribonucleoproteins (RNPs), which include crRNAs, tracrRNA, and the Cas9 protein, were assembled in the lab using Alt-R CRISPR-Cas9 components from Integrated DNA Technologies to form Cas9-RNP complexes. Protoplasts were mixed with Cas9-RNP complexes and the repair template, followed by transformation using polyethylene glycol (PEG)-$CaCl_2$ buffer (60 % [wt/vol] PEG 4000, 50 mM $CaCl_2 \cdot H_2O$, 450 mM Tris-HCl, pH 7.5). Subsequently, the transformation solution was mixed with liquid tryptone broth (TB3) medium (Per L: 3 g yeast extract, 3 g casamino acids, 200 g sucrose). This mixture was incubated at 25 °C with shaking at 100 rpm for 20 hrs to facilitate the regeneration of fungal cell walls. The following day, 300 µL of regenerated fungal protoplasts were mixed with 20 mL of liquid TB3 medium containing 0.7 % low melting point agarose and 100 mg/L hygromycin B. The mixture was then poured into sterile Petri dishes and incubated at 28 °C for 5-6 days until resistant colonies appeared on the surface. The potential

transformants were transferred to potato dextrose agar containing hygromycin at a final concentration of 150 µg/mL. I confirmed the successful knockout of *Hyd5* using Polymerase Chain Reaction (PCR) with gene-specific primers (see primer sequences in Table 3). Additionally, I verified the successful insertion of a single copy of the hygromycin gene using quantitative PCR (qPCR). Here, I estimated the hygromycin copy number by comparing the Cq value to that of a single-copy reference gene, *Tri6* (primer sequences listed in Table 3) using the formula $2^{[Cq\_TRI6 - Cq\_Hyg]}$). In *F. graminearum*, the transcriptional regulator *Tri6* is part of the trichothecene gene cluster and controls the expression of genes involved in the biosynthesis of the secondary metabolite deoxynivalenol (Nasmith et al., 2011; Sharma et al., 2022).

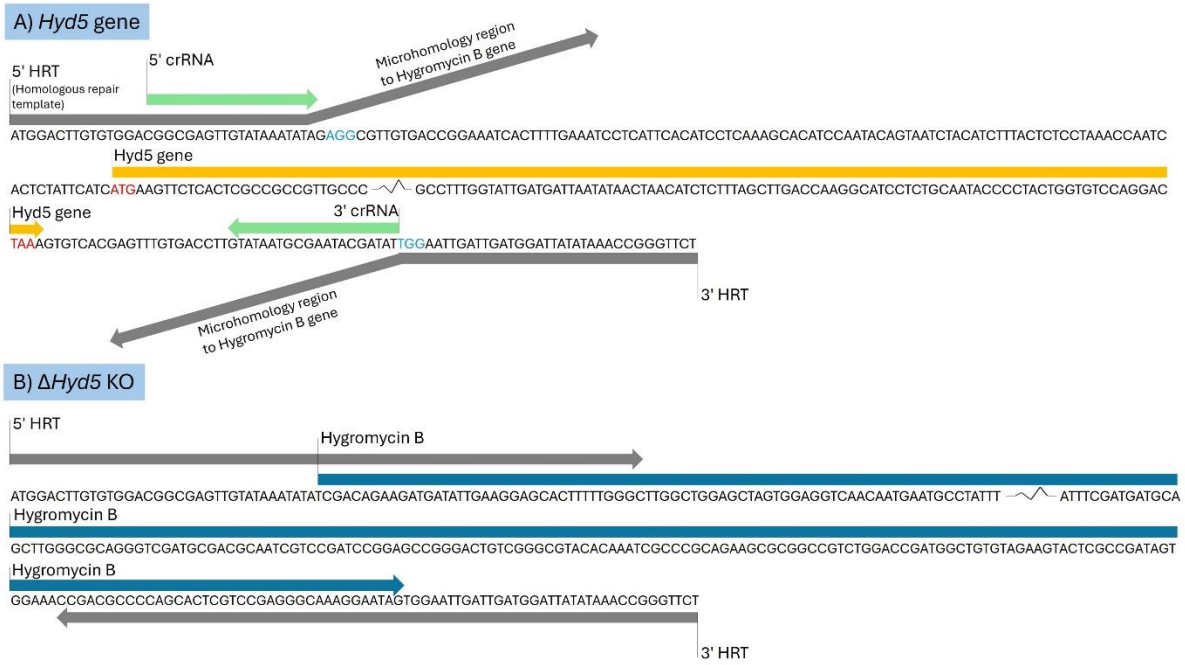

Figure 14: A schematic diagram illustrating the CRISPR-Cas9 *Hyd5* gene deletion process in *Fusarium graminearum*. A) The diagram shows the upstream and downstream regions of the *Hyd5* gene sequence. The protospacer sequences for the 5' and 3' crRNAs are indicated by green arrows, while the protospacer adjacent motif sequences are highlighted in blue. The homologous repair templates, targeting both the *Hyd5* gene and the hygromycin B resistance gene, are represented by grey arrows. The start and stop codons of the *Hyd5* gene are marked in red, and the gene itself is depicted by a yellow arrow. The blue arrow indicates the insertion of the hygromycin B gene following the Cas9-induced double-strand break in the *Hyd5* gene. B) The blue arrow indicates the insertion of the hygromycin B gene following the Cas9-induced double-strand break in the Hyd5 gene. The sequence in B) was verified by Sanger sequencing.

2.1.2 *In planta Hyd5* gene expression

A greenhouse experiment was conducted using two barley varieties (Newdale and AAC Goldman) and three inoculation treatments (*F. graminearum* DAOMC 233423 [wild type; WT], Δ*Hyd5* KO, or a non-inoculated water control). To prepare the planting medium, 100 g of Osmocote 14-14-14 (N-P-K) fertilizer and 15 g of Micromax nutrients were mixed into 20 L of SUNSHINE potting mix, along with 5 L of perlite to enhance aeration and drainage. The ingredients were thoroughly blended to ensure even nutrient distribution, and the soil was pre-soaked before being filled into pots (6.68 cm square at top; 8.89 cm deep). One seed was planted into a 2.5 cm deep hole in the center of each pot. Seedlings were transplanted after 7 days into 2.4 L pots, which had been lined with a double layer of paper towel and filled with the same potting mixture. The plants were watered whenever the soil appeared dry.

Three growth stages were selected for assessment of *Hyd5* gene expression: at heading, at flowering, and eight days post-flowering. Upon reaching the designated growth stage, heads were spray-inoculated (six sprays per head) with either the *F. graminearum* WT strain or the Δ*Hyd5* KO strain, at a concentration of 1×10^5 macroconidia/mL. For the non-inoculated control, heads were sprayed with sterile MilliQ water. After inoculation, heads were covered with plastic bags for 48 hrs to maintain the humidity necessary for pathogen infection. Nine replicates were conducted for each cultivar × time point × inoculation treatment.

At the grain-filling stage, disease severity was recorded as a percentage of symptomatic spikelets ([number of symptomatic kernels per head/mean number of kernels per head] × 100). Heads were then harvested, wrapped in aluminum foil, flash-frozen in liquid nitrogen, and stored at -80 °C until RNA extraction.

Gene expression analysis was conducted using RNA extracted from two spikelets (~100 mg) taken from the middle of each barley head. Spikelets were separated with forceps, ground in liquid nitrogen and mixed with 1.5 mL of TRIzol™ reagent (Thermo Fisher Scientific). After incubation for 5 min, 0.5 mL of chloroform was added. The mixture was shaken, incubated for 3 min, and centrifuged at 12,000 × g for 15 minutes at 4 °C. The aqueous phase was transferred to a new tube, followed by adding 0.7 mL isopropanol and incubating at -20 °C for 1 hour. The tubes were centrifuged at 12,000 × g for 10 min at 4 °C, the supernatant discarded, and the RNA pellet washed twice with 1 mL of 75 % ethanol. The RNA pellet was air-dried for 20 minutes, resuspended in 50 µL RNase-free water, and incubated at 60 °C for

15 minutes. The RNA quality was evaluated with the TapeStation System (Agilent), and only samples with RNA integrity number above 5 were selected, to ensure that analyses were based on high quality RNA. The samples were then stored at -80 °C until further use.

The *Hyd5* gene expression was examined via Reverse Transcription Quantitative Polymerase Chain Reaction (RT-qPCR). Complementary DNA (cDNA) synthesis began with a digestion reaction to remove potential contaminating genomic DNA, using the RNase-Free DNase kit (Qiagen). Two PCR tubes were prepared for each sample: one for the reverse transcriptase reaction and one for the no reverse transcriptase control. A 10 µL gDNA digestion reaction mix was prepared on ice, consisting of 3 µL Buffer RDD, 3 µL DNase I, and 4 µL template RNA. The mixture was incubated at 30 °C for 10 minutes in a thermal cycler (BioRad T100), then briefly centrifuged and placed on ice. cDNA was synthesized using the SuperScript™ IV VILO Master Mix (Thermo Fisher Scientific) according to the manufacturer's guidelines. The quality and concentration of the cDNA were assessed using the TapeStation System (Agilent). Due to low cDNA concentration, pre-amplification was performed using the SsoAdvanced™ PreAmp Supermix (BioRad) following the manufacturer's guidelines, targeting the *Hyd5* gene of interest and the reference gene glyceraldehyde-3-phosphate dehydrogenase (*GAPDH*) with specific primers (primer sequences Table 3). Each 20 µL RT-qPCR reaction mixture included PowerTrack™ SYBR Green Master Mix (Thermo Fisher Scientific), forward and reverse primers at 0.5 µM each, 1.0 ng/µL template DNA, and molecular biology grade water. Thermal cycling and fluorescence detection were performed with the QuantStudio™ 7 Pro Real-Time PCR System (Thermo Fisher Scientific). The thermal cycling protocol started with an initial hold at 95 °C for 2 minutes, followed by 40 cycles of denaturation at 95 °C for 15 seconds and annealing/extension at 60 °C for 1 minute. A melt curve analysis was performed after completion of amplification. The expression level of the *Hyd5* gene was determined relative to the expression level of *GAPDH* as: $2^{-[Cq\_Hyd5 - Cq\_GAPDH]}$. Some samples were excluded due to the inability to confidently detect gene expression of the housekeeping gene.

2.1.3 *Hyd5* gene expression during malting

A malting procedure was run using grain of the variety Newdale. Barley seeds were disinfested by exposure to dry heat 70 °C for 18 hrs (Gilbert et al., 2005). At steeping, 40 g of barley was placed in a sterile crystallizing dish (90×50 mm) and mixed with 80 mL of a spore suspension containing *F. graminearum* WT strain at a concentration of $1x10^5$ spores/mL (n = 3 replicate malting dishes). Dishes were incubated at room temperature for 16 hrs. After

draining, the grain underwent an 8-hour air rest with mixing halfway through. The grain was then submerged in 40 mL of sterile MilliQ water for 5 minutes, drained, and left for another 16-hour air rest. The dishes were transferred to a 20 °C incubator for germination, where the grain was sprayed with sterile MilliQ water after 8 hours and left for an additional 64 hours, with daily mixing. The grain was then kilned at 70 °C for 20 hrs, cleaned of rootlets, and ground to pass through a 2 mm sieve. The *Hyd5* gene expression was examined at steeping, germination, and final malt stages, via RT-qPCR. RNA extraction, cDNA synthesis, and PCR from infected barley were performed following the abovementioned procedures.

2.1.4 Malting with the Δ*Hyd5* KO strain and assessment of gushing potential

Seeds of barley variety Newdale were disinfested with dry heat and a small-scale malting procedure was carried out, as described above (n = 3 dishes per treatment). During the steeping stage, inoculum of either *F. graminearum* WT strain or the Δ*Hyd5* KO strains was added at a final concentration of 1×10^4 spores/mL, with sterile MilliQ water added for the non-inoculated control treatment. The seeds were germinated at 14 °C for 3 days, followed by kilning at 70 °C for 20 hours. Final ground malt was tested for gushing propensity through the modified Carlsberg assay as described in Chapter 1 section 2.6 (Jayathissa et al., 2024). Briefly, the bottles were shaken horizontally with a movement parallel to the longitudinal direction of the bottle (100 oscillations per minute; E6013 shaker, Eberbach Corporation) using a foam insert on the shaker table to hold the bottles in position. After shaking for 3 days at room temperature, the bottles were allowed to stand upright at room temperature for 1 hour. Each bottle was weighed, inverted three times, opened, dried with a paper towel, and then reweighed with the cap. The extent of beer gushing was measured by calculating the weight loss in grams.

2.2. The role of pure HYD5 protein in gushing

2.2.1 Heterologous expression and purification of hydrophobin HYD5 protein

Dr. David Langelaan and Raymond He at Dalhousie University fully conducted the heterologous expression and purification of the HYD5 protein as part of a collaborative effort for this project. Detailed methods are available in the appendices.

2.2.2 Beer gushing experiment for pure HYD5

Beer bottles (Heineken Original, 330 mL) were equilibrated to room temperature and uncapped. In the first set of bottles, pure hydrophobin (HYD5 from *F. graminearum*, heterologously expressed) was added as 4 µL of stock solution in water (2.2375 mg/mL; final

concentration 0.03 ppm), while the second set of bottles received 4 µL sterile water. All bottles (n = 10 bottles per treatment) were then recapped (Midwest Homebrewing and Winemaking Supplies) with new caps and processed through a modified Carlsberg assay as described in Chapter 1 section 2.6 (Jayathissa et al., 2024).

2.3. Hydrophobins in *Fusarium*

2.3.1 Identification of intraspecific *Hyd5* sequence variation in *Fusarium graminearum*

To identify whether strains of *F. graminearum* possess variants in the gene sequence of *Hyd5*, I used High Resolution Melting (HRM) analysis of amplicons from *Hyd5* exons to rapidly screen a set of 189 *F. graminearum* strains that originated from Saskatchewan, Alberta and Ontario (Oghenekaro et al., 2021). HRM analysis is a post-PCR method that can detect small differences in melting curves as PCR products dissociate. This method is used to identify variations in nucleic acid sequences (Tong & Giffard, 2012). Two primer sets (Table 3) were designed to amplify portions of the *F. graminearum Hyd5* gene, according to the guidelines of the MeltDoctor™ HRM kit (Applied Biosystems). Each 20 µL reaction mixture consisted of 10 µL of MeltDoctor™ master mixture, forward and reverse primers each at 0.5 µM, 1 µL of 20 ng/µL genomic DNA, and 6.6 µL molecular biology grade water. I performed PCR and fluorescence imaging via the QuantStudio™ 7 Pro Real-Time PCR system (Thermo Fisher Scientific). The thermal cycling protocol began with enzyme activation at 95 °C for 10 minutes, followed by 40 cycles of denaturation at 95 °C for 15 seconds, and annealing/extension at 60 °C for 1 minute. HRM analysis was performed following the PCR amplification, with temperature ramping from 60-95 °C, rising by 0.1 °C per second, with a plate read at each increment.

2.3.2 Sanger sequencing of the *Hyd5* gene

From the HRM results, a representative of each sequence variant was selected (represented by strains GU2-1, GU2-4, SB1.2, SB3.2b, SC.5a, CT2.b3, S01.1a, SW3.9, and SC.3; Oghenekaro et al., 2021). For each of these representative strains, I produced a longer amplicon for sequencing, using gene-specific primers designed in this work: Hyd5.f and Hyd5.r (primer sequences Table 3). Each 20 µL PCR reaction mixture consisted of KAPA HiFi HotStart Library Amplification master mixture (Roche), forward and reverse primers each at 0.5 µM, 1 ng/µL template DNA and molecular biology-grade water. PCR conditions were as follows: initial denaturation at 95°C for 3 minutes, followed by 25 cycles of 98 °C for 20 seconds, 62 °C for 15 seconds, and 72 °C for 15 minutes, with a final extension at 72 °C for 15 seconds. The PCR products were cleaned using the ChargeSwitch Pro PCR cleanup

kit (Thermo Fisher Scientific) and quantified using spectrophotometry (NanoDrop One; Thermo Fisher Scientific). The products were then analyzed on a FlashGel (Lonza). Amplicons from strains SW3.9 and SC.3 were present as multiple bands. To isolate the desired bands, gel extraction was performed using a 1% agarose gel and the Monarch DNA Gel Extraction Kit (New England Biolabs). The PCR products were Sanger sequenced, and sequences were manually trimmed and processed in CLC Genomics Workbench software to obtain the corresponding amino acid sequences of the HYD5 protein.

2.3.3 Interspecies variation in *Fusarium* hydrophobins

I obtained the DNA sequence of the *Hyd5* ortholog from 23 different *Fusarium* species via the National Center for Biotechnology Information, translated these sequences to protein sequences and created a protein alignment using the CLC Genomics Workbench (Qiagen). From these *Fusarium* species, I selected *F. avenaceum* to investigate whether its HYD5 protein could influence beer gushing when infecting malt, alongside *F. graminearum*.

Table 3: Primers used in this study. All the primers and probes were designed in this work.

Experiment	Primer name	Sequence (5' to 3')
CRISPR RNA sequences	5' crRNA	GGCGAGTTGTATAAATACAG
	3' crRNA	GTATAATGCGAATACGATAT
Homologous repair template	5' HRT	ATGGACTTGTGTGGACGGCGAGTTGT ATAAATACATCGACAGAAGATGATATT GAAGGAGCACTTTTTGGGC
	3' HRT	AGAACTCGGTTTATATAATCCATCAAT CAATTCCACTATTCCTTTGCCCTCGGA CGAGTGCTGGGGCGTCGG
Hyd5 gene-specific primers	FgHyd5_F1	TACAACAGGTTTCGAGGCTCCATTTAA GCTGCGATATAGACCGGGATGGTAGGT TTCAAAACGTCAACGG
	FgHyd5_R1	TTACAAGGTACATGCATTTTGTGGGAT CCGTAGATGGGCAAAACACACGGAGA CAACCATCGCAAAACAC
TRI6 reference gene	FgTRI6-5	GGCAAGACAAGGAAGGACAA
	FgTRI6-3	CGATCCCTCGTCAACACTTATG
High Resolution Melting analysis	FgHyd5.HRM.f1	CTTGGAGCCGTTGTCTCT
	FgHyd5.HRM.r1	GTTTCCGCAGTCGAGGT
	FgHyd5.HRM.f2	CTTCGTCTCCCACCGA
	FgHyd5.HRM.r2	GAGGACACAGCAGCGA
Hyd5 gene expression analysis	Hyd5.GE.a.F	GCTACTGATGTCTTGGGTGTT
	Hyd5.GE.a.R	ATGCCTTGGTCAAGGATGG
	Fg.GAPDH.F	ACCACCGTCCACTCCTACAC
	Fg.GAPDH.R	GGCGAACAGTCAAGTCAACA
Sanger sequencing of the *Hyd5* gene	Hyd5.f	CCTGGACACCAGTAGGGGTA
	Hyd5.r	CTTGGAGCCGTTGTCTCTG
Malting of *Fusarium* infected barley	Hv.Actin Forward	GTCTCCAGCTCCTGTTCATAAT
	Hv.Actin Reverse	GAGAGGTTACTCCTTCACAACC
	FaEF_F	CTGGGTTCTTGACAAGCTCA
	FaEF_R	CGGTGACATAGTAGCGAGGA

2.4. Hydrophobins in *Fusarium* during malting and their connections to beer gushing

2.4.1 Malting of *Fusarium* infected barley

To infect malt with both *F. graminearum* (WT strain DAOMC 233423) and *Fusarium avenaceum* (strain FaLH27), spores were produced in CMC broth as described above. Barley seeds (varieties Newdale and AAC Goldman) were disinfested by exposure to dry heat 70 °C for 18 hours (Gilbert et al., 2005). In a sterile crystallizing dish (90×50 mm), 40 g of barley was mixed with 80 mL of a spore suspension (1×10^5 spores/mL) containing either *F. graminearum* or *F. avenaceum* (separately), or a non-inoculated control (sterile MilliQ water added). Malting was done as in section 2.1.3.

Fusarium density was evaluated using qPCR. Total DNA was extracted from 0.1 g of ground malt with a Fungi/Yeast Genomic DNA Isolation Kit (Norgen), following the manufacturer's instructions. DNA purity and concentration were determined spectrophotometrically (NanoDrop One, Thermo Fisher Scientific). To avoid biases from variable DNA extraction efficiency in estimating F. *graminearum* density, the pathogen density was calculated as the ratio of *F. graminearum* gene copies to barley gene copies in each sample. The abundance of the barley actin gene was quantified using the primers Hv.Actin Forward and Hv.Actin Reverse (Table 3). For the amplification of *F. graminearum* DNA, the *GAPDH* region was targeted using the primers Fg.GAPDH.F, and Fg.GAPDH.R. For *F. avenaceum* DNA, the elongation factor 1-alpha region was amplified using the primers FaEF_F and FaEF_R (Table 3). In non-inoculated control samples, *F. graminearum and F. avenaceum* densities were quantified using the respective primers and designated as control 1 and control 2. *Fusarium* density in malt was measured following the protocol outlined in (Jayathissa et al., 2024).

2.4.2 Beer gushing in *Fusarium* infected malt

To evaluate the gushing potential of malt samples contaminated with *F. graminearum*, *F. avenaceum*, and control samples, I used the modified Carlsberg method as in Chapter 1 section 2.6 (Jayathissa et al., 2024). Beer was provided by the Canadian Malting Barley Technical Centre, Winnipeg, MB, from a single brewing batch. Beer bottles were equilibrated to room temperature. Twenty grams of ground malt was blended with 80 mL of sterile distilled water, and then centrifuged for 10 minutes at 4,500 × g at 25 °C. The supernatant was filtered through fluted filter paper. For each sample, 50 mL of beer was replaced with 50 mL of filtered malt extract in a bottle, which was recapped (Midwest Homebrewing and

Winemaking Supplies). The modified Carlsberg assay proceeded as described above (n = 8 bottles per treatment).

3. RESULTS

3.1 Deletion of *Hyd5* in *Fusarium graminearum*

I used an *in vitro* assembled CRISPR-Cas9 system for achieving complete *Hyd5* gene deletion in *F. graminearum*. I employed dual gRNAs targeting both upstream and downstream protospacer adjacent motif sites flanking the *Hyd5* gene. This approach resulted in efficient deletion of the *Hyd5* gene, demonstrating the efficacy of *in vitro*-assembled dual Cas9 ribonucleoprotein complexes with microhomology repair templates for precise genome manipulation in *F. graminearum*. Among the 17 putative transformants that were recovered, four strains were tested for the *Hyd5* gene deletion and hygromycin gene insertion. All four knockout strains (Δ*Hyd5* KO 1, Δ*Hyd5* KO 2, Δ*Hyd5* KO 11, Δ*Hyd5* KO 12) demonstrated successful *Hyd5* gene deletion, but estimated hygromycin resistance gene insertion copy number varied (2, 1, 1, and 13 copies, respectively). Only Δ*Hyd5* KO 2 and Δ*Hyd5* KO 11 were retained and stored at -80 °C. The Δ*Hyd5* KO 11 strain was selected for all subsequent applications in this study. The expected integration site was confirmed by Sanger sequencing (Figure 14).

3.2 *In planta Hyd5* gene expression

In this experiment, I tested whether loss of *Hyd5* impacts virulence and examined the *Hyd5 gene's expression in planta*. *Hyd5* gene expression was measured at different growth stages to assess its potential relationship to visual disease severity.

Visual disease severity was not significantly explained by inoculation treatment, cultivar, or growth stage (Table 4; Figures 15-17). When testing only the WT-inoculated treatment, disease severity was impacted by an interaction between growth stage and *Hyd5* gene expression ($p = 0.01$), which may indicate that the importance of *Hyd5* to disease development may differ among plant growth stages.

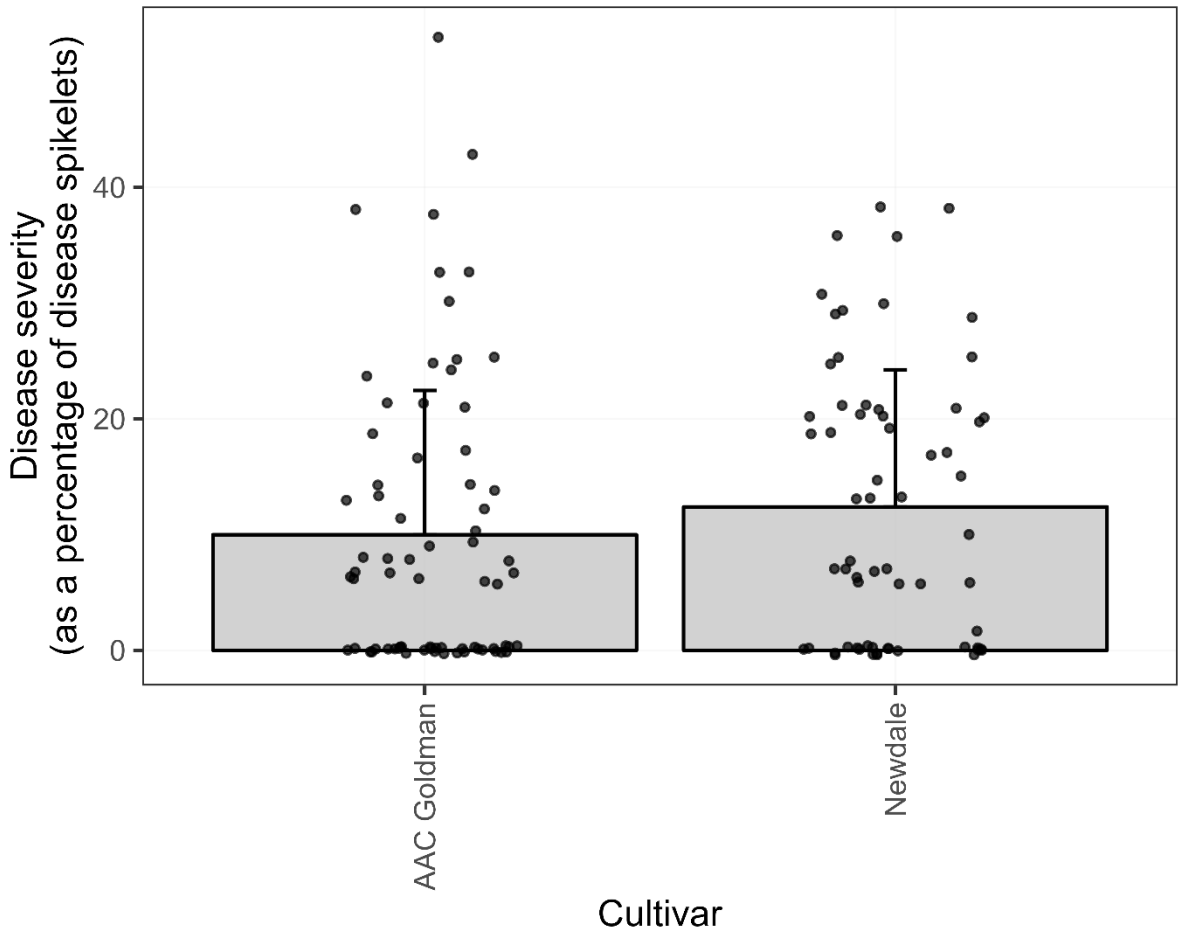

Figure 15: Fusarium head blight disease severity, expressed as the percentage of infected spikelets, compared between two barley cultivars, AAC Goldman and Newdale, across inoculation treatments. Error bars represent the standard deviations. See Table 4 for summary of statistical testing.

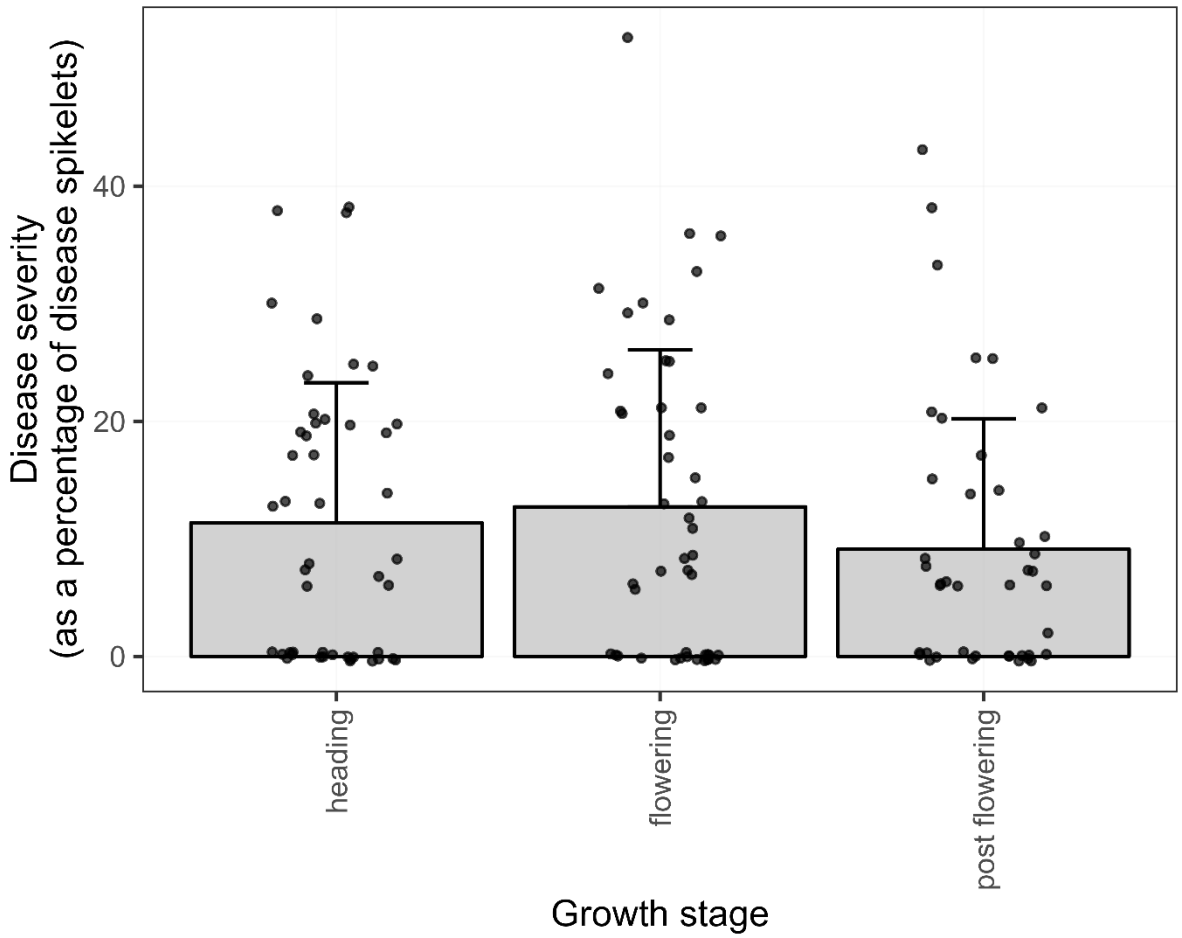

Figure 16: Fusarium head blight disease severity, expressed as the percentage of infected spikelets, compared between inoculation at three different growth stages, across barley cultivars. Error bars represent the standard deviations. See Table 4 for summary of statistical testing.

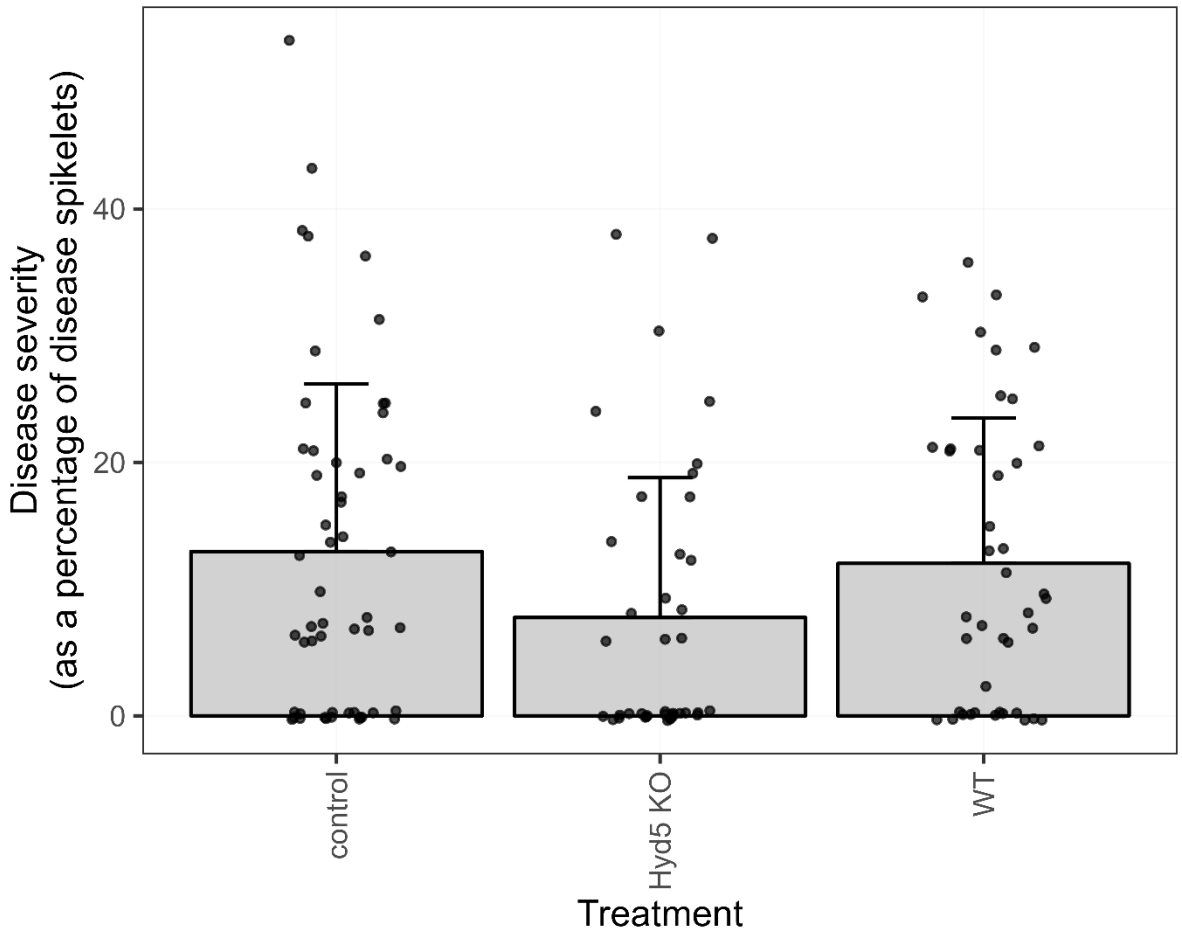

Figure 17: Fusarium head blight disease severity, expressed as the percentage of infected spikelets, compared between three different inoculation treatments (*F. graminearum* DAOMC 233423 WT, Δ*Hyd5* KO, and a water control), across barley cultivars and inoculation time points. See Table 4 for summary of statistical testing.

In explaining *Hyd5* gene expression during growth on barley heads (see Table 4 for model), the inoculation treatment factor (i.e., WT vs. Δ*Hyd5* KO strain vs. non-inoculated control) was highly significant (Figure 18; $p = 3.61 \times 10^{-5}$).

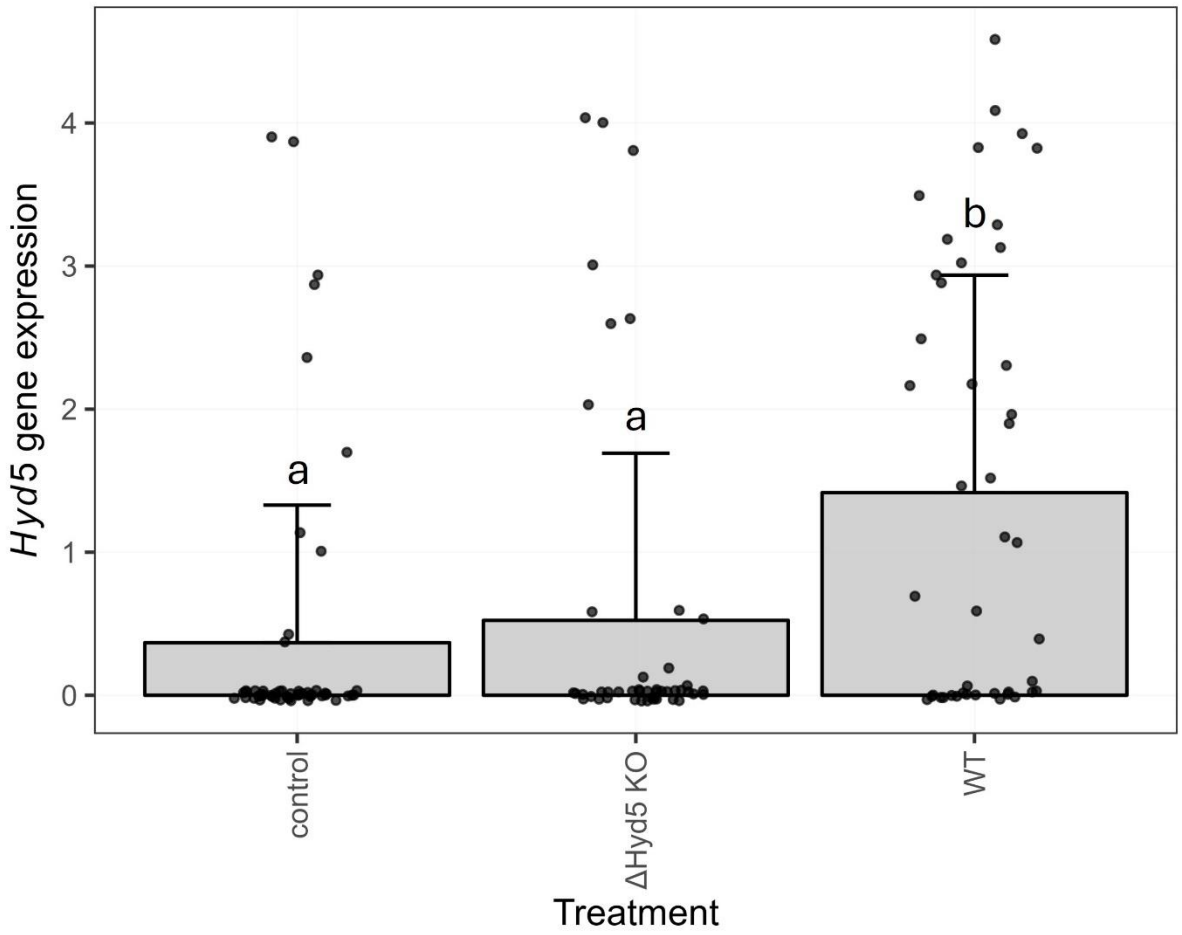

Figure 18: *Hyd5* was expressed during *in planta* growth on barley (relative to the housekeeping gene *GAPDH*). The experiment used two barley varieties (Newdale and AAC Goldman) and three inoculation treatments (*F. graminearum* DAOMC 233423 WT, Δ*Hyd5* KO, and water control). Significant differences among treatments are indicated by different lowercase letters. Error bars represent the standard deviation. See Table 4 for a summary of statistical testing.

As expected, the mean *Hyd5* gene expression for the WT treatment (1.42; a unitless ratio) was significantly higher than for either the Δ*Hyd5* KO or the control treatments (Tukey contrasts, $p < 0.05$), while there was no difference between the control and the Δ*Hyd5* KO treatments.

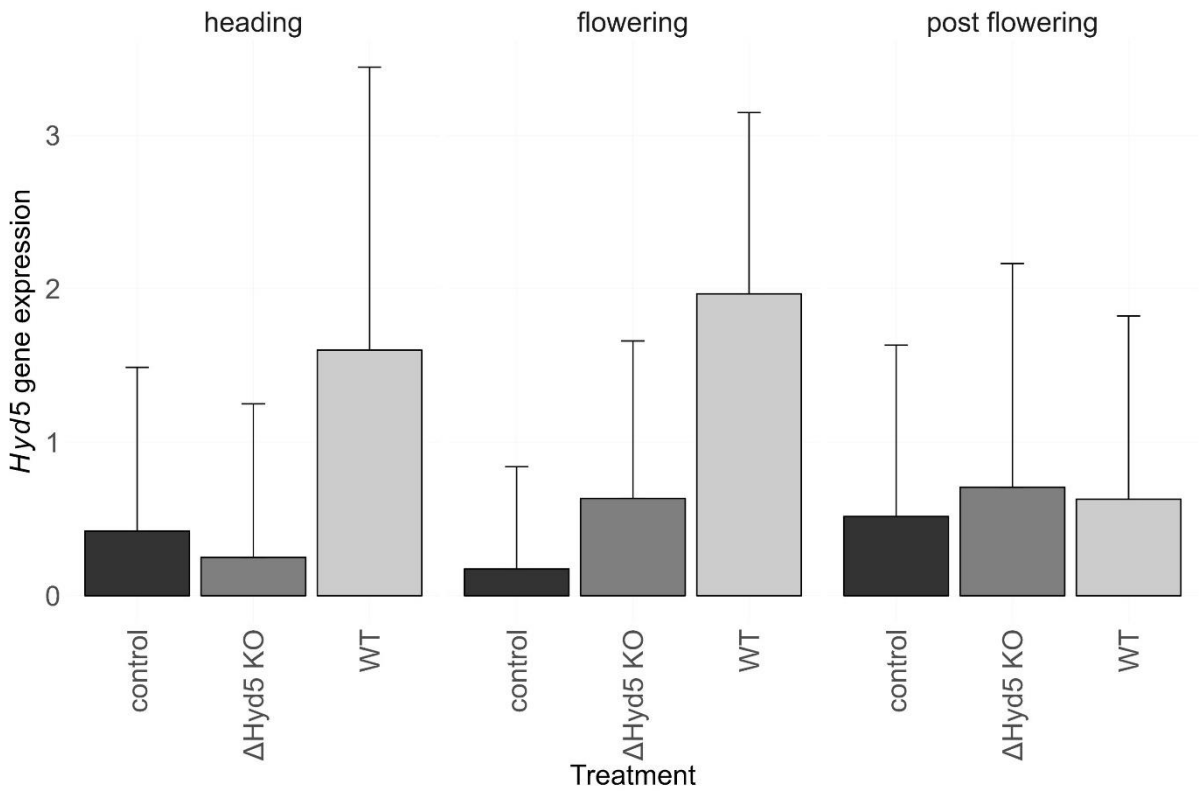

Figure 19: Expression of *Hyd5* (relative to the housekeeping gene *GAPDH*) was significantly impacted by an interaction between inoculation treatment and plant growth stage. Error bars represent the standard deviation. See Table 4 for a summary of statistical testing.

The inoculation treatment also interacted significantly with the plant growth stage (Figure 19; $p = 0.031$), indicating that differences in *Hyd5* gene expression among inoculation treatments were not consistent at every growth stage. Specifically, the WT treatment showed significantly higher *Hyd5* gene expression compared to both the Δ*Hyd5* KO and control treatments when inoculated at heading or at flowering ($p < 0.05$), but not when inoculated at the post-flowering growth stage. The interaction between cultivar and inoculation treatment was also significant ($p = 0.016$), indicating that differences in *Hyd5* gene expression among inoculation treatments were not consistent across both barley cultivars. Post-hoc pairwise comparisons revealed that *Hyd5* gene expression was significantly higher for the WT treatment than for either the Δ*Hyd5* KO or control treatments only on AAC Goldman but not on the Newdale variety (Figure 20).

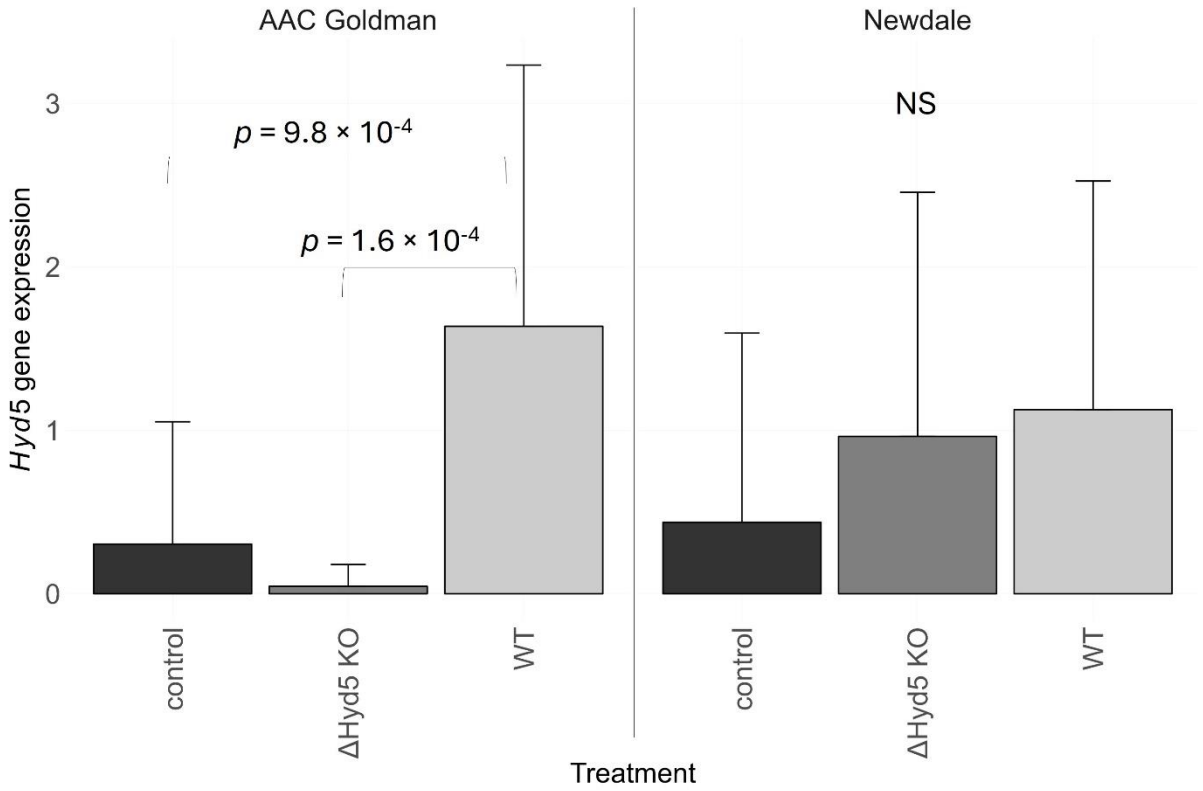

Figure 20: Expression of *Hyd5* (relative to the housekeeping gene *GAPDH*) was significantly impacted by an interaction between cultivar and inoculation treatment. Significant differences among treatments are shown by *p*-values, with "NS" indicating no significant difference. Error bars represent the standard deviation. See Table 2 for a summary of statistical testing.

3.3 *Hyd5* gene expression increased significantly from steeping to germination during malting

I was able to detect expression of the *F. graminearum Hyd5* gene during growth on barley under malting-like conditions. Furthermore, there was a significant increase in the *Hyd5* gene expression between the steeping and germination stages (Figure 21; $p = 0.03415$). I was unsuccessful in obtaining high quality RNA from the final malt stage, likely due to RNA degradation caused by the higher temperatures used during kilning; I am not able, therefore, to infer the extent of *Hyd5* expression during late stages of the malting process.

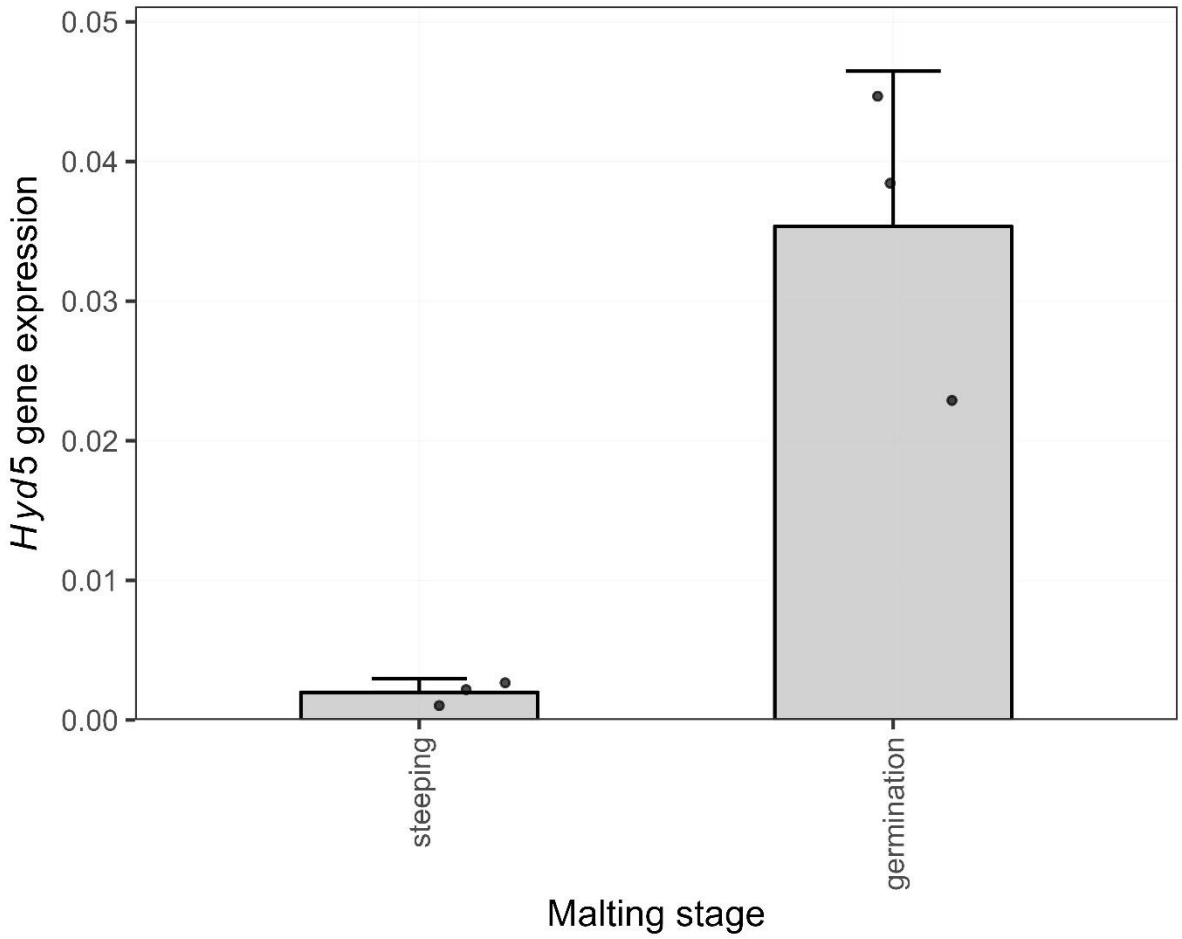

Figure 21: Expression of the *F. graminearum Hyd5* gene was detected during growth on barley under malting conditions. Expression of *Hyd5* (relative to the housekeeping gene *GAPDH*) was observed to increase significantly between the steeping and germination stages (T-test, $p = 0.03415$), as measured by quantitative PCR. Error bars represent the standard deviation (n = 3).

3.4 Reduced beer gushing in malt infected with the Δ*Hyd5* KO strain

There was a trend toward reduced beer gushing from malt that had been infected with the Δ*Hyd5* KO strain, compared to the WT strain. The water control (no malt extract added to the beer bottle) exhibited minimal gushing (2.67 g lost per bottle). The non-inoculated control and Δ*Hyd5* KO treated malt samples showed similar gushing levels (mean of 39.3 vs. 37.3 g lost, respectively). In contrast, malt infested with the WT strain, which contained the functional *Hyd5* gene, produced the highest average gushing (64.7 g lost). This supports the potential role of HYD5 in promoting beer gushing, although in this experiment the difference was not statistically significant (Figure 22; $p = 0.621$). The malt used here appears to have had some gushing-inducing capacity, perhaps associated with fungal growth in the field.

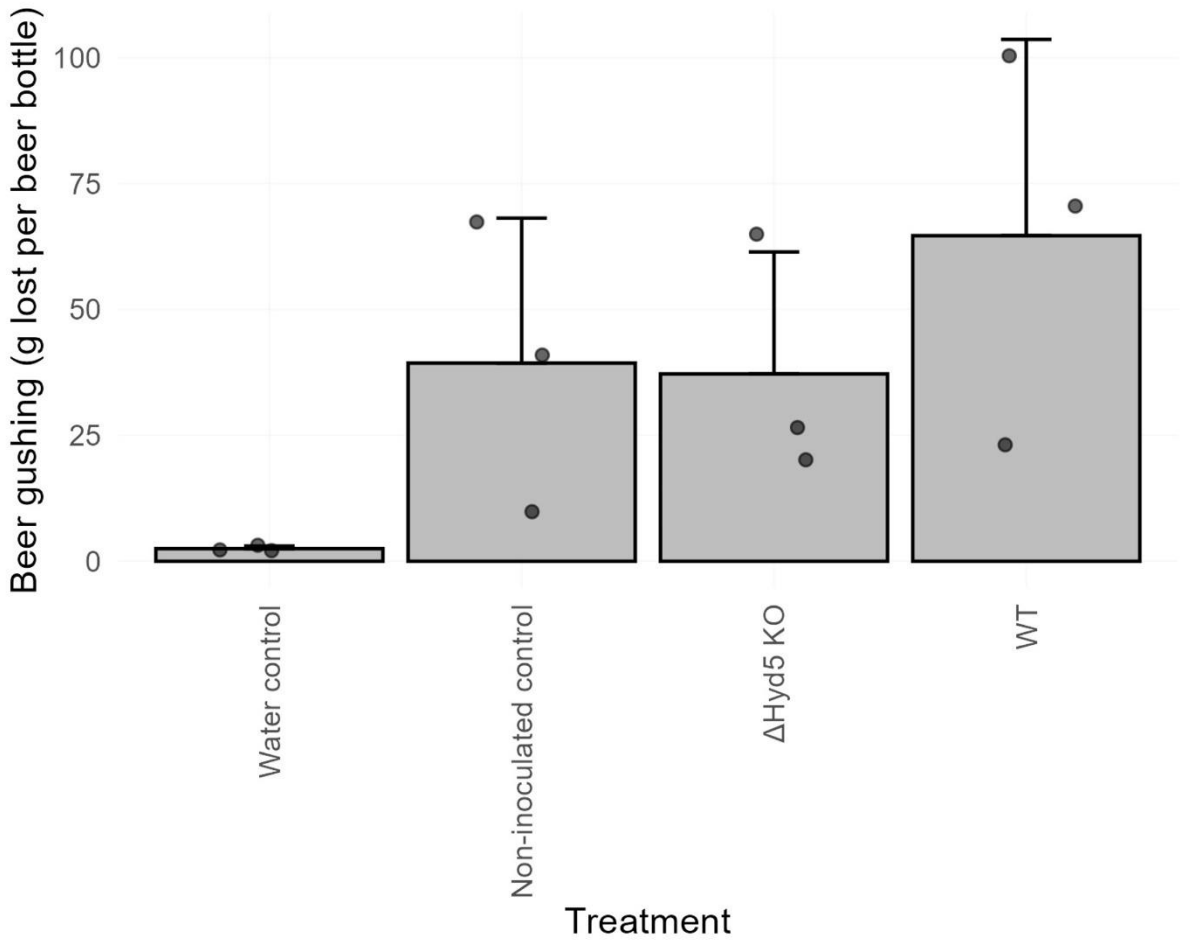

Figure 22: Malt infected with the WT strain, which has a functional *Hyd5* gene, showed the highest average beer gushing compared to the Δ*Hyd5* KO strain treatment (Tukey contrasts, $p = 0.621$). The x-axis represents different malt treatment conditions: water control, non-inoculated control, Δ*Hyd5* KO strain, and WT strain. Error bars represent standard deviations (n = 3).

3.5 Purification and characterization of recombinant HYD5 protein

The heterologous expression and purification of the HYD5 protein were entirely conducted by Dr. David Langelaan and Raymond He at Dalhousie University as part of a collaborative effort for this project. The results are available in the appendices.

3.6 Pure HYD5 induces severe gushing

The addition of purified HYD5 protein to bottled beer produced severe gushing, which was significantly greater than for water controls (Figure 23; T-test, $p = 3.35 \times 10^{-11}$). Bottles with hydrophobin added at a final concentration of 0.03 ppm showed 50 times more gushing compared to the control (150 vs. 3 g lost, respectively).

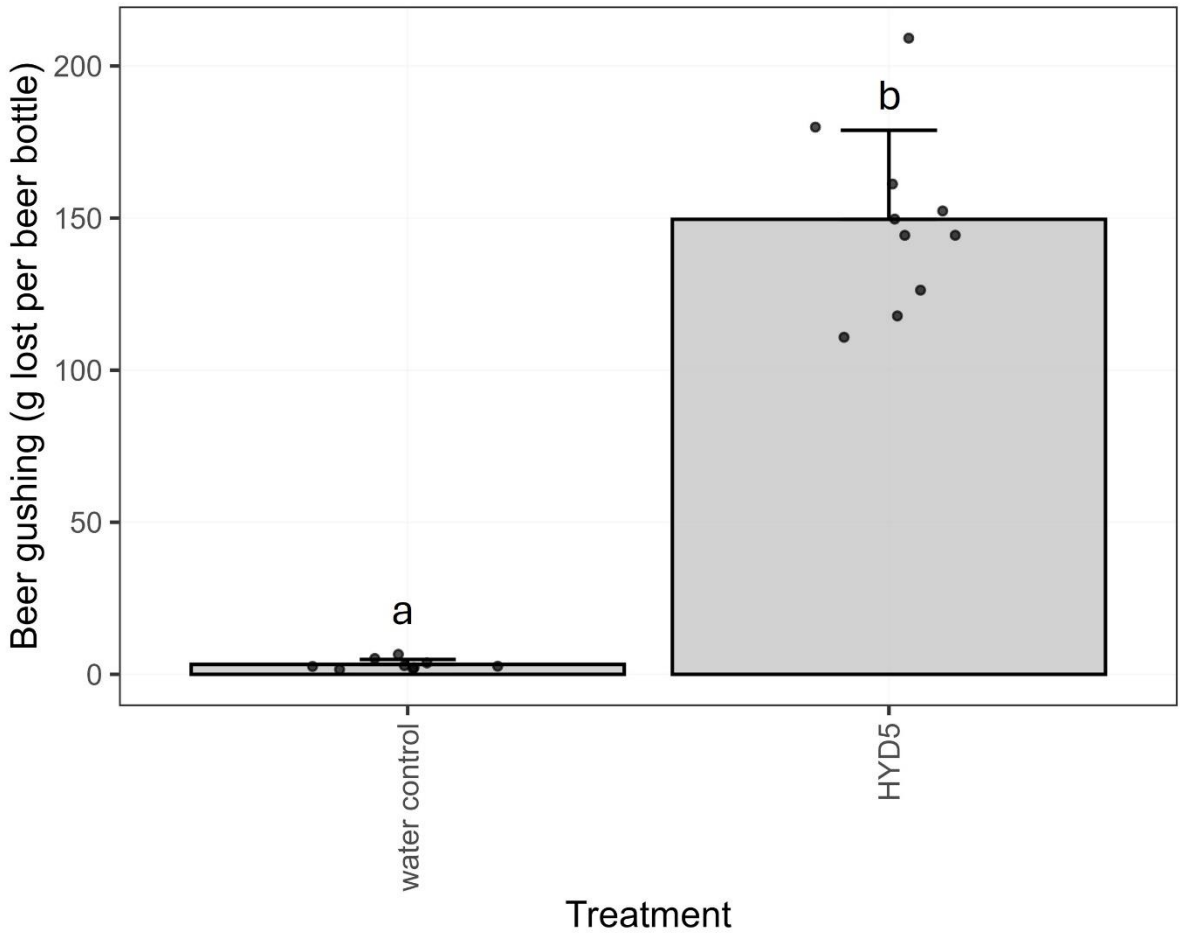

Figure 23: The addition of purified FgHYD5 protein from *F. graminearum* to bottled beer led to severe gushing, with significantly more beer lost compared to the water control (T-test, $p = 3.35 \times 10^{-11}$). Significant differences among treatments are indicated by different lowercase letters. Error bars indicate the standard deviation (n = 10).

3.7 Strains of *Fusarium graminearum* display variation in *Hyd5* gene sequence, but not in HYD5 protein sequence

High resolution melt analysis revealed multiple variants at the DNA level within the *Hyd5* gene. Among the 189 *F. graminearum* strains tested, nine distinct sequence variants were identified, represented by strains GU2-1, GU2-4, SB1.2, SB3.2b, SC.5a, CT2.b3, S01.1a, SW3.9, and SC.3. However, Sanger sequencing revealed that all isolates exhibited an identical amino acid sequence for HYD5. My HRM analysis was designed to avoid detecting intronic variants, which do not affect protein sequences, but even so, all identified nucleotide variants were silent mutations that translate to the same amino acid. Thus, no variations were observed in HYD5 at the protein level among the isolates studied (all strains matching existing NCBI accession: XP_011317673.1).

3.8 Species within the genus *Fusarium* display variations in HYD5 protein

Among the 23 *Fusarium* species investigated, the HYD5 protein sequence showed a high degree of similarity to that of *F. graminearum*, with identities ranging from 75-100 %. This indicates a conserved nature of the HYD5 protein across different *Fusarium* species, suggesting its potential functional importance within this genus. At the same time, differences in protein sequence suggest that some *Fusarium* species may produce HYD5 with greater or lesser propensity to cause gushing in beer. I chose to investigate *F. avenaceum* because it possesses differences in HYD5 amino acid sequence compared to *F. graminearum* (80 % similarity at the protein level for FgHYD5 vs. FaHYD5) and is commonly found in association with barley.

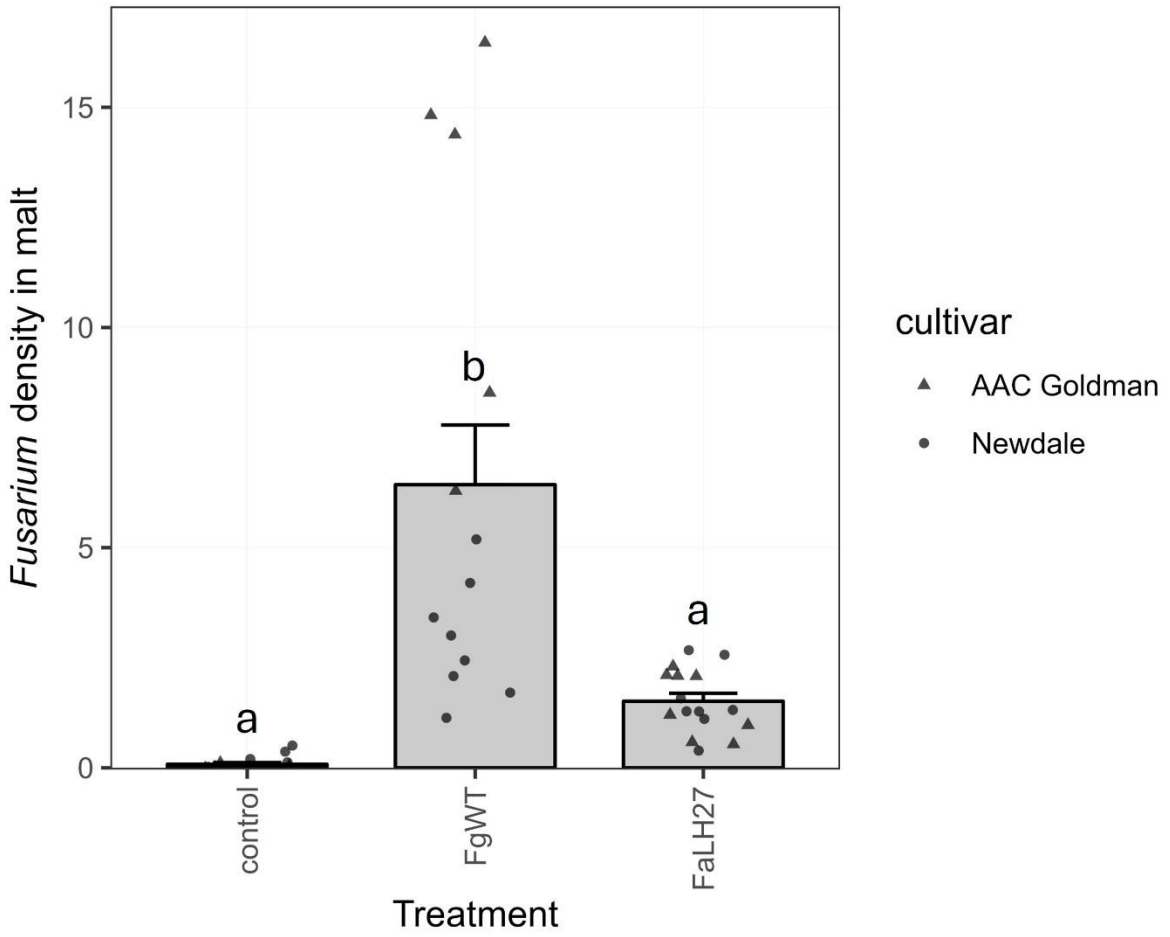

Figure 24: Both *Fusarium graminearum* and *F. avenaceum* can grow during malting. FgWT = *F. graminearum* DAOMC 233423; FaLH27 = *F. avenaceum* LH27; control = non-inoculated treatment. *Fusarium* density was quantified via qPCR using *Fusarium* specific primers, expressed relative to the abundance of a barley gene within each DNA extract. The graph displays the average *Fusarium* density in infected malt. Individual data points represent the *Fusarium* density in barley cultivars (Newdale and AAC Goldman), indicated by two distinct shapes. Significant differences among treatments are indicated by different lowercase letters. Standard deviations are represented by error bars (n = 8). See Table 4 for a summary of statistical testing.

3.9 *Fusarium avenaceum* grows in the malting environment and may induce gushing

Both fungal species achieved meaningful densities in the malting experiment with *F. graminearum* and *F. avenaceum* (Figure 24). The inoculation treatment was highly significant in explaining *Fusarium* density in malt (Table 4), with the FgWT treatment showing higher density compared to the control (Tukey contrasts, $p < 0.0001$) and compared to the FaLH27 treatment ($p = 0.0002$). Although the FaLH27 treatment showed numerically higher *Fusarium* density than the control (mean of X vs. Y), this difference was not significant ($p = 0.36$). The barley cultivar also significantly impacted *Fusarium* density ($p = 0.0018$), with AAC Goldman supporting a higher *Fusarium* density compared to Newdale (Figure 25A; 3.45 vs. 1.52 respectively; values are a unitless ratio). However, there were no significant differences in beer gushing between cultivars (Figure 25B) or among the inoculation treatments (Figure 26).

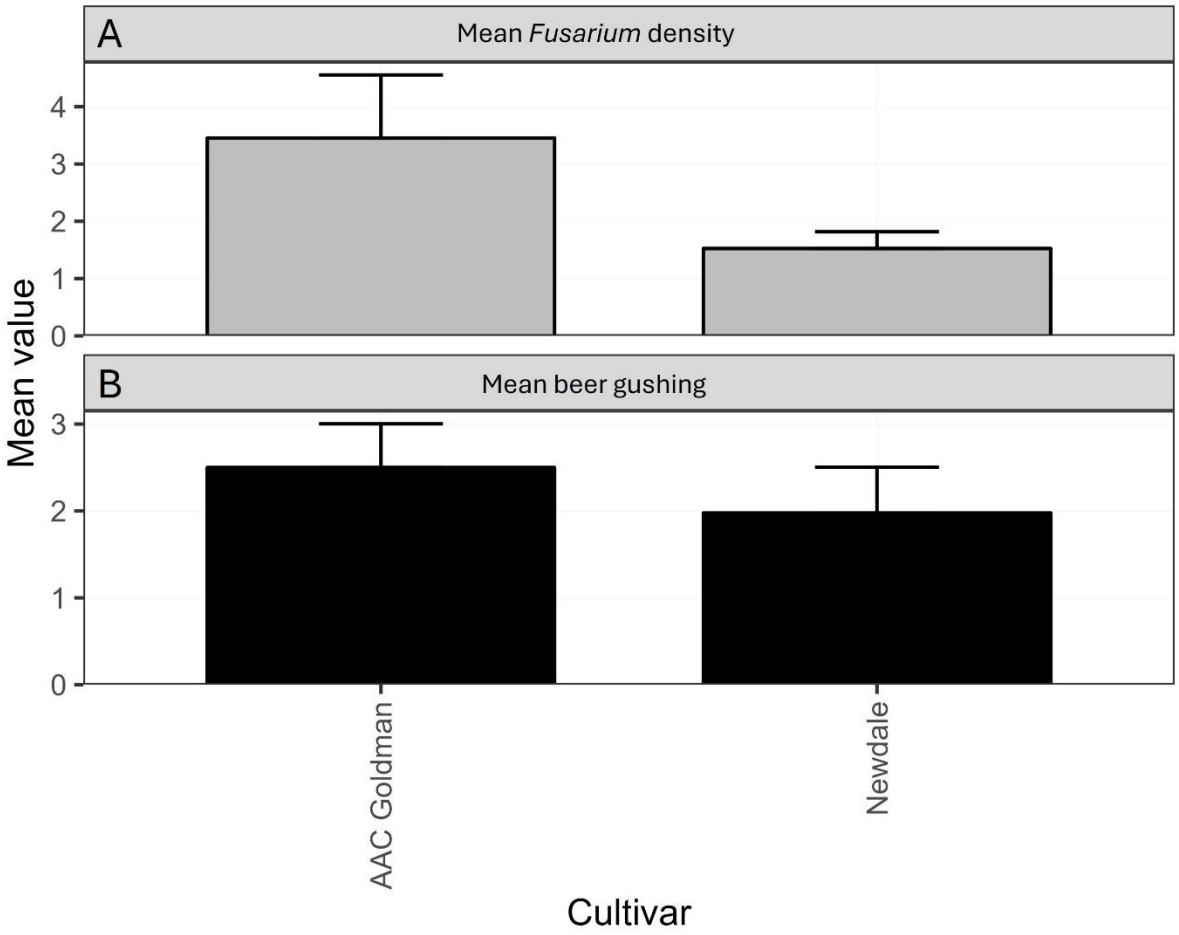

Figure 25: A) The mean *Fusarium* density was significantly greater in the AAC Goldman variety compared to the Newdale variety, while B) beer gushing did not differ significantly between the two (see Table 4 for statistical testing). *Fusarium* density is a unitless ratio of *Fusarium*:barley gene copies. Beer gushing is measured as g of beer lost upon bottle opening. Standard deviations (across *Fusarium* species) are shown with error bars (n = 12).

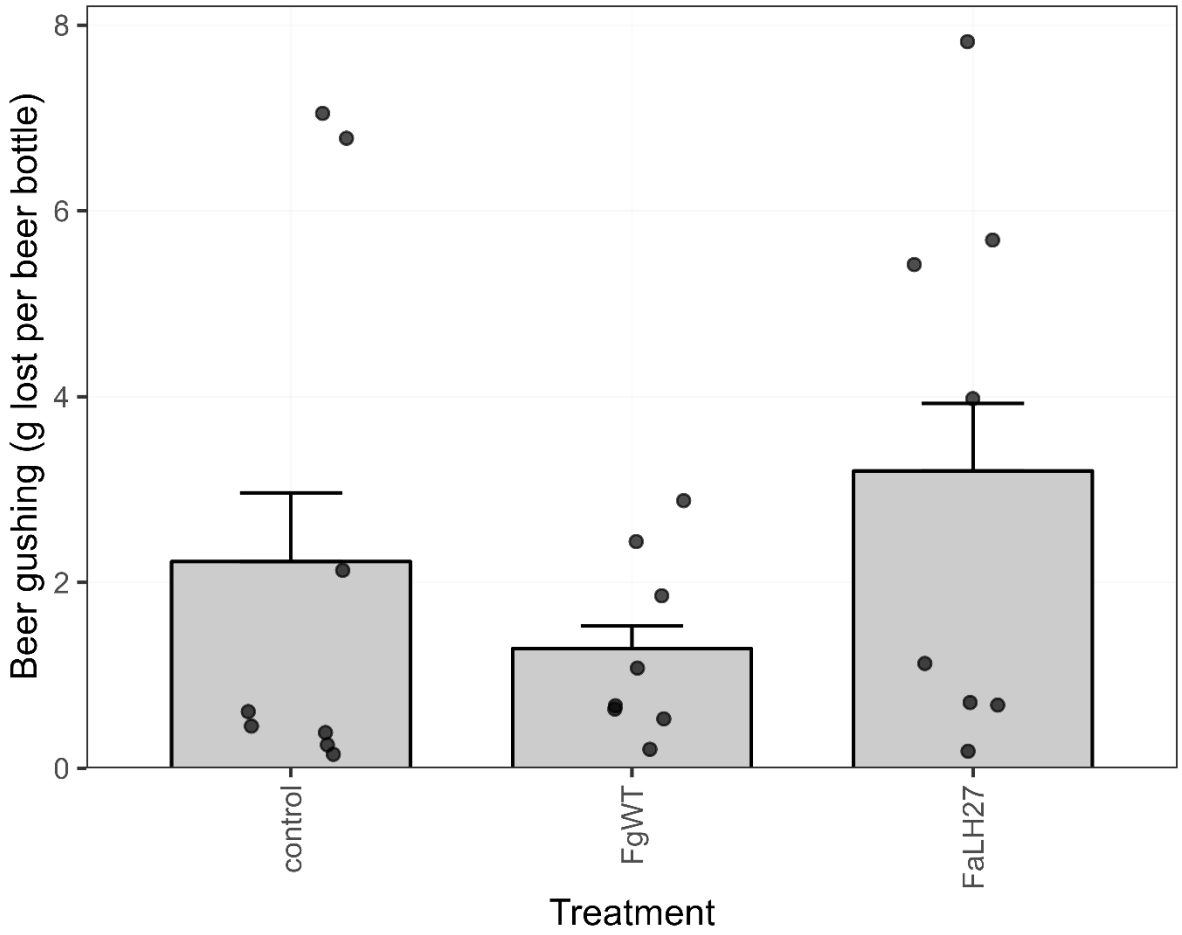

Figure 26: Gushing potential in beer (measured as g lost per bottle) for malts infected with *F. graminearum* DAOMC 233423 (FgWT), *F. avenaceum* LH27 (FaLH27), or a non-inoculated control. Shown are means + standard deviations (n = 8). There were no significant differences (ANOVA, $p = 0.717$).

Table 4: Summary of ANOVA results (*p*-values) examining the relationships between experimental variables (listed in rows) and different study measures (listed in columns).

	Hyd5 gene expression in barley	*Fusarium* density in infected malt	Disease severity in barley
Inoculation treatment	3.61×10^{-5} ***	3.20×10^{-6} ***	9.49×10^{-2}
Barley cultivar	0.49	1.83×10^{-3} **	0.21
Cultivar × Treatment	1.57×10^{-2} *	1.85×10^{-5} ***	8.95×10^{-2}
Cultivar × growth stage	0.32	NA	3.51×10^{-2} *
Treatment × Beer gushing	NA	3.21×10^{-2} *	NA
Cultivar × Treatment × Beer gushing	NA	7.54×10^{-3} **	NA
Growth stage × Treatment	3.12×10^{-2} *	NA	0.76

Note: These measures encompass *Hyd5* gene expression measured via RT-qPCR, *Fusarium* density measured via qPCR and disease severity measured via visual assessment. Linear models used to explain the observed values of each dependent variable (i.e., each column) incorporated all terms with a listed *p*-value; rows marked 'NA' indicate variables that were not included in the model for that particular dependent variable.

*** $p \leq 0.001$, ** $p \leq 0.01$, * $p \leq 0.05$

4. DISCUSSION

In this study, I investigated the roles of HYD5 from *Fusarium* in interactions with barley plants and grain (i.e., during malting) and its impact on beer gushing. My primary objective was to understand how *Hyd5* gene expression relates to fungal pathogenicity and malt quality.

In the greenhouse experiment, I investigated whether *Hyd5* gene expression is evident *in planta* and how the loss of the *Hyd5* gene affects the *Fusarium* activity. Detecting *Hyd5* expression *in planta* supports the idea that hydrophobins may be necessary to interactions with plant surfaces. Notably, when *F. graminearum* was introduced at the earlier stages of heading and flowering, there was an increased expression of the *Hyd5* gene, compared to when the pathogen was introduced post-flowering (Figure 19). This suggests a more prominent role for *Hyd5* during interaction with earlier developmental stages of the spike. However, it may also be the case that the last inoculation point (post-flowering) simply did not allow sufficient F. graminearum biomass accumulation to make *Hyd5* expression detectable.

Studies of the processes through which *F. graminearum* establishes within host tissue suggest that Hyd5 plays a reasonable role. Kang et al. (2005) studied *F. avenaceum* infection of winter wheat and observed that germ tubes did not immediately penetrate host tissues but extended and branched on the surface; this suggests an extended need for hyphae to interact with hydrophobic waxy plant surfaces. In my study, the increased expression of the *Hyd5* gene in the *F. graminearum* WT strain during the heading and flowering stages suggests that the pathogen may be more active and potentially preparing to invade the newly emerged, vulnerable plant tissues. This parallels the findings of Kang et al. (2005), where *Fusarium* species exhibit surface colonization before penetration, highlighting a common strategy among different *Fusarium* species to maximize infection success. Hydrophobins may help mediate the interaction with plant surfaces during this early stage of colonization. Luciano-Rosario et al., (2022) Six HfbG (class II hydrophobins) genes in *Penicillium expansum* were expressed during hyphal growth, suggesting that *F. graminearum* HYD5 might also be produced during hyphal growth.

However, in a previous study by Quarantin et al. (2019), wheat spikes inoculated with Δ*FgHyd5* mutants showed a similar percentage of infected spikelets compared to those inoculated with the WT, suggesting that the Δ*FgHyd5* mutation did not significantly impact

infection rates. My work extends this finding to a different *F. graminearum* strain background and to barley plants, as I also did not observe a difference in disease severity for my WT vs. Δ*Hyd5* KO strains (Figure 17). However, visual severity scores can be unreliable for fusarium head blight in barley (Jayathissa et al., 2024) as other pathogens may create similar symptoms, and successful infection by *F. graminearum* does not always produce visual symptoms. There are also some indications that cross-contamination or natural infection may have occurred in my greenhouse context. I observed *Hyd5* gene expression not only in the WT inoculated barley plants, but also in some plants from the Δ*Hyd5* KO and water control samples (Figure 19). Although I took precautions to prevent cross-contamination, the presence of both disease symptoms and *Hyd5* expression in the control and Δ*Hyd5* KO treatments suggests that there may have been background contamination. Possible sources of this contamination could be seed-borne *Fusarium* species on the seeds used in the experiment, inoculum spray drift, or insects disseminating spores that were applied to other plants. This background contamination was more evident on Newdale than AAC Goldman; for example, unexpected *Hyd5* expression was higher on Newdale (Figure 20). This fits with Newdale having a lower rating for fusarium head blight resistance, indicating the low levels of background contamination may have proliferated to greater extent on Newdale.

During initial fungal infection, various fungal genes are upregulated to aid in colonization, aiming to break through the cuticle covering the aerial epidermal cells of the host plant, which serves as the primary defense barrier. Pathogenic fungi use cutinases to penetrate this hydrophobic barrier. Espino-Rammer et al., (2013) found that novel class II hydrophobins (HFB4 and HFB7) in *Trichoderma* stimulate cutinase activity. This suggests that hydrophobins may facilitate infection by enhancing the activities of certain enzymes. By doing so, they could help breach the host's protective cuticle, promoting fungal entry and colonization.

Interaction with barley in a malting context represents quite a different environment for the fungus, compared to growth on barley heads during grain fill. For example, during the steeping process, the grain is submerged in water, which might trigger hydrophobin production to escape a submerged state. My validation of *Hyd5* expression during malting, and the significant increase in expression during the germination phase of malting, suggests that hydrophobins may be necessary to fungal activity in this environment. This upregulation indicates that *Hyd5* is involved in the pathogen's adaptation and response to the host. *Hyd5* may also be expressed in response to the stressful environment during malting. A previous

study found that CmHyd1, a class II hydrophobin in *Cordyceps militaris*, is involved in stress responses, including mycelial tolerance to osmotic and oxidative stresses, and conidial tolerance to high and low temperatures (Li et al., 2021). Osmotic stress, caused by changes in water availability during malting, can affect fungal growth. *Fusarium* can respond to osmotic stress by accumulating compatible solutes and modifying cell wall structures to maintain cellular integrity. During malting, as expected, the level of RNA from the final malt was low and quality was poor, so the samples at the malt stage were not included in the *Hyd5* gene expression analysis. This degradation in the final malt was likely due to the increased ribonuclease activity at higher temperatures during kilning (W. J. Lee & Pyler, 1985).

Hydrophobins produced during malting have been linked to beer gushing, but the gushing phenomenon remains unpredictable and poorly understood. Although not statistically significant, the higher gushing levels associated with malt infected by the WT strain, which possess the functional *Hyd5* gene, suggest a possible role of this gene in beer gushing. However, external factors, such as the fungal growth conditions in the field, could play a role, as the malt used in this experiment appears to have some intrinsic gushing-inducing capacity. The reduced beer gushing in malt infected with the Δ*Hyd5* KO strain is likely due to the altered surface properties resulting from the absence of functional HYD5 protein, which impairs the formation of hydrophobic barriers and aggregates that usually trigger gushing. This finding is consistent with Shokribousjein et al.'s (2011) suggestion that hydrophobins, due to their surface-active properties, can form nanostructures that stabilize gas bubbles, thereby creating nucleation sites for CO_2 bubbles. Consistent with our results, which showed significantly higher gushing in bottles containing pure hydrophobin, Sarlin et al., (2005) found a link between the level of hydrophobin in malt and the gushing potential. This implies that analyzing hydrophobin levels could help predict the risk of gushing in malt. Sarlin et al. (2005) examined the varying ability of hydrophobins to induce gushing. This was assumed to be due to differences in their structure, resulting from variation in amino acid sequences. Our initial hypothesis was that the structural differences in hydrophobins, such as variation in their amino acid sequences, can alter their surface activity in the beer. From our HRM analysis, the high degree of conservation among many strains does not support the idea that variations among *F. graminearum* HYD5 amino acid sequences could provide a significant explanation for the observed variation in gushing that maltsters face. There is a possibility that wild strains of *F. graminearum* could differ in the timing and quantity of HYD5 that they produce under malting conditions.

By comparing the crystal structures of three class II hydrophobins—HFBI, N-Cys HFBI variant, and HFBII from *Trichoderma reesei*—it was revealed that despite their low sequence identity (meaning their amino acid sequences differ significantly), their overall three-dimensional structures are conserved (Hakanpää et al., 2004 (a, b), 2006). Thus, there may be a high degree of functional redundancy among hydrophobins from diverse fungi, and multiple hydrophobin variants from a wide range of fungi may contribute to gushing. I began to explore this possibility by identifying interspecies variations in the HYD5 protein among *Fusarium* spp. and performing some experiments with *F. avenanceum*. A study by Mgbeahuruike et al. (2013), which examined the distribution and evolution of hydrophobin genes in fungi, including *Phlebia brevispora* and *Heterobasidion irregulare*, highlighted significant interspecies differences, which aligns with my findings on HYD5 protein variation among *Fusarium* species. Additionally, Mgbeahuruike et al. (2013) noted that different hydrophobins display distinct regulatory patterns during fungal growth on wood and in culture filtrates, underscoring the functional diversity of these proteins. Therefore, the observed interspecies variation in HYD5 protein suggests that gushing should not be unequivocally blamed on *F. graminearum*, as other fungi may also contribute to this quality defect. While I have demonstrated conclusively that HYD5 from *F. graminearum* can cause severe gushing, a similar demonstration could probably be made for hydrophobins from other filamentous fungi that also find the malting environment suitable for growth. Our previous study by Jayathissa et al. (2024) further supports this, as we found no clear correlation between *F. graminearum* density in barley and gushing in malt samples, indicating that *F. graminearum* alone may not be a reliable indicator of gushing potential.

In conclusion, this study underscores the complex interplay between *F. graminearum* hydrophobins, particularly HYD5, and the occurrence of beer gushing and fungal pathogenicity. My findings reveal that HYD5 plays a critical role in inducing gushing. At the same time, its involvement in pathogen activity appears to be significantly influenced by various stages of plant development and environmental conditions. The reduced gushing observed in malt infected with the Δ*Hyd5* KO strain highlights the protein's importance in the gushing phenomenon, while the variations in *Hyd5* gene expression across different stages of barley development emphasize its role in the pathogen's adaptation and colonization strategies. Moreover, this study supports the previously identified links between hydrophobins and the propensity of malt to cause gushing in beer. These insights suggest that managing hydrophobin levels and understanding their regulation could be crucial for both

disease control and brewing quality. Future research should investigate the molecular mechanisms underlying hydrophobin activity and explore targeted interventions to mitigate both fungal infection and malt gushing.

5. SUMMARY

In barley, *Fusarium graminearum* infection leads to FHB, affects malting quality, and contributes to beer gushing. Understanding the genetic and environmental factors that influence the severity of *Fusarium* infection, disease progression, and their impact on malting and brewing is critical for improving disease management and crop quality. This thesis aimed to investigate these dynamics by studying natural and greenhouse-inoculated barley-*Fusarium* interactions, focusing on *F. graminearum* strains and the role of the hydrophobin protein HYD5 in fungal pathogenicity and beer gushing.

The research highlighted the complex relationship between *F. graminearum* and its effects on barley, malt, and beer production. Significant variations in disease severity, *F. graminearum* density, and DON content were observed across different barley cultivars and growing seasons, underscoring the multifaceted nature of FHB. The involvement of hydrophobins, particularly HYD5, emerged as a crucial factor in both disease development and beer gushing, emphasizing the importance of this protein in *Fusarium*-barley interactions.

To investigate this further, I adapted an existing gene-editing protocol for *F. graminearum* by combining Cas9-gRNA in vitro assembly with a microhomology repair template, optimizing the process for *Fusarium* transformation. This work establishes a platform for site-specific gene targeting, which can be applied across different genetic backgrounds of *F. graminearum*. The reduced gushing observed in malt infected with the Δ*Hyd5* KO strain highlights the role of HYD5 in beer gushing, while variations in *Hyd5* gene expression across barley development stages reflect the pathogen's adaptive strategies.

Furthermore, the micromalting process demonstrated the limited influence of *F. graminearum* infection on DON accumulation in malt, and *F. graminearum* density was not a reliable predictor of gushing in beer. These findings suggest that gushing is influenced by a range of complex factors, with hydrophobin regulation playing a key role. Understanding and managing hydrophobin levels could improve both disease management and brewing quality.

Overall, this research underscores the need for continued exploration into the molecular mechanisms governing *F. graminearum* and its interaction with barley. For example, specific

antibodies against *Hyd5* could be used to develop ELISA assays to measure its levels in barley or malt samples. This knowledge will be crucial in developing effective disease control strategies and reducing the economic losses faced by the malting and brewing industries due to FHB and gushing.

6. REFERENCES

Smith's Diseases of Field and Garden Crops Diseases of Field and Garden Crops, Chiefly Such as are Caused by Fungi. Worthington G. Smith. (1885). *The American Naturalist*, *19*(4). https://doi.org/10.1086/273930

Al Abdallah Q, Ge W, Fortwendel JR. A simple and universal system for gene manipulation in *Aspergillus fumigatus*: in vitro-assembled Cas9-guide RNA ribonucleoproteins coupled with microhomology repair templates. Msphere. 2017 Dec 27;2(6):10-128. https://doi.org/10.1128/msphere.00446-17

Alisaac E, Mahlein AK. Fusarium head blight on wheat: biology, modern detection and diagnosis and integrated disease management. Toxins. 2023 Mar 3;15(3):192. https://doi.org/10.3390/toxins15030192

Alouane T, Rimbert H, Bormann J, González-Montiel GA, Loesgen S, Schäfer W, Freitag M, Langin T, Bonhomme L. Comparative genomics of eight *Fusarium graminearum* strains with contrasting aggressiveness reveals an expanded open pangenome and extended effector content signatures. International Journal of Molecular Sciences. 2021 Jun 10;22(12):6257. https://doi.org/10.3390/ijms22126257

Alukumbura AS, Bigi A, Sarrocco S, Fernando WD, Vannacci G, Mazzoncini M, Bakker MG. Minimal impacts on the wheat microbiome when *Trichoderma gamsii* T6085 is applied as a biocontrol agent to manage fusarium head blight disease. Frontiers in Microbiology. 2022 Sep 23;13:972016. https://doi.org/10.3389/fmicb.2022.972016

Askolin S, Linder M, Scholtmeijer K, Tenkanen M, Penttilä M, de Vocht ML, Wösten HA. Interaction and comparison of a class I hydrophobin from *Schizophyllum commune* and class II hydrophobins from *Trichoderma reesei*. Biomacromolecules. 2006 Apr 10;7(4):1295-301. https://doi.org/10.1021/bm050676s

Baik BK, Ullrich SE. Barley for food: Characteristics, improvement, and renewed interest. Journal of cereal science. 2008 Sep 1;48(2):233-42.

Bakker MG, Brown DW, Kelly AC, Kim HS, Kurtzman CP, Mccormick SP, O'Donnell KL, Proctor RH, Vaughan MM, Ward TJ. *Fusarium* mycotoxins: A trans-disciplinary overview. Canadian Journal of Plant Pathology. 2018 Apr 3;40(2):161-71. https://doi.org/10.1080/07060661.2018.1433720

Bakker, M. G., Jayathissa, A. U., Fernando, W. G. D., Badea, A., & Tucker, J. R. Microbiome dynamics during malting of barley grains infested by *Fusarium graminearum* strains. Plant Pathology. 2024 Sep;73(7):1886-1900. https://doi.org/10.1111/ppa.13946

Bamforth CW. Nutritional aspects of beer—a review. Nutrition research. 2002 Jan 1;22(1-2):227-37.

Bayry J, Aimanianda V, Guijarro JI, Sunde M, Latge JP. Hydrophobins—unique fungal proteins. PLoS pathogens. 2012 May 31;8(5):e1002700. https://doi.org/10.1371/journal.ppat.1002700

Beccari G, Prodi A, Tini F, Bonciarelli U, Onofri A, Oueslati S, Limayma M, Covarelli L. Changes in the Fusarium head blight complex of malting barley in a three-year field experiment in Italy. Toxins. 2017 Mar 29;9(4):120. https://doi.org/10.3390/toxins9040120

Beckerman JL, Ebbole DJ. MPG1, a gene encoding a fungal hydrophobin of *Magnaporthe grisea*, is involved in surface recognition. Molecular Plant-microbe Interactions: MPMI. 1996 Aug 1;9(6):450-6. https://doi.org/10.1094/MPMI-9-0450

Bertuzzi T, Rastelli S, Mulazzi A, Donadini G, Pietri A. Known and emerging mycotoxins in small-and large-scale brewed beer. Beverages. 2018 Jun 20;4(2):46. https://doi.org/10.3390/beverages4020046

Bills GF, Gloer JB. Biologically active secondary metabolites from the fungi. Microbiology spectrum. 2016 Dec 30;4(6):10-128. https://doi.org/10.1128/microbiolspec.funk-0009-2016

De Boevre M, Graniczkowska K, De Saeger S. Metabolism of modified mycotoxins studied through in vitro and in vivo models: An overview. Toxicology letters. 2015 Feb 17;233(1):24-8. https://doi.org/10.1016/j.toxlet.2014.12.011

Bokulich NA, Bamforth CW. The microbiology of malting and brewing. Microbiology and Molecular Biology Reviews. 2013 Jun;77(2):157-72. https://doi.org/10.1128/mmbr.00060-12

Carter JP, Rezanoor HN, Holden D, Desjardins AE, Plattner RD, Nicholson P. Variation in pathogenicity associated with the genetic diversity of *Fusarium graminearum*. European Journal of Plant Pathology. 2002 Jul;108:573-83. https://doi.org/10.1023/A:1019921203161

Castañares E, Albuquerque DR, Dinolfo MI, Pinto VF, Patriarca A, Stenglein SA. Trichothecene genotypes and production profiles of *Fusarium graminearum* isolates obtained from barley cultivated in Argentina. International journal of food microbiology. 2014 Jun 2;179:57-63. https://doi.org/10.1016/j.ijfoodmicro.2014.03.024

Chen C, Turna NS, Wu F. Risk assessment of dietary deoxynivalenol exposure in wheat products worldwide: Are new codex DON guidelines adequately protective?. Trends in Food Science & Technology. 2019 Jul 1;89:11-25.

Chylinski K, Makarova KS, Charpentier E, Koonin EV. Classification and evolution of type II CRISPR-Cas systems. Nucleic acids research. 2014 Jun 2;42(10):6091-105. https://doi.org/10.1093/nar/gku241

Cowger C, Beccari G, Dong Y. Timing of susceptibility to Fusarium head blight in winter wheat. Plant disease. 2020 Nov 16;104(11):2928-39. https://doi.org/10.1094/PDIS-03-20-0527-RE

Czembor, E., Stępień, Ł., & Waśkiewicz, A. (2015). Effect of environmental factors on Fusarium species and associated mycotoxins in maize grain grown in Poland. *PLoS ONE*, *10*(7). https://doi.org/10.1371/journal.pone.0133644

Denschlag, C., Vogel, R. F., & Niessen, L. (2013). Hyd5 gene based analysis of cereals and malt for gushing-inducing Fusarium spp. by real-time LAMP using fluorescence and turbidity measurements. *International Journal of Food Microbiology*, *162*(3). https://doi.org/10.1016/j.ijfoodmicro.2013.01.019

Dubey MK, Jensen DF, & Karlsson M. (2014). Hydrophobins are required for conidial hydrophobicity and plant root colonization in the fungal biocontrol agent Clonostachys rosea. *BMC Microbiology*, *14*, 1–4.

Dusabenyagasani, M., Dostaler, D., & Hamelin, R. C. (1999). Genetic diversity among Fusarium graminearum strains from Ontario and Quebec. *Canadian Journal of Plant Pathology*, *21*(3). https://doi.org/10.1080/07060669909501196

Environment and Climate Change Canada. (2022).

Espino-Rammer, L., Ribitsch, D., Przylucka, A., Marold, A., Greimel, K. J., Acero, E. H., Guebitz, G. M., Kubicek, C. P., & Druzhinina, I. S. (2013). Two novel class ii hydrophobins from Trichoderma spp. Stimulate enzymatic hydrolysis of poly(ethylene terephthalate) when expressed as fusion proteins. *Applied and Environmental Microbiology*, *79*(14). https://doi.org/10.1128/AEM.01132-13

Fabre, F., Bormann, J., Urbach, S., Roche, S., Langin, T., & Bonhomme, L. (2019). Unbalanced Roles of Fungal Aggressiveness and Host Cultivars in the Establishment of the Fusarium Head Blight in Bread Wheat. *Frontiers in Microbiology*, *10*. https://doi.org/10.3389/fmicb.2019.02857

Fernando, W. G. D., Oghenekaro, A. O., Tucker, J. R., & Badea, A. (2021). Building on a foundation: advances in epidemiology, resistance breeding, and forecasting research for reducing the impact of fusarium head blight in wheat and barley. In *Canadian Journal of Plant Pathology* (Vol. 43, Issue 4). https://doi.org/10.1080/07060661.2020.1861102

Foroud, N. A., McCormick, S. P., MacMillan, T., Badea, A., Kendra, D. F., Ellis, B. E., & Eudes, F. (2012). Greenhouse studies reveal increased aggressiveness of emergent Canadian Fusarium graminearum chemotypes in wheat. *Plant Disease*, *96*(9). https://doi.org/10.1094/PDIS-10-11-0863-RE

Gaj T, Gersbach CA, Barbas CF. ZFN, TALEN, and CRISPR/Cas-based methods for genome engineering. Trends in biotechnology. 2013 Jul 1;31(7):397-405. https://doi: 10.1016/j.tibtech.2013.04.004

Gilbert, J., Abramson, D., Mccallum, B., & Clear, R. (2002). Comparison of Canadian Fusarium graminearum isolates for aggressiveness, vegetative compatibility, and production of ergosterol and mycotoxins. *Mycopathologia*, *153*(4). https://doi.org/10.1023/A:1014940523921

Gilbert J, Tekauz A. Recent developments in research on Fusarium head blight of wheat in Canada. Canadian Journal of Plant Pathology. 2000 Mar 1;22(1):1-8. https://doi.org/10.1080/07060660009501155

Gilbert J, Woods SM, Turkington TK, Tekauz A. Effect of heat treatment to control Fusarium graminearum in wheat seed. Canadian Journal of Plant Pathology. 2005 Sep 1;27(3):448-52. https://doi.org/10.1080/07060660509507244

Góral T, Wiśniewska H, Ochodzki P, Nielsen LK, Walentyn-Góral D, Stępień Ł. Relationship between Fusarium head blight, kernel damage, concentration of *Fusarium* biomass, and *Fusarium* toxins in grain of winter wheat inoculated with *Fusarium culmorum*. Toxins. 2018 Dec 21;11(1):2. https://doi.org/10.3390/toxins11010002

Gosavi G, Yan F, Ren B, Kuang Y, Yan D, Zhou X, Zhou H. Applications of CRISPR technology in studying plant-pathogen interactions: overview and perspective. Phytopathology Research. 2020 Jul 31;2(1):21. https://doi.org/10.1186/s42483-020-00060-z

Gupta M, Abu-Ghannam N, Gallaghar E. Barley for brewing: Characteristic changes during malting, brewing and applications of its by-products. Comprehensive reviews in food science and food safety. 2010 May;9(3):318-28. https://doi.org/10.1111/j.1541-4337.2010.00112.x

Guzmán-Guzmán, P., Alemán-Duarte, M. I., Delaye, L., Herrera-Estrella, A., & Olmedo-Guzmán-Guzmán P, Alemán-Duarte MI, Delaye L, Herrera-Estrella A, Olmedo-Monfil V. Identification of effector-like proteins in *Trichoderma* spp. and role of a hydrophobin in the plant-fungus interaction and mycoparasitism. BMC genetics. 2017 Dec;18:1-20. https://doi.org/10.1186/s12863-017-0481-y

Gyllang H, Martinson E. Studies on the mycoflora of malt. Journal of the Institute of Brewing. 1976 Nov 12;82(6):350-2. https://doi.org/10.1002/j.2050-0416.1975.tb06962.x

Habschied, K., Krstanovic´, V., Velic´, N., Šantek, B., Novak, M., & Slačanac, V. Gushing potential of wheat malt infected with *Fusarium culmorum*. Journal of Hygienic Engineering and Design. 2014;*6*: 166-170.

Haikara A, Sarlin T, Nakari-Setala T, Penttila M, inventors. Method for determining a gushing factor for a beverage. United States patent application US 10/309,911. 2003 Aug 7.

Hakanpää J, Paananen A, Askolin S, Nakari-Setälä T, Parkkinen T, Penttilä M, Linder MB, Rouvinen J. Atomic resolution structure of the HFBII hydrophobin, a self-assembling amphiphile. Journal of Biological Chemistry. 2004 (a) Jan 2;279(1):534-9. https://doi.org/10.1074/jbc.M309650200

Hakanpaa J, Parkkinen T, Hakulinen N, Linder M, Rouvinen J. Crystallization and preliminary X-ray characterization of *Trichoderma reesei* hydrophobin HFBII. Acta

Crystallographica Section D: Biological Crystallography. 2004 (b) Jan 1;60(1):163-5. https://doi.org/10.1107/S0907444903024430

Hakanpää J, Szilvay GR, Kaljunen H, Maksimainen M, Linder M, Rouvinen J. Two crystal structures of *Trichoderma reesei* hydrophobin HFBI—the structure of a protein amphiphile with and without detergent interaction. Protein science. 2006 Sep;15(9):2129-40. https://doi.org/10.1110/ps.062326706

Harris LJ, Balcerzak M, Johnston A, Schneiderman D, Ouellet T. Host-preferential *Fusarium graminearum* gene expression during infection of wheat, barley, and maize. Fungal Biology. 2016 Jan 1;120(1):111-23. https://doi.org/10.1016/j.funbio.2015.10.010

Hofgaard IS, Seehusen T, Aamot HU, Riley H, Razzaghian J, Le VH, Hjelkrem AG, Dill-Macky R, Brodal G. Inoculum potential of *Fusarium* spp. relates to tillage and straw management in Norwegian fields of spring oats. Frontiers in Microbiology. 2016 Apr 22;7:556. https://doi.org/10.3389/fmicb.2016.00556

Huang H, Gao X, Li Y, Tian P, Nima Y, Laba Z, Ci Z, Wei X, Qu J, Guan W, Liao W. Content analysis of vitamins, dietary fibers and amino acids in a wide collection of barley (*Hordeum vulgare* L.) from Tibet, China. Bioinformation. 2020;16(4):314. https://doi.org/10.6026/97320630016314

Ilgen P, Hadeler B, Maier FJ, Schäfer W. Developing kernel and rachis node induce the trichothecene pathway of *Fusarium graminearum* during wheat head infection. Molecular plant-microbe interactions. 2009 Aug;22(8):899-908. https://doi.org/10.1094/MPMI-22-8-0899

Izydorczyk, M. S. Prediction of germination energy of malting barley during long-time storage. Canadian Grain Commission. 2004.

Ishino Y, Krupovic M, Forterre P. History of CRISPR-Cas from encounter with a mysterious repeated sequence to genome editing technology. Journal of bacteriology. 2018 Apr 1;200(7):10-128.

Janssen EM, Liu C, Van der Fels-Klerx HJ. *Fusarium* infection and trichothecenes in barley and its comparison with wheat. World Mycotoxin Journal. 2018 Feb 23;11(1):33-46. https://doi.org/10.3920/WMJ2017.2255

Jayathissa, A. U., Tucker, J. R., Badea, A., Fernando, W. G. D., & Bakker, M. G. Impacts of pathogen strain and barley cultivar on Fusarium head blight in barley and during malting. Plant Pathology. 2024 Sep;73(7):1874-1885. https://doi.org/10.1111/ppa.13918

Jensen BG, Andersen MR, Pedersen MH, Frisvad JC, Søndergaard I. Hydrophobins from *Aspergillus* species cannot be clearly divided into two classes. BMC Research Notes. 2010 Dec;3:1-6. https://doi.org/10.1186/1756-0500-3-344

Jin Z, Solanki S, Ameen G, Gross T, Poudel RS, Borowicz P, Brueggeman RS, Schwarz P. Expansion of internal hyphal growth in fusarium head blight–infected grains contributes to the elevated mycotoxin production during the malting process. Molecular Plant-

Microbe Interactions. 2021 Jul 30;34(7):793-802. https://doi.org/10.1094/MPMI-01-21-0024-R

Kang Z, Zingen-Sell I, Buchenauer H. Infection of wheat spikes by *Fusarium avenaceum* and alterations of cell wall components in the infected tissue. European Journal of Plant Pathology. 2005 Jan;111:19-28. https://doi.org/10.1007/s10658-004-1983-9

Kassambara, A., & Kassambara, M. A. (2019). Package 'ggcorrplot'. R Package. version 0.1.4.1.

Kelly A, Proctor RH, Belzile F, Chulze SN, Clear RM, Cowger C, Elmer W, Lee T, Obanor F, Waalwijk C, Ward TJ. The geographic distribution and complex evolutionary history of the NX-2 trichothecene chemotype from *Fusarium graminearum*. Fungal Genetics and Biology. 2016 Oct 1;95:39-48. https://doi.org/10.1016/j.fgb.2016.08.003

Khalesi M, Gebruers K, Derdelinckx G. Recent advances in fungal hydrophobin towards using in industry. The protein journal. 2015 Aug;34:243-55. https://doi.org/10.1007/s10930-015-9621-2

Khanzadi MN, Khan AA. CRISPR/Cas9: Nature's gift to prokaryotes and an auspicious tool in genome editing. Journal of basic microbiology. 2020 Feb;60(2):91-102. https://doi.org/10.1002/jobm.201900420

Kim S, Ahn IP, Rho HS, Lee YH. MHP1, a *Magnaporthe grisea* hydrophobin gene, is required for fungal development and plant colonization. Molecular Microbiology. 2005 Sep;57(5):1224-37. https://doi.org/10.1111/j.1365-2958.2005.04750.x

Kitabatake K, Amaha M. Effect of chemical modifications on the gushing-inducing activity of a hydrophobic protein produced by a *Nigrospora* sp. Agricultural and Biological Chemistry. 1977 Jun 1;41(6):1011-9. https://doi.org/10.1271/bbb1961.41.1011

Kleemola, T., Nakari-Setälä, T., Linder, M., Penttilä, M., Kotaviita, E., Olkku, J., & Haikara, A. Characterisation and detection of the gushing factors produced by fungi. Proceedings of the European Brewery Convention Congress, Budapest. 2001.

EFSA Panel on Contaminants in the Food Chain (CONTAM), Knutsen HK, Alexander J, Barregård L, Bignami M, Brüschweiler B, Ceccatelli S, Cottrill B, Dinovi M, Edler L, Grasl-Kraupp B. Risk to human health related to the presence of perfluorooctane sulfonic acid and perfluorooctanoic acid in food. EFSA journal. 2018 Dec;16(12):e05194. https://doi.org/10.2903/j.efsa.2017.4718

Koonin EV, Makarova KS. Origins and evolution of CRISPR-Cas systems. Philosophical Transactions of the Royal Society B. 2019 May 13;374(1772):20180087. https://doi.org/10.1098/rstb.2018.0087

Kranz B, Koch M, Schapfl M, Fischer L. Investigation of the germination of barley and wheat grains with a design of experiments for the production of hydrolases. Food Technology and Biotechnology. 2015 Jun 23;53(2):127-35. https://doi.org/10.17113/ftb.53.02.15.3718

Krstanović V, Habschied K, Mastanjević K. Research of malting procedures for winter hard wheat varieties—part I. Foods. 2020 Dec 28;10(1):52. https://doi.org/10.3390/foods10010052

Kulkarni SS, Nene SN, Joshi KS. Exploring malted barley waste for fungi producing surface active proteins like hydrophobins. SN Applied Sciences. 2020 Nov;2:1-4. https://doi.org/10.1007/s42452-020-03696-w

Kushiro M. Effects of milling and cooking processes on the deoxynivalenol content in wheat. International journal of molecular sciences. 2008 Nov 5;9(11):2127-45. https://doi.org/10.3390/ijms9112127

Laitila, A. (2007). Microbes in the tailoring of barley malt properties. VTT Publications, *645*.

Lau G, Hamer JE. Regulatory genes controlling MPG1 expression and pathogenicity in the rice blast fungus *Magnaporthe grisea*. The Plant Cell. 1996 May 1;8(5):771-81. https://doi.org/10.1105/tpc.8.5.771

Laurent B, Moinard M, Spataro C, Ponts N, Barreau C, Foulongne-Oriol M. Landscape of genomic diversity and host adaptation in *Fusarium graminearum*. BMC genomics. 2017 Dec;18:1-9. https://doi.org/10.1186/s12864-017-3524-x

Lee T, Oh DW, Kim HS, Lee J, Kim YH, Yun SH, Lee YW. Identification of deoxynivalenol- and nivalenol-producing chemotypes of *Gibberella zeae* by using PCR. Applied and Environmental Microbiology. 2001 Jul 1;67(7):2966-72. https://doi.org/10.1128/AEM.67.7.2966-2972.2001

Lee WJ, Pyler RE. Nucleic acid degrading enzymes of barley malt. I. Nucleases and phosphatases. Journal of the American Society of Brewing Chemists. 1985 Jan 1;43(1):1-6. https://doi.org/10.1094/asbcj-43-0001

Legge WG, Badea A, Tucker JR, Fetch Jr TG, Banik M, Haber S, Menzies JG, Tekauz A, Turkington TK, Martin RA, Choo TM. AAC Goldman barley. Canadian Journal of Plant Science. 2018 Apr 15;98(5):1203-11. https://doi.org/10.1139/cjps-2017-0361

Legge WG, Haber S, Harder DE, Menzies JG, Noll JS, Tekauz A, Thomas PL, Turkington TK, Bizimungu B. Newdale barley. Canadian journal of plant science. 2008 Jul 1;88(4):717-23. https://doi.org/10.4141/CJPS07194

Leplat J, Héraud C, Gautheron E, Mangin P, Falchetto L, Steinberg C. Colonization dynamic of various crop residues by *Fusarium graminearum* monitored through real-time PCR measurements. Journal of applied microbiology. 2016 Nov 1;121(5):1394-405. https://doi.org/10.1111/jam.13259

Leung RK, Whittaker PA. RNA interference: from gene silencing to gene-specific therapeutics. Pharmacology & therapeutics. 2005 Aug 1;107(2):222-39. https://doi.org/10.1016/j.pharmthera.2005.03.004

Lewandowski SM, Bushnell WR, Evans CK. Distribution of mycelial colonies and lesions in field-grown barley inoculated with *Fusarium graminearum*. Phytopathology. 2006 Jun;96(6):567-81. https://doi.org/10.1094/PHYTO-96-0567

Li X, Wang F, Liu M, Dong C. Hydrophobin CmHYD1 is involved in conidiation, infection and primordium formation, and regulated by GATA transcription factor CmAreA in edible fungus, Cordyceps militaris. Journal of Fungi. 2021 Aug 20;7(8):674. https://doi.org/10.3390/jof7080674

Liang J, Lofgren L, Ma Z, Ward TJ, Kistler HC. Population subdivision of *Fusarium graminearum* from barley and wheat in the Upper Midwestern United States at the turn of the century. Phytopathology. 2015 Nov 18;105(11):1466-74. https://doi.org/10.1094/PHYTO-01-15-0021-R

Linder MB. Hydrophobins: proteins that self assemble at interfaces. Current Opinion in Colloid & Interface Science. 2009 Oct 1;14(5):356-63. https://doi.org/10.1016/j.cocis.2009.04.001

Linder MB, Szilvay GR, Nakari-Setälä T, Penttilä ME. Hydrophobins: the protein-amphiphiles of filamentous fungi. FEMS microbiology reviews. 2005 Nov 1;29(5):877-96. https://doi.org/10.1016/j.femsre.2005.01.004

Linkmeyer A, Hofer K, Rychlik M, Herz M, Hausladen H, Hückelhoven R, Hess M. Influence of inoculum and climatic factors on the severity of Fusarium head blight in German spring and winter barley. Food Additives & Contaminants: Part A. 2016 Mar 3;33(3):489-99. https://doi.org/10.1080/19440049.2015.1133932

Littlejohn KA, Hooley P, Cox PW. Bioinformatics predicts diverse Aspergillus hydrophobins with novel properties. Food Hydrocolloids. 2012 Jun 1;27(2):503-16. https://doi.org/10.1016/j.foodhyd.2011.08.018

Lofgren L, Riddle J, Dong Y, Kuhnem PR, Cummings JA, Del Ponte EM, Bergstrom GC, Kistler HC. A high proportion of NX-2 genotype strains are found among *Fusarium graminearum* isolates from northeastern New York State. European Journal of Plant Pathology. 2018 Mar;150:791-6. https://doi.org/10.1007/s10658-017-1314-6

Luciano-Rosario D, Eagan JL, Aryal N, Dominguez EG, Hull CM, Keller NP. The hydrophobin gene family confers a fitness trade-off between spore dispersal and host colonization in *Penicillium expansum*. Mbio. 2022 Dec 20;13(6):e02754-22. https://doi.org/10.1128/mbio.02754-22

Lutterschmid G, Muranyi M, Stübner M, Vogel RF, Niessen L. Heterologous expression of surface-active proteins from barley and filamentous fungi in *Pichia pastoris* and characterization of their contribution to beer gushing. International journal of food microbiology. 2011 May 14;147(1):17-25. https://doi.org/10.1016/j.ijfoodmicro.2011.02.030

Malbrán I, Mourelos CA, Girotti JR, Aulicino MB, Balatti PA, Lori GA. Aggressiveness variation of *Fusarium graminearum* isolates from Argentina following point inoculation of field grown wheat spikes. Crop Protection. 2012 Dec 1;42:234-43. https://doi.org/10.1016/j.cropro.2012.05.025

Maldonado-Ramirez SL, Schmale III DG, Shields EJ, Bergstrom GC. The relative abundance of viable spores of *Gibberella zeae* in the planetary boundary layer suggests the role of long-distance transport in regional epidemics of Fusarium head blight. Agricultural and Forest Meteorology. 2005 Sep 20;132(1-2):20-7. https://doi.org/10.1016/j.agrformet.2005.06.007

Manstretta V, Rossi V. Effects of weather variables on ascospore discharge from *Fusarium graminearum* perithecia. PloS one. 2015 Sep 24;10(9):e0138860. https://doi.org/10.1371/journal.pone.0138860

Mastanjević K, Krstanović V, Mastanjević K, Šarkanj B. Malting and brewing industries encounter *Fusarium* spp. related problems. Fermentation. 2018 Jan 9;4(1):3. https://doi.org/10.3390/fermentation4010003

Mastanjević K, Lukinac J, Jukić M, Šarkanj B, Krstanović V, Mastanjević K. Multi-(myco) toxins in malting and brewing by-products. Toxins. 2019 Jan 9;11(1):30. https://doi.org/10.3390/toxins11010030

Mastanjević K, Mastanjević K, Krstanović V. The gushing experience—a quick overview. Beverages. 2017 Jun 12;3(2):25. https://doi.org/10.3390/beverages3020025

Maul R, Müller C, Rieß S, Koch M, Methner FJ, Irene N. Germination induces the glucosylation of the *Fusarium* mycotoxin deoxynivalenol in various grains. Food Chemistry. 2012 Mar 1;131(1):274-9. https://doi.org/10.1016/j.foodchem.2011.08.077

McMullen M, Bergstrom G, De Wolf E, Dill-Macky R, Hershman D, Shaner G, Van Sanford D. A unified effort to fight an enemy of wheat and barley: Fusarium head blight. Plant disease. 2012 Dec;96(12):1712-28. https://doi.org/10.1094/PDIS-03-12-0291-FE

Mesterhazy A. Updating the breeding philosophy of wheat to Fusarium head blight (FHB): Resistance components, QTL identification, and phenotyping—A review. Plants. 2020 Dec 3;9(12):1702. https://doi.org/10.3390/plants9121702

Mesterhazy A, Gyorgy A, Varga M, Toth B. Methodical considerations and resistance evaluation against *F. graminearum* and *F. culmorum* head blight in wheat. The influence of mixture of isolates on aggressiveness and resistance expression. Microorganisms. 2020 Jul 13;8(7):1036. https://doi.org/10.3390/microorganisms8071036

Mgbeahuruike AC, Kovalchuk A, Chen H, Ubhayasekera W, Asiegbu FO. Evolutionary analysis of hydrophobin gene family in two wood-degrading basidiomycetes, *Phlebia brevispora* and *Heterobasidion annosum* sl. BMC Evolutionary Biology. 2013 Dec;13:1-6. https://doi.org/10.1186/1471-2148-13-240

Miedaner T, Schilling AG, Geiger HH. Molecular genetic diversity and variation for aggressiveness in populations of *Fusarium graminearum* and *Fusarium culmorum* sampled from wheat fields in different countries. Journal of Phytopathology. 2001 Dec;149(11-12):641-8. https://doi.org/10.1046/j.1439-0434.2001.00687.x

Minenko E, Vogel RF, Niessen L. Significance of the class II hydrophobin FgHyd5p for the life cycle of *Fusarium graminearum*. Fungal biology. 2014 Apr 1;118(4):385-93. https://doi.org/10.1016/j.funbio.2014.02.003

Morooka, N., Uratsuji, N., Yoshizawa, T., & Yamamoto, H. Studies on the Toxic Substances in Barley Infected with *Fusarium* spp. Food Hygiene and Safety Science (Shokuhin Eiseigaku Zasshi). 1972 Oct 5;13(5):368-75. https://doi.org/10.3358/shokueishi.13.368

Narwal S, Kumar D, Sheoran S, Verma RP, Gupta RK. Hulless barley as a promising source to improve the nutritional quality of wheat products. Journal of food science and technology. 2017 Aug;54:2638-44. https://doi.org/10.1007/s13197-017-2669-6

Nasmith CG, Walkowiak S, Wang L, Leung WW, Gong Y, Johnston A, Harris LJ, Guttman DS, Subramaniam R. Tri6 is a global transcription regulator in the phytopathogen *Fusarium graminearum*. PLoS pathogens. 2011 Sep 29;7(9):e1002266. https://doi.org/10.1371/journal.ppat.1002266

Newman CW, Newman RK. A brief history of barley foods. Cereal foods world. 2006 Jan 1;51(1):4-7. https://doi.org/10.1094/cfw-51-0004

Neylon E, Arendt EK, Lynch KM, Zannini E, Bazzoli P, Monin T, Sahin AW. Rootlets, a malting by-product with great potential. Fermentation. 2020 Nov 26;6(4):117. https://doi.org/10.3390/fermentation6040117

Nicolli CP, Machado FJ, Spolti P, Del Ponte EM. Fitness traits of deoxynivalenol and nivalenol-producing *Fusarium graminearum* species complex strains from wheat. Plant disease. 2018 Jul 18;102(7):1341-7. https://doi.org/10.1094/PDIS-12-17-1943-RE

Oghenekaro AO, Oviedo-Ludena MA, Serajazari M, Wang X, Henriquez MA, Wenner NG, Kuldau GA, Navabi A, Kutcher HR, Fernando WD. Population genetic structure and chemotype diversity of *Fusarium graminearum* populations from wheat in Canada and North Eastern United States. Toxins. 2021 Mar 1;13(3):180. https://doi.org/10.3390/TOXINS13030180

Okorski A, Milewska A, Pszczółkowska A, Karpiesiuk K, Kozera W, Dąbrowska JA, Radwińska J. Prevalence of *Fusarium* fungi and deoxynivalenol levels in winter wheat grain in different climatic regions of Poland. Toxins. 2022 Jan 28;14(2):102.

Okungbowa FI, Shittu HO. Fusarium wilts: An overview. Environ. Res. J. 2012 Apr 1;6(2):83-102.

Pariaud B, Ravigné V, Halkett F, Goyeau H, Carlier J, Lannou C. Aggressiveness and its role in the adaptation of plant pathogens. Plant Pathology. 2009 Jun;58(3):409-24. https://doi.org/10.1111/j.1365-3059.2009.02039.x

Parry DW, Jenkinson P, McLeod L. Fusarium ear blight (scab) in small grain cereals—a review. Plant pathology. 1995 Apr;44(2):207-38. https://doi.org/10.1111/j.1365-3059.1995.tb02773.x

Peiris KH, Pumphrey MO, Dong Y, Maghirang EB, Berzonsky W, Dowell FE. Near-infrared spectroscopic method for identification of fusarium head blight damage and prediction of deoxynivalenol in single wheat kernels. Cereal Chemistry. 2010 Nov;87(6):511-7.

Piacentini KC, Běláková S, Rocha LO, Savi GD, Benešová K, Pernica M, Hartman I, Čáslavský J, Boško R, Corrêa B. Gushing phenomenon and gene Hyd5 from *Fusarium* species in barley samples from Brazil. Kvasny prumysl. 2021 Apr 15;67(2):435-41. https://doi.org/10.18832/kp2021.67.435

Pinton P, Tsybulskyy D, Lucioli J, Laffitte J, Callu P, Lyazhri F, Grosjean F, Bracarense AP, Kolf-Clauw M, Oswald IP. Toxicity of deoxynivalenol and its acetylated derivatives on the intestine: differential effects on morphology, barrier function, tight junction proteins, and mitogen-activated protein kinases. Toxicological Sciences. 2012 Nov 1;130(1):180-90. https://doi.org/10.1093/toxsci/kfs239

Quarantin A, Hadeler B, Kröger C, Schäfer W, Favaron F, Sella L, Martínez-Rocha AL. Different hydrophobins of *Fusarium graminearum* are involved in hyphal growth, attachment, water-air interface penetration and plant infection. Frontiers in Microbiology. 2019 Apr 12;10:751. https://doi.org/10.3389/fmicb.2019.00751

R Core Team. R: a language and environment for statistical computing. Vienna: R Foundation for Statistical Computing. 2021.

Ramakrishna N, Lacey J, Candlish AA, Smith JE, Goodbrand IA. Monoclonal antibody-based enzyme linked immunosorbent assay of aflatoxin B1, T-2 toxin, and ochratoxin A in barley. Journal of the Association of Official Analytical Chemists. 1990 Jan 1;73(1):71-6. https://doi.org/10.1093/jaoac/73.1.71

Ran R, Wang C, Han Z, Wu A, Zhang D, Shi J. Determination of deoxynivalenol (DON) and its derivatives: Current status of analytical methods. Food control. 2013 Nov 1;34(1):138-48. https://doi.org/10.1016/j.foodcont.2013.04.026

Rani H, Bhardwaj RD. Quality attributes for barley malt:“The backbone of beer”. Journal of Food Science. 2021 Aug;86(8):3322-40. https://doi.org/10.1111/1750-3841.15858

Righetti L, Galaverna G, Dall’Asta C. Group detection of DON and its modified forms by an ELISA kit. Food Additives & Contaminants: Part A. 2017 Feb 1;34(2):248-54. https://doi.org/10.1080/19440049.2016.1265671

Rodgers K, McVey M. Error-prone repair of DNA double-strand breaks. Journal of cellular physiology. 2016 Jan;231(1):15-24. https://doi.org/10.1002/jcp.25053

Roy, K. The effect of germination conditions on growth of *Fusarium graminearum* and secretion of deoxynivalenol during floor malting of barley. University of Dalhousie. 2021.

Salas B, Steffenson BJ, Casper HH, Tacke B, Prom LK, Fetch Jr TG, Schwarz PB. *Fusarium* species pathogenic to barley and their associated mycotoxins. Plant disease. 1999 Jul;83(7):667-74. https://doi.org/10.1094/PDIS.1999.83.7.667

Sarlin T. Detection and characterisation of *Fusarium* hydrophobins inducing gushing in beer. VTT Technical Research Centre of Finland; 2012.

Sarlin T, Kivioja T, Kalkkinen N, Linder MB, Nakari-Setälä T. Identification and characterization of gushing-active hydrophobins from *Fusarium graminearum* and related species. Journal of basic microbiology. 2012 Apr;52(2):184-94. https://doi.org/10.1002/jobm.201100053

Sarlin T, Nakari-Setälä T, Linder M, Penttilä M, Haikara A. Fungal hydrophobins as predictors of the gushing activity of malt. Journal of the Institute of Brewing. 2005;111(2):105-11. https://doi.org/10.1002/j.2050-0416.2005.tb00655.x

Sarlin T, Vilpola A, Kotaviita E, Olkku J, Haikara A. Fungal hydrophobins in the barley-to-beer chain. Journal of the Institute of Brewing. 2007;113(2):147-53. https://doi.org/10.1002/j.2050-0416.2007.tb00271.x

Schmale III DG, Leslie JF, Zeller KA, Saleh AA, Shields EJ, Bergstrom GC. Genetic structure of atmospheric populations of *Gibberella zeae*. Phytopathology. 2006 Sep;96(9):1021-6. https://doi.org/10.1094/PHYTO-96-1021

Schöneberg T, Musa T, Forrer HR, Mascher F, Bucheli TD, Bertossa M, Keller B, Vogelgsang S. Infection conditions of *Fusarium graminearum* in barley are variety specific and different from those in wheat. European journal of plant pathology. 2018 Aug;151:975-89. https://doi.org/10.1007/s10658-018-1434-7

Schroeder, H. W., & Christensen, J. J. (1963). Factors affecting resistance of wheat to scab caused by *Gibberella zeae*. *Phytopathology*, *53*.

Schuren FH, Wessels JG. Two genes specifically expressed in fruiting dikaryons of *Schizophyllum commune*: homologies with a gene not regulated by mating-type genes. Gene. 1990 Jan 1;90(2):199-205. https://doi.org/10.1016/0378-1119(90)90180-Y

Schuren FH, Wessels JG. Two genes specifically expressed in fruiting dikaryons of *Schizophyllum commune*: homologies with a gene not regulated by mating-type genes. Gene. 1990 Jan 1;90(2):199-205. https://doi.org/10.1016/0378-1119(90)90180-Y

Schwarz PB. Fusarium head blight and deoxynivalenol in malting and brewing: successes and future challenges. Tropical Plant Pathology. 2017 Jun;42:153-64. https://doi.org/10.1007/s40858-017-0146-4

Schwarz PB, Beattie S, Casper HH. Relationship between *Fusarium* infestation of barley and the gushing potential of malt. Journal of the Institute of Brewing. 1996 Mar 4;102(2):93-6. https://doi.org/10.1002/j.2050-0416.1996.tb00899.x

Schwarz PB, Jones BL, Steffenson BJ. Enzymes associated with *Fusarium* infection of barley. Journal of the American Society of Brewing Chemists. 2002 Jun 1;60(3):130-4. https://doi.org/10.1094/asbcj-60-0130

Schwarz, P. B., Schwarz, J. G., Zhou, A., Prom, L. K., & Steffenson, B. J. Effect of *Fusarium graminearum* and *F. Poae* infection on barley and malt quality. Monatsschrift Fur Brauwissenschaft. 2001 Dec:54(3–4).

Schwarz P, Li Y. Malting and brewing uses of barley. Barley: Production, improvement, and uses. 2010 Jan 25:478-521. https://doi.org/10.1002/9780470958636.ch15

Sharma T, Sridhar PS, Blackman C, Foote SJ, Allingham JS, Subramaniam R, Loewen MC. *Fusarium graminearum* ste3 G-protein coupled receptor: A mediator of hyphal chemotropism and pathogenesis. Msphere. 2022 Dec 21;7(6):e00456-22. https://doi.org/10.1128/msphere.00456-22

Shokribousjein Z, Deckers SM, Gebruers K, Lorgouilloux Y, Baggerman G, Verachtert H, Delcour JA, Etienne P, Rock JM, Michiels C, Derdelinckx G. Hydrophobins, beer foaming and gushing. Cerevisia. 2011 Jan 1;35(4):85-101. https://doi.org/10.1016/j.cervis.2010.12.001

Siou D, Gelisse S, Laval V, Repinçay C, Canalès R, Suffert F, Lannou C. Effect of wheat spike infection timing on Fusarium head blight development and mycotoxin accumulation. Plant pathology. 2014 Apr;63(2):390-9. https://doi.org/10.1111/ppa.12106

Sobrova P, Adam V, Vasatkova A, Beklova M, Zeman L, Kizek R. Deoxynivalenol and its toxicity. Interdisciplinary toxicology. 2010 Sep 1;3(3):94-9. https://doi.org/10.2478/v10102-010-0019-x

Specker C. Analysis of the interaction of gushing inducing hydrophobins with beer foam proteins (Doctoral dissertation, Technische Universität München).

Sullivan P, Arendt E, Gallagher E. The increasing use of barley and barley by-products in the production of healthier baked goods. Trends in Food Science & Technology. 2013 Feb 1;29(2):124-34. https://doi.org/10.1016/j.tifs.2012.10.005

Sultana S, Adhikary SK, Islam MM, Rahman SM. Evaluation of pathogenic variability based on leaf blotch disease development components of *Bipolaris sorokiniana* in *Triticum aestivum* and agroclimatic origin. The plant pathology journal. 2018 Apr;34(2):93.

Sun J, Wu Y. Evaluation of dietary exposure to deoxynivalenol (DON) and its derivatives from cereals in China. Food control. 2016 Nov 1;69:90-9. https://doi.org/10.1016/j.foodcont.2016.04.040

Sunde M, Kwan AH, Templeton MD, Beever RE, Mackay JP. Structural analysis of hydrophobins. Micron. 2008 Oct 1;39(7):773-84. https://doi.org/10.1016/j.micron.2007.08.003

Szilvay GR, Paananen A, Laurikainen K, Vuorimaa E, Lemmetyinen H, Peltonen J, Linder MB. Self-assembled hydrophobin protein films at the air− water interface: Structural analysis and molecular engineering. Biochemistry. 2007 Mar 6;46(9):2345-54. https://doi.org/10.1021/bi602358h

Talbot NJ, Ebbole DJ, Hamer JE. Identification and characterization of MPG1, a gene involved in pathogenicity from the rice blast fungus *Magnaporthe grisea*. The Plant Cell. 1993 Nov 1;5(11):1575-90. https://doi.org/10.2307/3869740

Talbot NJ, Kershaw MJ, Wakley GE, De Vries OM, Wessels JG, Hamer JE. MPG1 encodes a fungal hydrophobin involved in surface interactions during infection-related development of *Magnaporthe grisea*. The Plant Cell. 1996 Jun 1;8(6):985-99. https://doi.org/10.1105/tpc.8.6.985

Tong SY, Giffard PM. Microbiological applications of high-resolution melting analysis. Journal of clinical microbiology. 2012 Nov;50(11):3418-21. https://doi.org/10.1128/JCM.01709-12

Tucker JR, Badea A, Blagden R, Pleskach K, Tittlemier SA, Fernando WD. Deoxynivalenol-3-glucoside content is highly associated with deoxynivalenol levels in two-row barley genotypes of importance to Canadian barley breeding programs. Toxins. 2019 Jun 5;11(6):319. https://doi.org/10.3390/toxins11060319

Ualema NJ, Dos Santos LN, Bogusz S, Ferreira NR. From conventional to craft beer: Perception, source, and production of beer color-A systematic review and bibliometric analysis. Foods. 2024 Sep 18;13(18):2956. https://doi.org/10.3390/foods13182956

Vaag, P. (2023). Immunological detection of Fusarium in barley and malt . In European brewery convention. https://doi.org/10.1093/oso/9780199632831.003.0068

Valsecchi I, Dupres V, Stephen-Victor E, Guijarro JI, Gibbons J, Beau R, Bayry J, Coppee JY, Lafont F, Latgé JP, Beauvais A. Role of hydrophobins in *Aspergillus fumigatus*. Journal of fungi. 2017 Dec 24;4(1):2. https://doi.org/10.3390/jof4010002

van der Lee T, Zhang H, van Diepeningen A, Waalwijk C. Biogeography of *Fusarium graminearum* species complex and chemotypes: a review. Food Additives & Contaminants: Part A. 2015 Apr 3;32(4):453-60. https://doi.org/10.1080/19440049.2014.984244

Varga E, Wiesenberger G, Hametner C, Ward TJ, Dong Y, Schöfbeck D, McCormick S, Broz K, Stückler R, Schuhmacher R, Krska R. New tricks of an old enemy: isolates of *Fusarium graminearum* produce a type A trichothecene mycotoxin. Environmental Microbiology. 2015 Aug;17(8):2588-600. https://doi.org/10.1111/1462-2920.12718

Virkajärvi V, Sarlin T, Laitila A. *Fusarium* profiling and barley malt gushing propensity. Journal of the American Society of Brewing Chemists. 2017 Jun 1;75(3):181-92. https://doi.org/10.1094/ASBCJ-2017-3321-01

Walkowiak S, Bonner CT, Wang L, Blackwell B, Rowland O, Subramaniam R. Intraspecies interaction of *Fusarium graminearum* contributes to reduced toxin production and virulence. Molecular plant-microbe interactions. 2015 Nov 19;28(11):1256-67. https://doi.org/10.1094/MPMI-06-15-0120-R

Mary Wanjiru W, Zhensheng K, Buchenauer H. Importance of cell wall degrading enzymes produced by *Fusarium graminearum* during infection of wheat heads. European Journal of Plant Pathology. 2002 Oct;108:803-10. https://doi.org/10.1023/A:1020847216155

Ward TJ, Clear RM, Rooney AP, O'Donnell K, Gaba D, Patrick S, Starkey DE, Gilbert J, Geiser DM, Nowicki TW. An adaptive evolutionary shift in Fusarium head blight pathogen populations is driving the rapid spread of more toxigenic *Fusarium graminearum* in North America. Fungal Genetics and Biology. 2008 Apr 1;45(4):473-84. https://doi.org/10.1016/j.fgb.2007.10.003

Warth B, Sulyok M, Fruhmann P, Berthiller F, Schuhmacher R, Hametner C, Adam G, Fröhlich J, Krska R. Assessment of human deoxynivalenol exposure using an LC–MS/MS based biomarker method. Toxicology letters. 2012 May 20;211(1):85-90. https://doi.org/10.1016/j.toxlet.2012.02.023

Wessels, J. G. H. Developmental regulation of fungal cell wall formation. Annual Review of Phytopathology. 1994;32:413-437. https://doi.org/10.1146/annurev.py.32.090194.002213

Wessels JG. Fungal hydrophobins: proteins that function at an interface. Trends in plant science. 1996 Jan 1;1(1):9-15. https://doi.org/10.1016/S1360-1385(96)80017-3

Wessels JG. Hydrophobins: proteins that change the nature of the fungal surface. Advances in microbial physiology. 1996 Jan 1;38:1-45. https://doi.org/10.1016/s0065-2911(08)60154-x

Wessels JG. Hydrophobins, unique fungal proteins. Mycologist. 2000 Jan 1;14(4):153. https://doi.org/10.1016/S0269-915X(00)80030-0

Wickham H. ggplot2. Wiley interdisciplinary reviews: computational statistics. 2011 Mar;3(2):180-5. https://doi.org/10.1002/wics.147

Woelflingseder L, Gruber N, Adam G, Marko D. Pro-inflammatory effects of NX-3 toxin are comparable to deoxynivalenol and not modulated by the co-occurring pro-oxidant aurofusarin. Microorganisms. 2020 Apr 21;8(4):603.

Wösten HA. Hydrophobins: multipurpose proteins. Annual Reviews in Microbiology. 2001 Oct;55(1):625-46. https://doi.org/10.1146/annurev.micro.55.1.625

Wösten HA, de Vocht ML. Hydrophobins, the fungal coat unravelled. Biochimica et Biophysica Acta (BBA)-Reviews on Biomembranes. 2000 Sep 18;1469(2):79-86. https://doi.org/10.1016/S0304-4157(00)00002-2

Wösten HA, Schuren FH, Wessels JG. Interfacial self-assembly of a hydrophobin into an amphipathic protein membrane mediates fungal attachment to hydrophobic surfaces. The EMBO Journal. 1994 Dec 15;13(24):5848-54. https://doi.org/10.1002/j.1460-2075.1994.tb06929.x

Wösten HA, van Wetter MA, Lugones LG, van der Mei HC, Busscher HJ, Wessels JG. How a fungus escapes the water to grow into the air. Current Biology. 1999 Jan 28;9(2):85-8. https://doi.org/10.1016/S0960-9822(99)80019-0

Wösten HA, Wessels JG. Hydrophobins, from molecular structure to multiple functions in fungal development. Mycoscience. 1997 Oct;38:363-74. https://doi.org/10.1007/bf02464099

Xie Y, Xu M, Han B, Chen T, Cai G, Lu J. Barley husk degraded by *Fusarium graminearum* MH1 induced premature yeast flocculation. Journal of Agricultural and Food Chemistry. 2022 Aug 10;70(33):10296-304.

Xue AG, Ho KM, Butler G, Vigier BJ, Babcock C. Pathogenicity of *Fusarium* species causing head blight in barley. Phytoprotection. 2006 Aug;87(2):55-61. https://doi.org/10.7202/013973ar

Yang H, Ren S, Yu S, Pan H, Li T, Ge S, Zhang J, Xia N. Methods favoring homology-directed repair choice in response to CRISPR/Cas9 induced-double strand breaks. International journal of molecular sciences. 2020 Sep 4;21(18):6461. https://doi.org/10.3390/ijms21186461

Yin, X. S. Practical Brewing Sciences - MALT. Book by the American Society of Brewing Chemists. 2021. St Paul, USA. Chapter 14.

Zeller KA, Bowden RL, Leslie JF. Diversity of epidemic populations of *Gibberella zeae* from small quadrats in Kansas and North Dakota. Phytopathology. 2003 Jul;93(7):874-80. https://doi.org/10.1094/PHYTO.2003.93.7.874

Zhang H, Sun J, Zhang Y, Lu M, Sun L, Li W, Hu X, Wang B. Retention of deoxynivalenol and its derivatives during storage of wheat grain and flour. Food Control. 2016 Jul 1;65:177-81. https://doi.org/10.1016/j.foodcont.2015.12.019

Zhang H, Van der Lee T, Waalwijk C, Chen W, Xu J, Xu J, Zhang Y, Feng J. Population analysis of the *Fusarium graminearum* species complex from wheat in China show a shift to more aggressive isolates. PLoS One. 2012 Feb 20;7(2):e31722. https://doi.org/10.1371/journal.pone.0031722

Zhang JB, Li HP, Dang FJ, Qu B, Xu YB, Zhao CS, Liao YC. Determination of the trichothecene mycotoxin chemotypes and associated geographical distribution and phylogenetic species of the *Fusarium graminearum* clade from China. Mycological research. 2007 Aug 1;111(8):967-75. https://doi.org/10.1016/j.mycres.2007.06.008

Zhou MX. Barley production and consumption. Genetics and improvement of barley malt quality 2009 (pp. 1-17). Berlin, Heidelberg: Springer Berlin Heidelberg. https://doi.org/10.1007/978-3-642-01279-2_1

Zohary D, Hopf M, Weiss E. Domestication of Plants in the Old World: The origin and spread of domesticated plants in Southwest Asia, Europe, and the Mediterranean Basin. Oxford University Press; 2012 Mar 1. https://doi.org/10.5860/choice.50-4995

7. APPENDICES

7.1 Supporting information

7.1.1 Heterologous expression and purification of hydrophobin HYD5 protein

A codon-optimized sequence coding for HYD5 (*Fusarium graminearum* v3.0|scaffold_1:6013270-6014092) was purchased from BioBasic Inc. and ligated into a modified pET-21 derived plasmid so that the open reading frame coded for a hexahistidine-tag (H), the B1 domain of Streptococcal protein G (GB1), a thrombin cleavage site (Th), and HYD5 (HGB1ThHYD5). Chemically competent *E. coli* SHuffle (DE3) (New England Biolabs) was transformed with the plasmid and grown overnight on selective plates at 37 °C. Bacterial cultures (1 L) were inoculated from a single colony and grown in lysogeny broth (LB) media with ampicillin (100 μg/mL) at 37 °C. When the optical density at 600 nm reached 0.6-0.8, protein expression was induced by the addition of isopropyl β-D-1-thiogalactopyranoside to a final concentration of 0.5 mM. Following overnight incubation at 20 °C, cells were collected by centrifugation (4550 × g) and then resuspended in lysis buffer (20 mM Tris pH 8, 250 mM NaCl). Cells were lysed by sonication (2 min) and the lysate was clarified by centrifugation for 20 min at 25,000 × g. The supernatant was applied to a gravity column containing Ni2+ charged nitrilotriacetic acid coupled to agarose resin (MCLAB), washed with lysis buffer containing 10 mM imidazole, and eluted with elution buffer (20 mM Tris pH 8, 250 mM NaCl, 300 mM imidazole). After elution, 500 U of thrombin was added and the sample was dialyzed overnight at 4 ℃ against 20 mM Tris pH 8, 50 mM NaCl and 1 mM $CaCl_2$. After cleavage, the HYD5 was isolated using Ni^{2+} affinity chromatography. Reduced glutathione (2 mM) and oxidized glutathione (1 mM) were added and the protein was allowed to refold overnight at 4 ℃. Anion exchange chromatography (Q Sepharose, Cytiva) via fast protein liquid chromatography (AKTA) was used to further purify HYD5. Sample quality was checked by sodium dodecyl sulfate polyacrylamide gel electrophoresis (SDS-PAGE), and reverse phase high-performance liquid chromatography (Beckman System Gold with a C18 column, gradient of 5-55 % acetonitrile containing 0.5 % trifluoroacetic acid over 20 min).

7.1.2 Purification and characterization of recombinant HYD5 protein

The HYD5 protein from *F. graminearum* was successfully produced in *E. coli* and purified. After Ni^{2+} affinity chromatography, one major band was visible by SDS-PAGE (Supplementary Figure S1). The second run of Ni^{2+} affinity chromatography isolated pure HYD5. However, the FPLC purification chromatogram showed several peaks (data not

shown), suggesting a mixture of HYD5 conformations. Such conformational differences could arise from different disulfide bonding patterns during the refold of HYD5. Additionally, the HPLC result showed that HYD5 (22 min) from FPLC only contains a single peak (17 min), which suggests a homogeneous conformation of HYD5 was obtained after FPLC. The overall yield of HYD5 was about 3-5 mg/L induced culture.

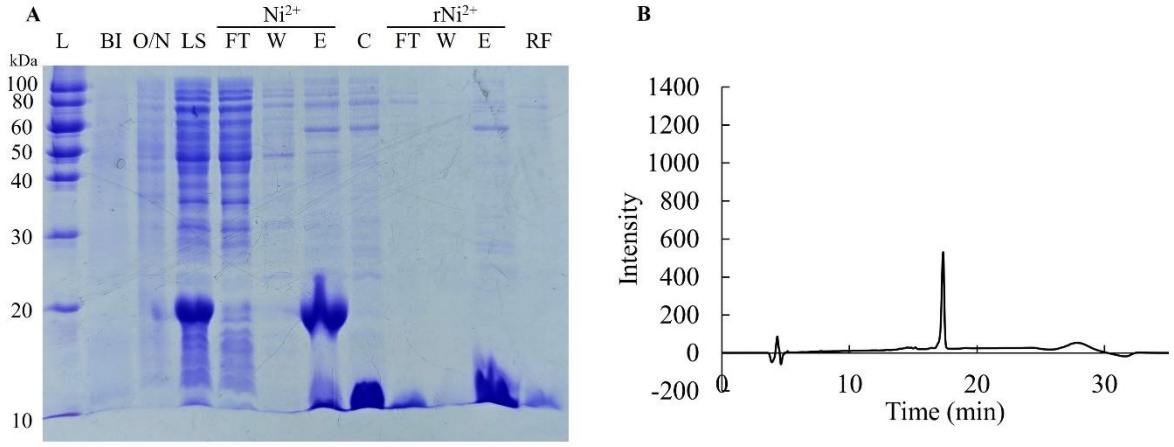

Supplementary Figure S1: SDS-PAGE monitoring of HYD5 purification. A) the Ni^{2+} affinity chromatography purification of HYD5, L: ladder; BI: before induction; O/N: overnight expression; LS: lysis sample; Ni^{2+}: the first run of Ni^{2+} affinity chromatography; FT: flow through; W: wash; E: elution; C: cut; rNi^{2+}: the second run of Ni^{2+} affinity chromatography; RF: refold. B) HPLC qualification of HYD5 purification. The single peak indicates the homogenous formation of HYD5, which was used for further analysis.

7.2 List of abbreviations

15-ADON	15-acetyl deoxynivalenol
3-ADON	3-acetyl deoxynivalenol
ANOVA	Analysis of Variance
Cas	CRISPR-associated
cDNA	Complementary DNA
CMC	Carboxymethyl Cellulose
CRISPR	Clustered Regularly Interspaced Short Palindromic Repeats
crRNA	CRISPR RNA
DNA	Deoxyribonucleic Acid
DON	Deoxynivalenol
DSB	Double Strand Break
ELISA	Enzyme Linked Immunosorbent Assay
FHB	Fusarium Head Blight
FPLC	Fast Protein Liquid Chromatography

GAPDH	Glyceraldehyde-3-phosphate dehydrogenase
HDR	Homologous-Directed Repair
HPLC	High-performance liquid chromatography
HRM	High Resolution Melting Analysis
HRT	Homologous Repair Template
HSW	Henriquez Spring Wheat
HYD	Hydrophobin
ITS	Internal Transcribed Spacer
KO	Knockout
NHEJ	Non-Homologous End Joining
NIV	Nivalenol
PAM	Protospacer Adjacent Motif
PCR	Polymerase Chain Reaction
PDA	Potato Dextrose Agar
PEG	Polyethylene Glycol
qPCR	Quantitative PCR
RNA	Ribonucleic Acid
RNP	Ribonucleoproteins
RT-qPCR	Reverse Transcription Quantitative Polymerase Chain Reaction
SDS-PAGE	Sodium dodecyl sulfate-polyacrylamide gel electrophoresis
sgRNA	Single-guide RNA
tracrRNA	trans-activating crRNA
PYF	premature yeast flocculation